# THE
# PROCEEDINGS
## OF
# THE PHYSICAL SOCIETY

## CONTENTS

# THE PHYSICAL SOCIETY

## INSTRUCTIONS TO AUTHORS

Note. The acceptance of a paper for publication in the Proceedings rests with the Council, advised by its Editing Committee. The high cost of printing renders it imperative to exclude matter that is not novel and not of importance to the understanding of the paper.

Authors offering original contributions for publication in the Proceedings should observe the following directions; failure to comply with these may cause considerable delay in publication. Fuller directions, including special instructions on the arrangement of mathematical work, are contained in a leaflet obtainable from the Assistant Secretary.

*Manuscript.*—In drafting the paper a clear and concise style should be adopted. The utmost brevity consistent with effective presentation of the original subject-matter should be used. The copy should be easily legible, preferably typewritten and double-spaced. It should receive a careful final revision before communication, since alterations are costly when once the type has been set up. Mathematical expressions should be set out clearly, in the simplest possible notation.

*Drawings and tables.*—Diagrams must be carefully drawn in Indian ink on white paper or card. Their size and thickness of line must be sufficient to allow of reduction. *Lettering and numbering should be in pencil*, to allow of printing in a uniform style. The number of diagrams should be kept down to the minimum. Data should in general be presented in the form of either curves or tables, but not both. Footlines descriptive of figures, and headlines indicative of contents of tables, should be supplied.

*Abstracts.*—Every paper must be accompanied by an abstract, brief but sufficient to indicate the scope of the paper and to summarize all novel results.

*Proofs.*—Proofs of accepted papers will be forwarded to authors. They should be returned promptly with errors corrected, but additions to or other deviations from the original copy should be avoided.

*Reprints.*—Fifty copies of printed papers will be supplied gratis. Extra copies may be purchased at cost price.

*Contributions by non-Fellows.*—Papers by non-Fellows must be communicated to the Society through a Fellow.

*Republication.*—Permission to reproduce papers or illustrations contained therein may be granted by the Council on application to the Hon. Secretaries.

# ──MACMILLAN──

**STANDARD FOUR-FIGURE MATHEMATICAL TABLES.** By L. M. MILNE-THOMSON, M.A., and L. J. COMRIE, M.A., Ph.D. Edition A: With Positive Characteristics in the Logarithms. Edition B: With Negative Characteristics in the Logarithms. 10s. 6d. net each Edition.

---

**INTRODUCTION TO THE THEORY OF FOURIER'S SERIES AND INTEGRALS.** By H. S. CARSLAW, Sc.D., LL.D., F.R.S.E. *Third Edition, revised and enlarged.* 20s. net.

---

**ASTRONOMY.** An Introduction. By ROBERT H. BAKER, Ph.D., Professor of Astronomy in the University of Illinois. 16s. net.

---

**ALTERNATING CURRENTS FOR TECHNICAL STUDENTS.** By CALVIN C. BISHOP, E.E., Head of the Department of Drafting and Design, Technical High School, Buffalo, N.Y. 8s. 6d. net.
This book is written to explain graphically and with simple mathematics the fundamental principles of alternating-current theory, circuits and apparatus. It is intended for technical and vocational students, engineering students, and any others who may desire to become acquainted with the subject.

---

**THE THEORY OF THE GYROSCOPIC COMPASS, and its Deviations.** By A. L. RAWLINGS, Ph.D., B.Sc. (London), late Principal Scientific Assistant in the Department of Scientific Research, Admiralty; formerly Superintendent of Instruction and Experiment at the Admiralty Compass Department. 10s. 6d. net.

---

**SPEECH AND HEARING.** By HARVEY FLETCHER, Ph.D., Acoustical Research Director, Bell Telephone Laboratories, Inc. With an Introduction by H. D. ARNOLD, Ph.D. 21s. net.

---

**A HISTORY OF PHYSICS IN ITS ELEMENTARY BRANCHES; INCLUDING THE EVOLUTION OF PHYSICAL LABORATORIES.** By FLORIAN CAJORI, Ph.D., Professor of the History of Mathematics in the University of California. *Revised and Enlarged Edition.* 15s. net.

---

**LECTURES ON THEORETICAL PHYSICS.** By the late Professor H. A. LORENTZ. Authorised Translation by L. SILBERSTEIN, Ph.D., and A. P. H. TRIVELLI. Volume I. Aether Theories and Aether Models. Edited by H. BREMEKAMP, Ph.D.—Kinetical Problems. Edited by E. D. BRUINS, Ph.D., and J. REUDLER, Ph.D. With Figures. 12s. 6d. net. Volume II. Thermodynamics. Edited by T. C. CLAY-JOLLES.—Entropy and Probability. Edited by C. A. CROMMELIN, Ph.D.—The Theory of Radiation. Edited by A. D. FOKKER, Ph.D.—The Theory of Quanta. Edited by G. L. DE HAAS-LORENTZ, Ph.D. 21s. net. Volume III. The Principle of Relativity for Uniform Translations (Special Theory of Relativity). [*Shortly*]

---

**GAUGES AND FINE MEASUREMENTS.** By F. H. ROLT, M.B.E., B.Sc., Senior Assistant, Metrology Department, National Physical Laboratory. Edited by Sir RICHARD GLAZEBROOK, K.C.B., D.Sc., F.R.S., Editor of *A Dictionary of Applied Physics.* 2 volumes. 42s. net.

---

**DICTIONARY OF APPLIED PHYSICS.** By Various Writers. Edited by Sir RICHARD GLAZEBROOK, K.C.B., D.Sc., F.R.S. Illustrated. In 5 volumes. £3. 3s. net each. The set of 5 volumes, £14. 14s. net. Volume I. Mechanics—Engineering—Heat. Volume II. Electricity. Volume III. Meteorology, Metrology, and Measuring Apparatus. Volume IV. Light, Sound and Radiology. Volume V. Aeronautics—Metallurgy—General Index.

*\*\** *Macmillan's Classified Catalogue, post free on application*

## ──MACMILLAN & CO. LTD. LONDON W.C. 2──

# ❁ New Cambridge Books ❁

## THE PHYSICAL PRINCIPLES OF THE QUANTUM THEORY

By *WERNER HEISENBERG*

*Translated into English by Carl Eckart and Frank C. Hoyt*

With 19 text-figures.     Crown 8vo.     8s. 6d. net.

## BAND SPECTRA AND MOLECULAR STUCTURE

By *R. de L. KRONIG*

Demy 8vo.     10s. 6d. net.

An attempt to obtain a fuller understanding of molecular structure from spectral evidence. The investigation in particular throws light on the macroscopic properties of molecular gases and the theory of chemical binding.

## AN OUTLINE OF WAVE MECHANICS

By *N. F. MOTT*

Demy 8vo.     8s. 6d. net.

Mr Mott, who is lecturer in Theoretical Physics in the University of Manchester, has written an account of the methods of the New Quantum Theory. The book is intended for the advanced student of experimental physics and for the research worker.

CAMBRIDGE UNIVERSITY PRESS

Fetter Lane     LONDON     E.C. 4
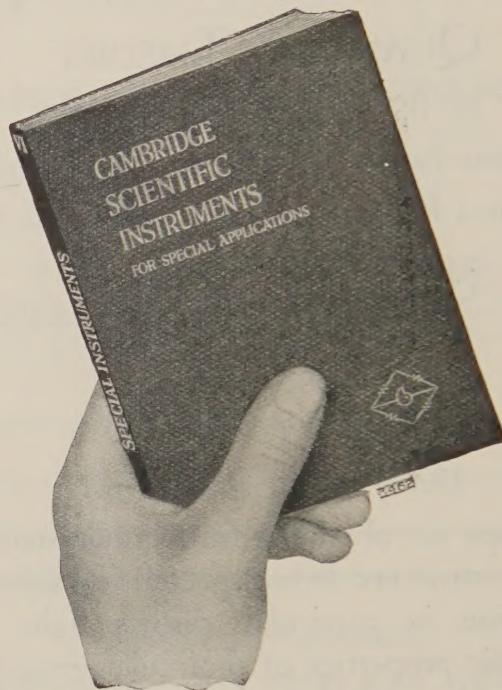
## A SIMPLE APPROXIMATE THEORY OF THE PRESSURE BETWEEN TWO BODIES IN CONTACT*

BY J. P. ANDREWS, M.Sc., F.Inst.P.

*ABSTRACT.* When two solid bodies are pressed together without at any point exceeding the elastic limit, their common area of contact is frequently circular, and in such cases the normal stress at each point of this area may be calculated by a simple approximate method giving results correct, as a rule, to within 1 or 2 per cent. The approximation makes use of two principles: (*a*) The displacement at the centre of the circle of contact is twice that at its edge, and (*b*) for the purpose of calculating the stresses we may replace the two bodies by a single sphere of which the circle of contact is a diametral section, and write the strain at any point as the ratio of the displacement of that point to the length of the line drawn from the point to the sphere in the direction of displacement. When the elastic modulus with which this is multiplied is taken as that appropriate to a rod with sides fixed, the agreement with accurate theory is close. It is shown that the principle (*a*) remains nearly true for elliptical areas of contact.

THE problem of the stresses called forth when two bodies are pressed together, a problem of considerable practical interest, has been thoroughly worked out by Hertz†, and it is possible to obtain from his theory all that is required in practice, provided that the elastic limit is not surpassed. It is nevertheless a fact that the mathematical processes involved in the analysis are far from elementary, and it is not a simple matter to deduce the formulae required in simple instances. This complexity arises in part from the thoroughness of the solution, which includes the distribution of stresses in the interior of the substances. Now in practice we rarely need to know anything beyond the pressure at each point of the surface of contact, and the dimensions of that area, which is generally circular or approximately so. In cases where this information will suffice, a much easier approximate calculation is possible.

This simpler method rests on the fact that in either of a pair of bodies in contact the normal displacement at the centre of a circular area of contact is twice that at its

---

\* Portion of thesis approved for the degree of Doctor of Science in the University of London.

† See A. E. H. Love, *Elasticity*, p. 194 (Cambridge, 1927).

edge. This may be deduced from Hertz's theory, or may be regarded as an experi-
mental fact true for perfectly elastic bodies. The following experiment is a verifica-
tion of the rule for the case of a solid rubber sphere in contact with a glass plane.

A solid rubber ball (Croydex type), about 6·2 cm. in diameter, was compressed
between two parallel planes in such a way that the total force employed and the
corresponding diminution of the diameter of the rubber ball could both be measured.
If the ball behaves in a perfectly elastic fashion in the sense employed by Hertz, and
$H, k$     $H$ is the total diminution of the diameter under a thrust $F$, $F = kH^{\frac{3}{2}}$, where $k$ is a
constant.

Figure 1 *a* shows that, for small compressions, the ball may be considered
perfectly elastic.
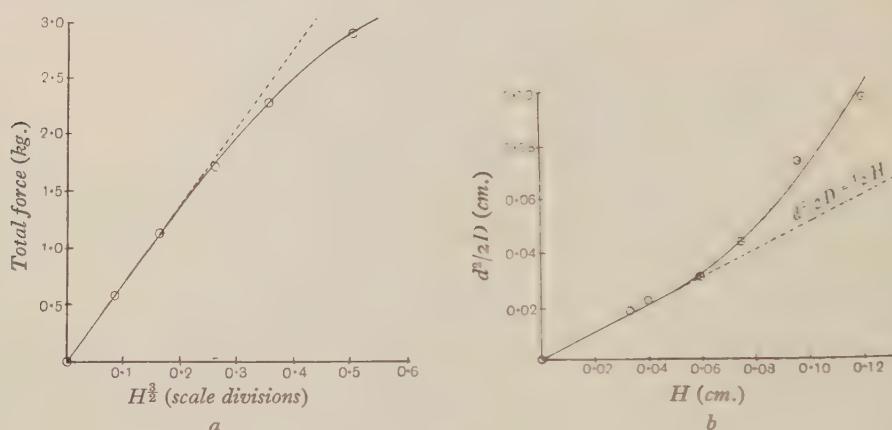


Fig. 1.

Next, the ball was inserted in the apparatus shown in figure 2, in which it is
compressed between two blocks of glass. In order to avoid the errors due to its
weight, the ball was floated in water, so that it just touched the bottom glass. The
levels of the two glass surfaces were read through a microscope, with the aid of stiff
glass pointers projecting from them, the upper glass being kept stationary and the
ball gradually pressed on to it by means of a screw which raised the bottom block.
The bottom of the upper block had been smeared very thinly with a minute
quantity of grease, just sufficient to alter the reflecting power of the surface; and
when the compressed ball was flattened against this surface, the circle of contact
was clearly visible through the glass and was measured microscopically.

$D, d$     If the diameter of the ball is $D$ and that of the area of contact $d$ the height of the
spherical cap whose base is a circle of diameter $d$ is $d^2/4D$. Hence, if the compression
merely takes place where contact is made, the total diminution $H$ of the diameter,
considering both top and bottom, should be $d^2/2D$. If, on the other hand, this only
accounts for half the diminution, as we have assumed, $H = d^2/D$. Figure 1 *b* shows
the actual experimental results. Evidently for small compressions, up to 1 per cent.
of the radius of the ball, our assumption is justified; and this is the order of strain
to which Hertz's theory is supposed to apply.

Consider therefore two spheres, of radii $R_1$, $R_2$ respectively, just touching as in figure 3 $a$, so that the distance between their centres is $(R_1 + R_2)$. Press them together, figure 3 $b$, so that their centres, originally at $B_0$, $B_1$, are now at $B_0$, $B_2$ respectively. If with $B_0$, $B_2$ as centres we draw two spheres of radii $R_1$, $R_2$, they intersect in the circle whose diameter is $CD$ and cut off $GH$ on the line $B_0B_2$. The actual shapes of the surfaces are shown by unbroken lines, that of the first sphere having become the surface $AEOFJ$, and that of the second $KEOFL$, $EOF$ being the surface of contact. Draw through $E$ a line parallel to $B_0B_2$, cutting the dotted spheres in $M$, $N$. Then the principle quoted at the beginning of the paper indicates that $MN = \frac{1}{2}GH$.
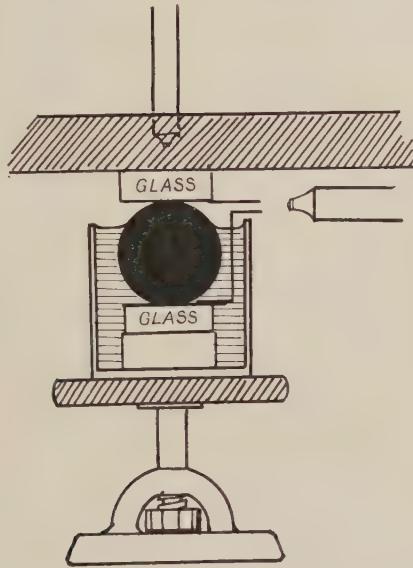


Fig. 2.

In the approximation to be given we assume that the surfaces $AE$, $KE$ do not differ appreciably from spheres of the radii $R_1$, $R_2$, at any rate near the point $E$, so that we account for the intersection of the actual surfaces at $E$ instead of at $C$ by assuming the spherical masses surrounding the area of contact to have been simply pressed back, without appreciable deformation, by amounts $ME$, $EN$ respectively, where $ME = \frac{1}{2}GO$ and $EN = \frac{1}{2}OH$. It follows then that if through $E$ and $F$ we continue the spherical surfaces $AE$, $KE$, etc., these will cut off a length $PQ$ on $B_0B_2$, where $PQ = \frac{1}{2}GH = \frac{1}{2}B_1B_2$, and the circle of contact is the circle of intersection of these two spheres. The process of compression may then be thought of as the production of (*a*) a mass displacement of the material surrounding the area of contact, and (*b*) an additional displacement of points within the area of contact which increases from the edge to the centre and makes the total displacement at the centre just double that at the edge.

Turning now to an actual example of the approximate method, consider the pressing together of two different bodies whose surfaces in the neighbourhood of

the points of contact are parts of spheres of radii $R_1$, $R_2$ respectively. Since we are only concerned with displacements in this neighbourhood we may replace the bodies by complete spheres of radii $R_1$, $R_2$. In order, now, to find the radius of the circle of contact when the centres of the spheres have approached by $B_1B_2$ or $\alpha$ after the surfaces have touched, we draw two intersecting spheres representing the bodies in
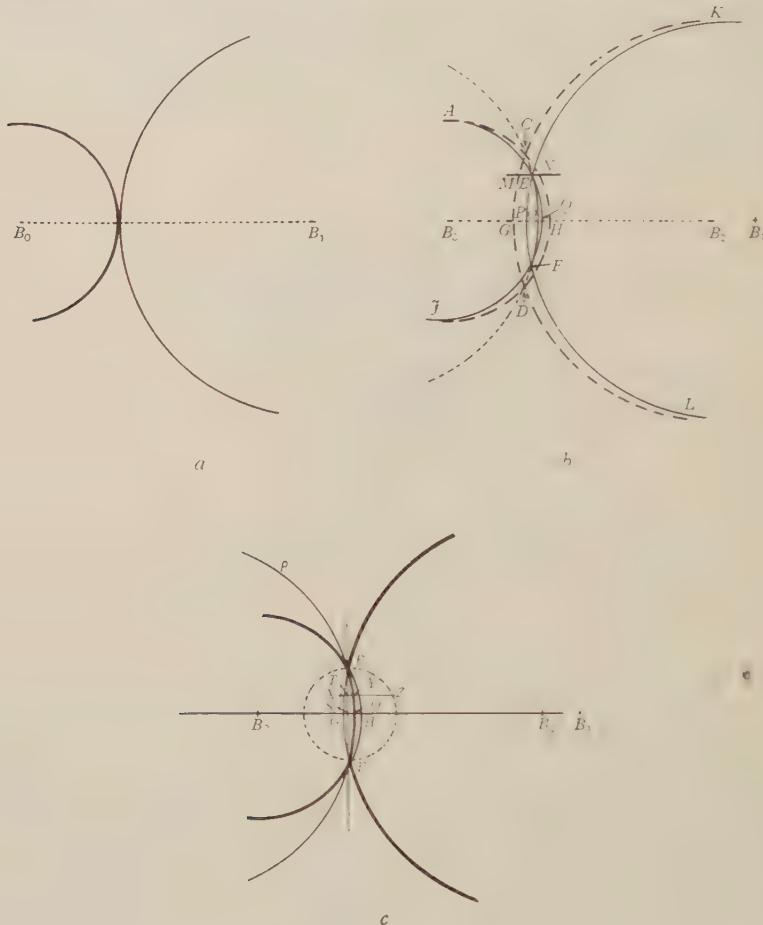


Fig. 3.

contact, figure 3 *c*, and if *EF* is small compared with the radius of curvature of either sphere

$$SG \times 2R_1 = SE^2 = a^2, \text{ where } 2a = EF,$$

$$SH \times 2R_2 = SE^2 = a^2,$$

$$SG + SH = \alpha/2.$$

Hence

$$a^2 = \alpha R_1 R_2/(R_1 + R_2).$$

This is the expression given by Love.

The pressure at each point of the area of contact may be calculated thus. In the figure the unbroken lines represent the two spheres and the surface of contact (part of a sphere of radius $\rho$, say). The displacement of the point $X$ on the surface of one of the spheres is then $XY$. To calculate the pressure at $Y$, we first require the strain at that point, and the second part of the approximation enters here. On $EF$ as diameter construct the sphere shown by the dotted line. We will suppose that at the surface of contact the normal stresses in, say, the larger sphere of figure 3 $c$ are the same as those at the upper surface of a body bounded originally by the spherical surfaces $EGF$, $EZF$, when $EGF$ is depressed to $EYF$, and $EZF$ is held rigidly fixed. The appropriate strain of an element such as $XZ$ is $XY/XZ$. Draw the straight line $EF$ cutting $XZ$ in $T$. Let $EF$ be equal to $2a$ and $ST$ to $r$, where $S$ is the mid-point of $EF$. Then from the figure we have, if the displacements are all small,

$$2R_1 XT = a^2 - r^2 = 2\rho \cdot TY = (TZ)^2.$$

Remembering that $YZ = TZ$ very nearly, in all cases where Hertz's theory applies, there is no difficulty in showing that

$$XY = (1 - R_1/\rho)\,(a^2 - r^2)/2R_1,$$

and the strain, to the same approximation, is then $(a^2 - r^2)^{\frac{1}{2}}\,(1 - R_1/\rho)/2R_1$, while the stress at $Y$ is $E_1$ times this quantity, where $E_1$ is the appropriate elastic modulus. But since the normal stresses must be the same in both bodies

$$\tfrac{1}{2}E_1\,(a^2 - r^2)^{\frac{1}{2}}\,(1/R_1 - 1/\rho) = \tfrac{1}{2}E_2\,(a^2 - r^2)^{\frac{1}{2}}\,(1/R_2 + 1/\rho).$$

From which we derive
$$1/\rho = (E_1/R_1 - E_2/R_2)/(E_1 + E_2).$$

The stress may finally be written

$$\tfrac{1}{2}\,(1/R_1 + 1/R_2)\,(a^2 - r^2)^{\frac{1}{2}}/(1/E_1 + 1/E_2).$$

The proper elastic modulus appears from general considerations to be that appropriate to the longitudinal compression of a rod whose sides are fixed, or one with a value between this and Young's modulus $q$. For a rod with sides fixed, $E$ would have the value $E = q/[1 - 2\sigma^2/(1 - \sigma)]$, where $\sigma$ is Poisson's ratio.

We may now compare these results with those of accurate theory. The stress at $Y$ is, on Hertz's theory,

$$[2/\pi]\,[1/R_1 + 1/R_2]\,(a^2 - r^2)^{\frac{1}{2}}\,[(1 - \sigma_1^2)/q_1 + (1 - \sigma_2^2)/q_2].$$

The coefficient of $(1/R_1 + 1/R_2)\,(a^2 - r^2)^{\frac{1}{2}}$ in the accurate case is

$$[2/\pi]\,\{1/[(1 - \sigma_1^2)/q_1 + (1 - \sigma_2^2)/q_2]\},$$

where $\sigma_1$, $\sigma_2$ are the values of Poisson's ratio for the two materials, and in the simple theory $\tfrac{1}{2}\,\{1/[\{1 - 2\sigma_1^2/(1 - \sigma_1)\}/q_1 + \{1 - 2\sigma_2^2/(1 - \sigma_2)\}/q_2]\}.$

To illustrate the extent of the agreement, consider the two spheres to be made of the same material, and Poisson's ratio to be 0·3. Then the values of the coefficients in the two cases are,

by the accurate theory,     0·349$q$,

by the approximate theory, 0·336$q$.

*(marginal notes:)* $\rho$ ; $a, r$ ; $E_1$ ; $E_2$ ; $q$ ; $\sigma$

This agreement is quite good enough for most purposes. The following example relates to a practical case. A steel ball of radius 1 inch is pressed into a flat copper plate. The values of Young's modulus for the steel and the copper are respectively $2 \times 10^{12}$ dynes/cm.$^2$ and $1 \cdot 2 \times 10^{12}$ dynes cm.$^2$, while the values of Poisson's ratio are $0 \cdot 30$ and $0 \cdot 26$ respectively. We suppose the centre of the ball to have been pressed down, after the ball rested on the copper, by $0 \cdot 001$ cm. It is required to find the pressure at the centre of the area of contact.

By the method already explained, we find that the radius of this area is $0 \cdot 0316$ cm. Employing this value in the necessary calculation, and remembering that $R_2 = \infty$, we have, for the pressure at the centre of the area of contact, by the accurate method $6 \cdot 46 \times 10^9$ dynes/cm.$^2$ or $9 \cdot 38 \times 10^3$ lb. in.$^2$, and by the approximate method $6 \cdot 56 \times 10^9$ dynes/cm.$^2$ or $9 \cdot 51 \times 10^3$ lb. in.$^2$. The total force on the ball could be calculated by the usual simple integration, and the degree of approximation is the same.

As a further example let us consider two equal cylinders of the same substance, with their axes perpendicular, to be pressed into one another. Now two cylindrical surfaces of radius $R$, when allowed to intersect, cut in a curve which is approximately a circle if its area is small compared with $R^2$. Simple calculation gives the radius of this circle as $(2R\alpha)^{\frac{1}{2}}$, where $(2R - \alpha)$ is the perpendicular distance between the axes. In the case of the solid cylinders, however, the surrounding surface is pressed back, and the flattened area of contact is that obtained when the approach is considered as $\alpha/2$. This is merely the application of the first principle of approximation laid down in this paper. The radius $a$ of the area of contact is therefore $(R\alpha)^{\frac{1}{2}}$.

α

The actual area of contact will be an anticlastic surface, the two radii of curvature in this instance being equal to $\rho$, say. If we take the origin of coordinates to be at the centre of this area, and the coordinate axes to be parallel to the axes of the cylinders, elementary geometry shows that the displacement of a point on the surface of either cylinder, reckoned as in the case of the spheres, is

ρ

$$(a^2 - x^2)(1/2R - 1/2\rho) - y^2/2\rho.$$

In order to find the strain at the point in question, we construct as before a sphere with the circle of contact as its diametral section. If we divide this into longitudinal prisms supposed to be uniformly compressed in the direction of their length, and proceed exactly as before, we find the strain to be

$$\{(a^2 - x^2)(1/2R - 1/2\rho) - y^2/2\rho\}/(a^2 - r^2)^{\frac{1}{2}}.$$

The condition that the stress in the direction of pressure must be the same at the surface in each cylinder leads to the relation

$$\rho = 2R,$$

and the stress, finally, may be written

$$[E/4R](a^2 - r^2)^{\frac{1}{2}},$$

where, as before, $E$ is the appropriate elastic modulus, which we may take to be that for the compression of a rod with sides fixed. The full expression then becomes

$$q(a^2 - r^2)^{\frac{1}{2}}/4R\{1 - 2\sigma^2/(1 - \sigma)\}.$$

The stress calculated from Hertz's theory is

$$q (a^2 - r^2)^{\frac{1}{2}}/\pi R (1 - \sigma^2),$$

and this is of the same order of agreement as in the case of spheres.

The validity of these methods depends upon the fact that when the area of contact has a circular perimeter the ratio of two definite integrals which occur in Hertz's theory is equal to 2·0*. These integrals are

$$\int_0^\infty du/\{(1 + u)^{\frac{3}{2}} [u (1 - e^2 + u)]^{\frac{1}{2}}\}, \text{ which} = \pi/2 \text{ when } e = 0,$$

and 
$$\int_0^\infty du/\{u (1 + u) (1 - e^2 + u)\}^{\frac{1}{2}}, \text{ which} = \pi \text{ when } e = 0.$$

In these expressions, $e$ is the eccentricity of the perimeter of the area of contact,     $e$
proved by Hertz to be always elliptical, within the limits laid down in his theory.

It is owing to this simple relation that what is called in this paper the first principle is accurately true for circular areas of contact. In so far however as the ratio mentioned approximates to 2 over a wide range of values of $e$ no serious inaccuracy would be caused by using the approximate method for elliptical areas of contact. The list below indicates how the ratio varies for different values of $e$, the numbers having been calculated from the approximations

$$\int_0^\infty du/(1 + u)^{\frac{3}{2}} \{u (1 - e^2 + u)\}^{\frac{1}{2}} = \pi/2 (1 + \tfrac{3}{8}e^2),$$

$$\int_0^\infty du/\{u (1 + u) (1 - e^2 + u)\}^{\frac{1}{2}} = \pi (1 + e^2/4),$$

which values apply when $e$ is not too near to unity.

The test thus provides a guide to the accuracy of the approximation in any unusual case where the area of contact is elliptical. In such a case the method of reckoning the strain is similar; but it now becomes necessary to construct an

| $e$ | o | 0·2 | 0·4 | 0·6 | 0·8 |
|---|---|---|---|---|---|
| Ratio of integrals | 2·0 | 1·990 | 1·960 | 1·910 | 1·840 |

ellipsoid on the elliptical area of contact. Simple comparison with accurate theory suggests that the length of the third semi-diameter of this ellipsoid should be taken as the harmonic mean of the lengths of the other two.

In conclusion I have pleasure in thanking Prof. C. H. Lees for his interest and advice in the preparation of this paper.

## DISCUSSION

* A. E. H. Love, *loc. cit.* p. 197, equations (56) and (57).

# EXPERIMENTS ON IMPACT*

## By J. P. ANDREWS, M.Sc., F.Inst.P.

*ABSTRACT.* This paper, which describes the continuation of a research upon the impact of soft metallic bodies, contains the results of four investigations, as follows: (1) Impact of equal spheres for low values of the velocity of approach $v$. The duration of contact is found to vary inversely as $v^{\frac{1}{3}}$, while the coefficients of restitution $e$ in the same cases are found to be unity for all speeds below a value characteristic of each material, as though the metals were perfectly elastic for smaller speeds. (2) The effect of duration of contact upon the size of the permanent deformations. No effect was observed. (3) The variation of duration of contact $t$ with mass of sphere at high speeds of approach. Within the limits of experimental error, $t$ varies as the square root of the mass, as theory predicts. (4) The impact of crossed cylinders. No important new phenomena are found.

---

## §1. INTRODUCTION

THE experiments to be described in this paper continue a previously published series of investigations† into the impact of soft metallic bodies. The ultimate goal of the research was the elucidation of the phenomenon of the flow of solids under pressure; the method employed, that of impact of pairs of similar spheres of soft metal, for in this method the phenomena are all of such brief duration that it is possible to neglect cumulative effects such as the elastic after-effect, etc. The duration of contact during collision, and the size of the flattened parts generally produced, afforded the data; and the chief results recorded in these previous investigations are summarised below and in figures 3 and 4.

(a) The duration of contact is related to the velocity of approach in the manner shown in figure 3. The empirical equation $t = t_0 - a\,v^n$, where $t$ is the duration of contact and $t_0$, $a$, $n$ are constants, fits these results fairly well, but smooths over the characteristic inward bend at $\alpha$. (b) The circular permanent deformations are bounded by a rim. (c) The diameters $d$ of these rims are related to the velocity of impact $v$ by the law $d = b\,(v - v_0)^m$ (see figure 4), where $b$, $v_0$, and $m$ are constants. When $v < v_0$, no deformations are produced.

These results, together with the discovery by C. V. Raman that the coefficients of restitution of solid spheres approach unity at very slow speeds of approach, were all explained in detail by a theory of impact‡ based on the following two fundamental principles: (1) That all the metals employed are perfectly elastic until the pressure exerted between them attains a value $p_0$ characteristic of the material; (2) that this pressure $p_0$ is never exceeded, any further mutual approach of the spheres producing plastic flow of the material.

$t$

$t_0$, $a$, $n$

$d$,

$v$, $b$, $v_0$, $m$

$p_0$

---

While the theory very satisfactorily explained all the results obtained, it was felt that the evidence for it was still deficient in one particular, namely the direct experimental verification of perfect elasticity for small stresses. To supply this deficiency, therefore, a more accurate method of investigating the variation of duration of contact with velocity of approach at very small speeds, is described in this paper. An additional assumption, implicit in the theory, that "time-effects" have no influence on the results owing to the extreme brevity of the impact, which is of the order $10^{-4}$ sec., had no experimental support: and this point also is dealt with. It was felt desirable also to test the consequences of the theory in some particular case, and for this purpose, experiments were performed at comparatively high speeds of approach (about 150 cm./sec.), when the duration of contact is primarily determined by the plastic properties of the metal, and defects due to the elastic reaction may be considered as secondary. The variation of the duration of contact with the mass of the spheres was investigated, though with some difficulty. Finally, experiments on the impact of crossed cylinders were tried, to find out whether the shapes of the bodies in contact had any important significance not taken into account in the theory.

## §2. EXPERIMENTS AT LOW SPEEDS

For these experiments it was essential that the velocity of approach should not exceed 1 or 2 cm./sec. and in any case should be less than that required to initiate permanent deformation. The method of measuring this speed consequently became very important. The method finally adopted was suggested by Raman's device for measuring coefficients of restitution at low speeds. The chief improvement adopted in the present case consisted in an accurate timing device, without which absolute measurement of velocity is impossible.

The image of a fine slit $S$, figure 2 ($a$), strongly illuminated from a pointolite $P$ is focussed at $M$ above the line joining the centres of the spheres. The further progress of the light is prevented, when the balls are touching, by two small pieces of mica $M$ attached to the little brass blocks to which the balls also are attached, figure 2 ($b$). When the balls are drawn apart, light passes through the lens $L$, figure 2 ($a$), and a magnified image of the gap at $M$ is produced on a photographic plate $F$. (In the diagram the rays are drawn for one point only in the gap at $M$.) A cylindrical lens— a thick glass rod—at $C$ concentrates the light into a fine line on the plate, and an electrically maintained tuning-fork $T$ cuts off the light 64 times a second. If the balls are withdrawn through a fixed small distance and the plate is pushed down by hand, it will show on development a series of fine lines of equal length. If, however, the spheres are slowly approaching, the lengths of the lines will slowly diminish, and after impact slowly increase, giving a negative such as those from which the prints of plate 1 were taken. To obtain the speed of approach, the negative is measured under low magnification; and the lengths of the lines are plotted as the ordinates of a graph whose abscissae are times measured in periods of the tuning-fork. Figure 5 shows a series of such graphs.

The slope of a line at the moment of impact determines the required velocity, since the magnification and the frequency of the fork are known; in the same way

the speed of separation may be measured. The prints in plate 1 are examples for three different speeds of approach. In practice, measurements were always made on the negative itself; by this means the velocities could be measured to an accuracy of 2 or 3 per cent.
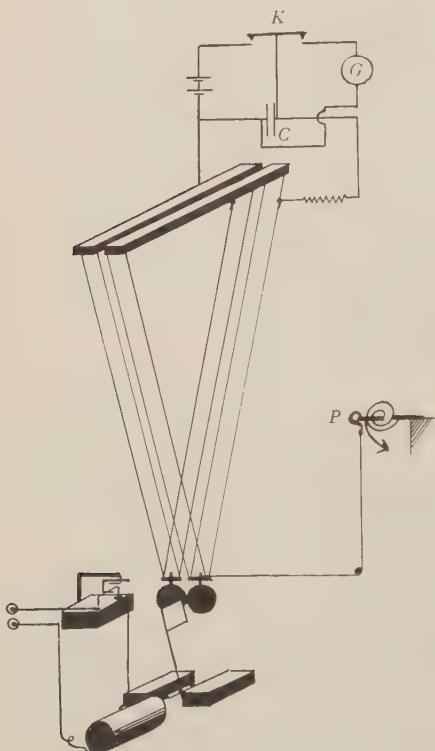


Fig. 1.  Diagram of apparatus, apart from the
          timing arrangement of Fig. 2 (a).
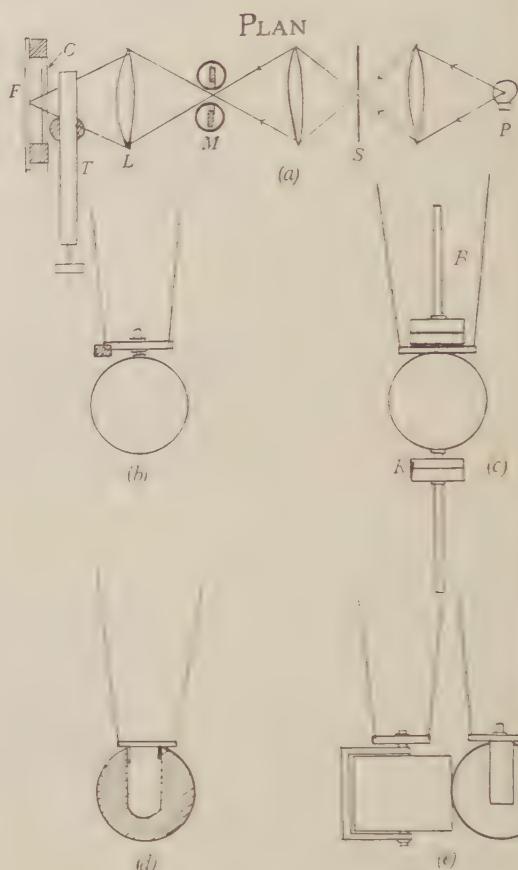
Fig. 2.

Connected to the spheres, figure 1, was an electrical circuit for measuring the duration of contact. When the spheres touched they partially discharged condenser $C$ through a resistance; and when the key $K$ was subsequently depressed to the right, the charge remaining passed through the ballistic galvanometer $G$ whose throw afforded a means of calculating the time of contact.

The results are rather more scattered than the method seems to justify. In order to test the reliability of the electrical circuit, the balls were separated and the condenser charged and immediately discharged. This process was repeated in one experiment twelve times, care being taken that all other conditions were those which would obtain in an actual observation. The average deflection was 33·767, the mean deviation from the average was 0·019, and the maximum deviation 0·033.

This indicates that the electrical circuit is not to blame for the scattering. The optical arrangement suggests one possible source of chance variation. The distance between the balls and the lens $L$ may vary slightly. The change in the magnification produced by an alteration of 1 mm. in this distance is about 0·01, or about 1 in 600; this cannot therefore account for the effect. The conclusion must be that the spheres differ slightly at different parts of their surfaces in regard to either shape or elastic properties. This has been fairly obvious throughout the work on impact; in the case of aluminium the surface was pitted with minute cavities, while with Babbitt's metal a lens revealed small crystals of dark substance (possibly antimony) scattered
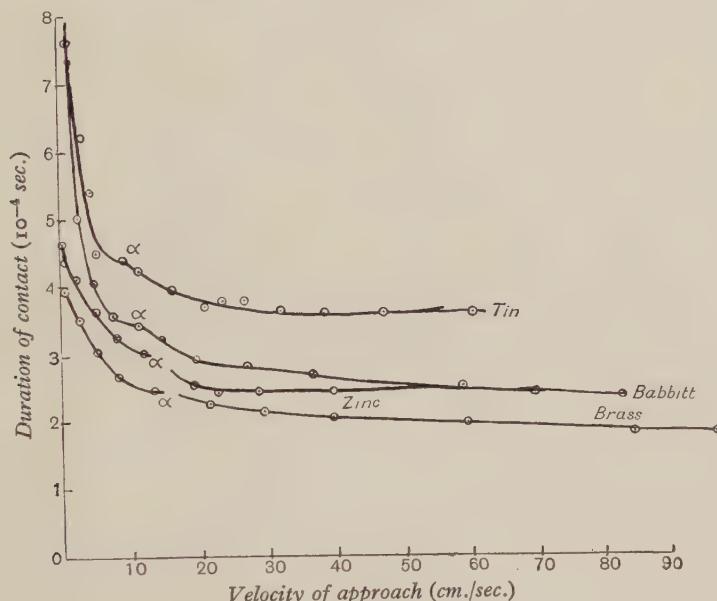


Fig. 3.

through the material. The speeds of approach are so small in the experiments that the maximum area of contact is small, and the method becomes one which deals with minute samples of the material in which small variations do not average out.

The results were treated as follows. From the electrical circuit we know that

$$t = RC \log_e (\theta_0/\theta),$$

where $R$ is the resistance in series with the spheres, $C$ the capacitance of the condenser, $\theta_0$ the deflection of the galvanometer on immediate discharge, $\theta$ after the spheres have collided. If $R$ remains constant throughout a series of experiments on a pair of spheres,

$$t = k_1 \log_{10} (\theta_0/\theta),$$

where $k_1$ is a constant. Now, according to Hertz's theory,

$$t = k_2 v^{-\frac{1}{5}},$$

$R, C$

$\theta_0, \theta$

$k_1$

$v$

where $v$ is the velocity of approach. Let us suppose that in these experiments $t = k_2 v^{-n}$. Then we have the relation

$n$

$$\log \log (\theta_0/\theta) = -n \log v + \text{const.}$$

The value of the constant depends upon the radius of the spheres, their mass and elastic properties, and the constants of the electric circuit. We are not at present concerned with its value.

If then we plot $\log \log (\theta_0/\theta)$ as ordinate and $\log v$ as abscissa, the slope of the graph gives $n$. Typical graphs are shown in figure 6.

The results for the materials investigated are tabulated in the second column of table 1, the value of $n$ having been calculated from the observations by the method described by J. H. Awbery*.

Table 1

| Material | $-n$ | $e$ and mean deviation |
|---|---|---|
| Aluminium | 0·21 | 1·00 ± 0·013 |
| Zinc | 0·20 | 0·99 ± 0·005 |
| Lead-Tin | 0·21 | 0·97 ± 0·06 |
| Babbitt | 0·20 | 1·00 ± 0·018 |
| Brass | 0·21 | 1·00 ± 0·024 |

$e$

In the case of tin the values of the coefficients of restitution $e$ showed that small permanent deformations were being produced down to about 0·3 cm. sec., although these were not visible. Figure 6 $a$ illustrates this. The variation is like that found previously by Raman.

The coefficients of restitution were investigated and these, like the results just recorded, varied somewhat. Table 2 gives a typical list of results, while in the third column of table 1 are the mean values of these coefficients and the mean deviations for the various materials. The coefficients cannot of course actually exceed 1·00 but they are recorded as measured, to indicate the order of accuracy of the method.

Table 2. Coefficients of restitution for brass

| Speed of approach | 0·39 | 0·57 | 0·55 | 1·08 | 1·18 | 1·65 | 1·49 | 1·72 | 2·04 | 2·22 |
|---|---|---|---|---|---|---|---|---|---|---|
| $e$ | 1·02 | 1·02 | 1·00 | 0·95 | 1·02 | 0·93 | 1·00 | 1·04 | 1·00 | 1·02 |

The evidence is decidedly in favour of perfect elasticity at very low speeds, the deviations of $n$ from $-\frac{1}{5}$ and of $e$ from 1·00 being of the same order as the experimental error.

### §3. VARIATION OF DURATION OF CONTACT WITH MASS OF SPHERE, AND INVESTIGATION OF TIME EFFECTS

The best manner of increasing the mass of the spheres, while keeping other variables constant, was considered to consist in the loading of the spheres with riders. Rods $B$ were screwed into the spheres, figure 2 ($c$), and brass weights $R$ (50 gm. each) were fixed thereon. When the experiments were performed, however,

* J. H. Awbery, *Proc. Phys. Soc.* **41**, 384 (1929).

Fig. 4.



Fig. 5.

# J. P. Andrews
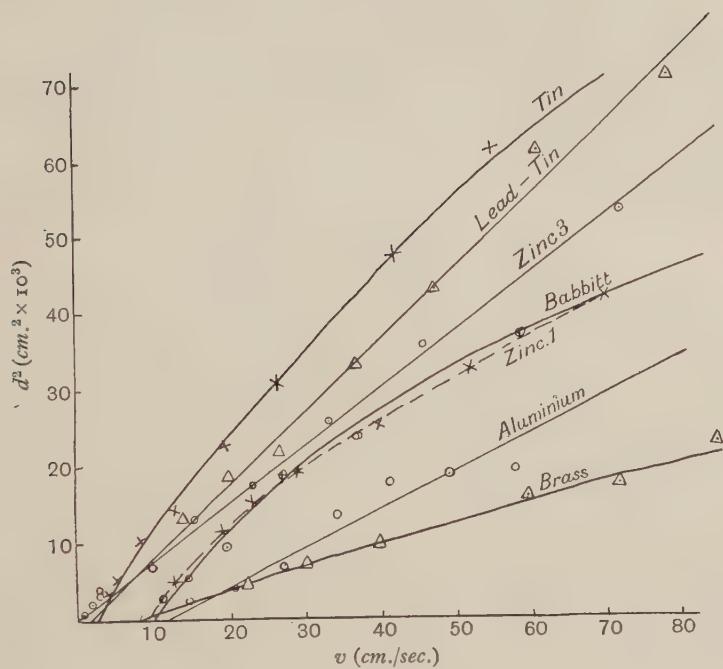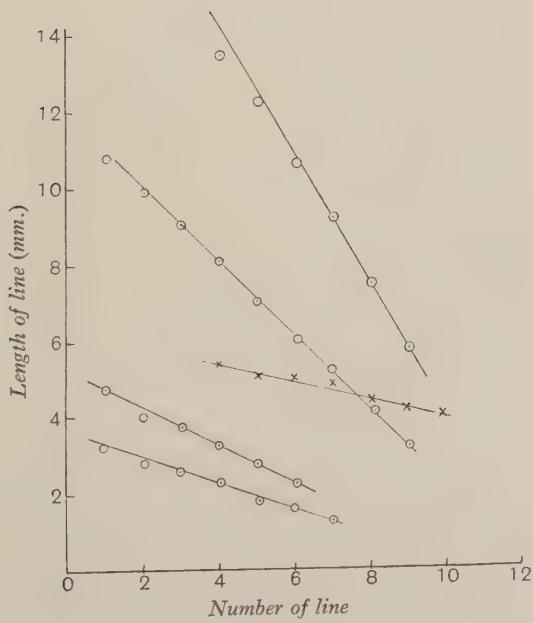
it was soon discovered that a vitiating effect had been introduced. The impact appears to have generated a transverse oscillation whose half period controlled the duration of contact, just as the longitudinal vibrations in a long rod govern that duration. In order to test this matter, one rider above and one below each sphere
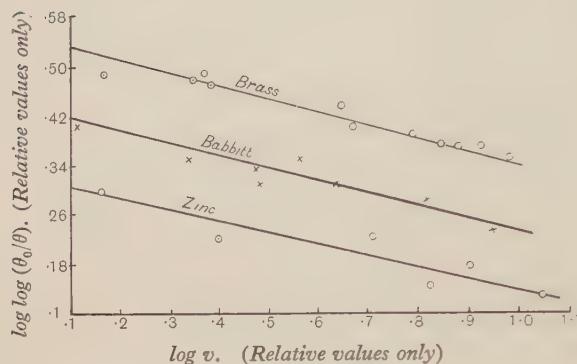


Fig. 6.
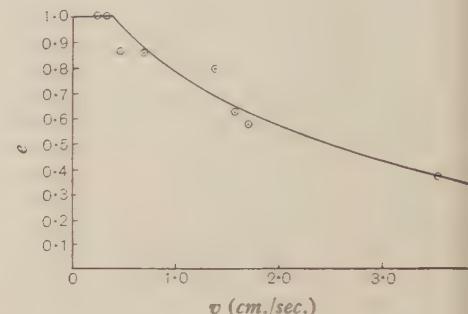
Fig. 6 a.
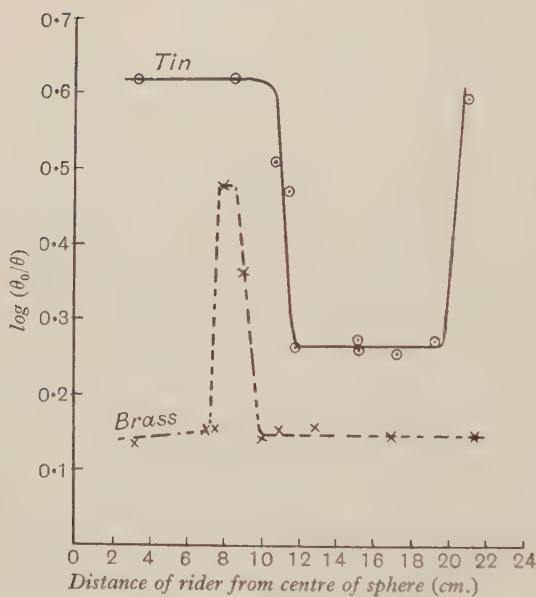


Fig. 7.
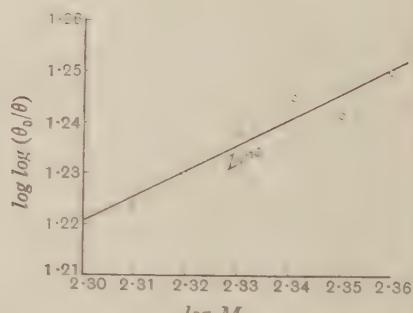
Fig. 8.

were used, and the velocity of approach being kept constant, the distance of the riders from the centres of the spheres was varied. The duration of contact was then observed. The graphs, figure 7, show that the tendency was for the duration to remain unchanged up to a certain position of the rider, then to pass suddenly to another position, and finally to return. If we call the ratio of the two durations $T$, and let $L$ be the ratio of the total length of rod $R$ to the length between sphere and

rider when the first sudden change occurs, then for brass $T = 3\cdot2$, $L = 3\cdot3$, and for tin, $T = 2\cdot4$, $L = 2\cdot2$. This suggests that the rod tends to vibrate so that the rider is at a node, the upper and lower ends of the rod being antinodes; and the duration of the contact is determined by the period of this vibration. This effect was employed to investigate the influence of longer or shorter contact on the size of the deformations. Times varying in the ratio 3 : 1 were thus obtainable. Upon measurement of the deformations, no significant difference was observable in their size. Table 3 is typical.

Table 3. Deformation of tin

| Duration of contact × 10⁻⁴ (sec.) | 7·0 | 3·17 | 3·13 | 3·02 | 3·22 | 2·96 |
|---|---|---|---|---|---|---|
| Diameter of deformation (cm.) | 0·397 | 0·356 | 0·388 | 0·385 | 0·377 | 0·395 |
| Duration of contact × 10⁻⁴ (sec.) | 7·32 | 7·35 | 3·09 | 6·02 | 5·59 | — |
| Diameter of deformation (cm.) | 0·387 | 0·352 | 0·355 | 0·365 | 0·357 | — |

We may therefore conclude that only negligible differences are made to the results by longer or shorter duration of contact.

The problem of variation with mass now becomes more difficult, since any arrangement for carrying riders involves a risk similar to that which has just been discussed. The only safe method appears to be the hollowing of the spheres and subsequent filling with heavy material. The range of variation of the mass is thereby made very restricted, however; for if the hollowing is carried too far, the sphere will vibrate as an elastic shell. Figure 2 (*d*) shows the dimensions finally adopted for the boring. An experiment on duration of contact was tried first with the spheres empty: then with an increasing quantity of lead shot, fixed with paraffin wax poured in hot. (After the wax had been inserted, 40 minutes were allowed to elapse before an observation was taken, so that temperatures should recover.) The speed of approach, kept as constant as possible, was made large—of the order 150 cm./sec.—so that plastic properties were most important. Under these circumstances, the duration of contact $t_0$ is given by

$$t_0 = \pi/2 \, (M/\pi R p_0)^{\frac{1}{2}} \text{ approximately} \qquad \ldots\ldots(1).$$

Experiment has already shown that at these high speeds the duration $t$ is practically a constant. All metals were known to behave similarly, so only three were investigated, namely aluminium, zinc and tin. In figure 8 is a typical graph, in which log log $(\theta_0/\theta)$ is plotted against log $M$. The slopes calculated for the three cases are given in table 4. They would all be 0·50 if equation (1) held good.

Table 4. Values of $x$ where $t = kM^x$

| Substance | Aluminium | Zinc | Tin |
|---|---|---|---|
| $x$ | 0·52 | 0·49 | 0·53 |

The restricted range of variation of the masses accounts for the deviation from 0·50.
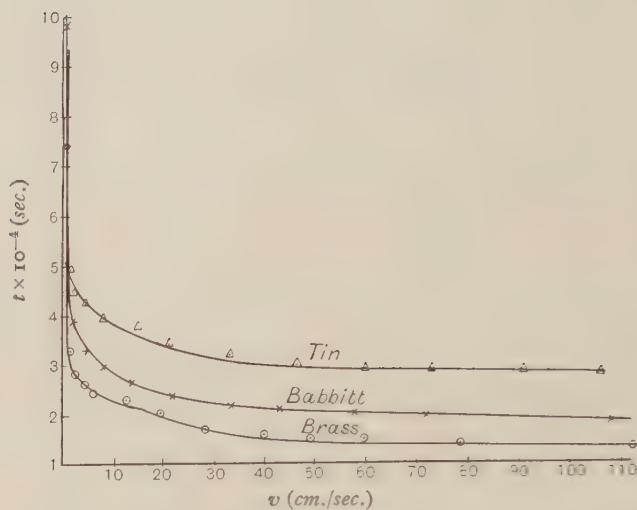
Fig. 9. Duration of contact and velocity of approach (cylinders).
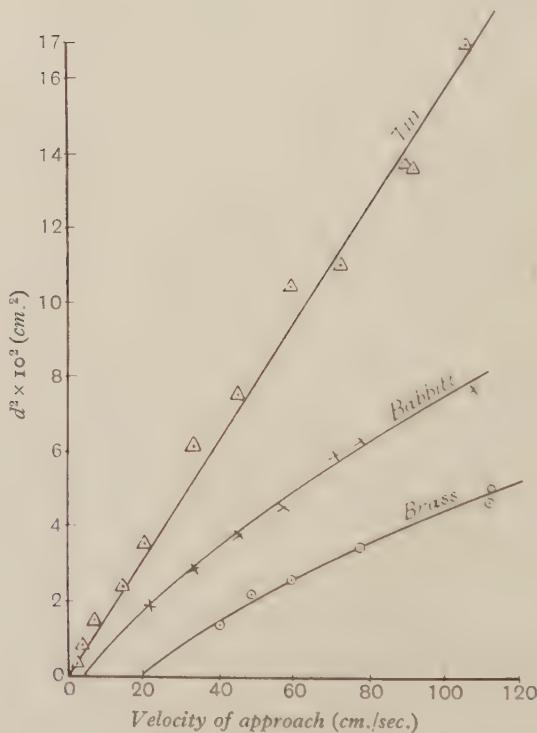


Fig. 10. (Diameter)² and velocity of approach (cylinders).

## §4. EXPERIMENTS ON CROSSED CYLINDERS

The theory was based upon experiments on spheres only, and there remained a possibility that some essential part of the variation of duration of contact and of size of deformation may have been due to shape of surface. Two equal cylinders of radius 2 cm. were therefore taken, one suspended with its axis vertical the other with its axis horizontal as in figure 2 (*e*), and the time of contact, etc. were investigated. The same precautions were taken to present a fresh surface at every collision. Nothing new emerged from these experiments, and their results are represented graphically in figures 9 and 10.

The conclusion may be drawn that while the value of the duration of contact may depend on the shapes of the surfaces, its variation with velocity does not change in any fundamental manner when the shapes of the surfaces are altered. The variation of the size of the permanent deformations also follows no new law.

## §5. CONCLUSION

The experiments justify the assumption of perfect elasticity at low speeds and the neglect of any cumulative effect due to the differences in the times of contact. The variation in this time for different colliding masses is in accordance with the theoretical results, and when the shape of the colliding surfaces is changed from spherical to cylindrical no new factor is introduced.

## §6. ACKNOWLEDGMENT

My thanks are due to Prof. C. H. Lees both for the facilities given me for the work and for advice during its progress.

## DISCUSSION

# OBSERVATIONS ON PERCUSSION FIGURES*

## By J. P. ANDREWS, M.Sc., F.Inst.P.

*Received May 8, 1930. Read and discussed October 17, 1930*

*ABSTRACT.* The formation of percussion figures by the pressure of a steel ball on glass blocks is here traced out, and an investigation suggested by this exploration elicits the following facts: (1) The diameter of the innermost circular or part-circular crack remains constant for one specimen of glass, and is independent of the maximum pressure exerted by the ball on the glass. (2) The diameter of the outermost circular or part-circular crack varies with the maximum pressure in a manner which suggests that the crack tends to keep to the outer edge of the area of contact. (3) No crack is formed until the pressure exceeds a value characteristic of the glass. A method of testing the fragility of glass is developed: and finally some observations on percussion figures upon spherical surfaces are mentioned.

## § 1. INTRODUCTION

THE principal names associated with the study of percussion figures—the ring-formed cracks produced when a steel ball is pressed into, or is allowed to fall upon a flat glass block—are those of C. V. Raman†, K. Banerji‡, and J. W. French§. The characteristics of such figures, as described by these observers, may be summarized thus. A plane circular area is surrounded by a double ring-crack, the annulus enclosed between the rings often being broken up by cross cracks. The diameters of the internal and external rings increase with the final static pressure upon the steel ball, or the height from which it is dropped (Banerji), the external ring being roughly coincident with the circumference of the area of contact as calculated by Hertz's theory for perfectly elastic bodies. The plane area within the rings is at a slightly lower level than the surrounding glass, which is heaped up into a minute rim just outside the annular region (Raman). The two cracks extend into the interior of the glass, forming circular truncated cones with bases below the glass surface.

## § 2. PROCESS OF FORMATION OF PERCUSSION FIGURES

During some work on the collision of spheres of soft metals I had met with percussion figures of a different kind, namely the flattened patches formed when two spheres of such metal collide. An outstanding characteristic of these circular patches was the thread-like rim surrounding each of them; and a less prominent feature, not invariably visible, was the convex curvature of the surface within this rim. Comparison with the glass percussion figures of Raman was suggested, and experiments

---

PLATE 2

(a)

(b)

(c)

(d)

(e)

(f)

(g)

(h)

(i)

(j)

were made with two objects in view, namely (1) to investigate the somewhat surprising observation of Banerji that the diameter of the internal crack varies with the final static pressure, or the height of fall, and (2) to find how far the character of percussion figures on glass throws light upon the formation of similar figures on metal spheres.

In figure 1 is plotted an example of Banerji's observations, showing how the two diameters were found to increase with the height of fall of a steel ball on a glass block. Such a result seems to imply that the crack was formed at the moment of recoil of the sphere. Similarly, for static pressure, if Banerji is right, the crack must have been formed as the pressure was released. An attempt to demonstrate this with
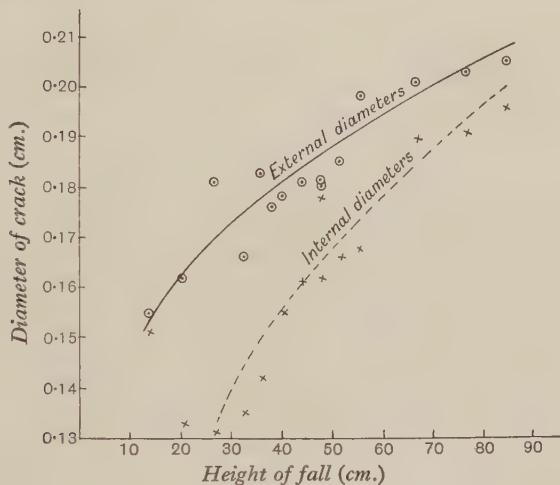


Fig. 1.

static pressure threw light on the problem. A crack does not form all at once, but starts at one point or simultaneously at several points on the surface. If a block of glass is carefully pressed in a parallel-jawed vice against a steel ball, the genesis and development of the crack may be watched through the side of the block. Figure (a) of plate 2 shows what is usually seen for a moderate pressure*. A click is sometimes heard when the glass cracks, and one cannot always see where the breakdown has occurred. Thus, in the case of (a), which promised a perfectly circular crack, when the pressure was released only two or three short cracks were found, of which (b) is the photograph from the top of the plate. This view from above may, however, tell only part of the story. The cracks which appear are often remarkably black, a fact which probably indicates an actual gap in the glass: and it is conceivable that the fracture extends further than appears. I have indeed succeeded in one or two instances in reflecting light from a surface inside the glass which did not end in a visible crack on the surface: while in one case, while the fracture was being examined between crossed nicols, a short crack appeared to continue in a thread of

* The upper half is the reflected image of the lower half.

light through a much larger arc of a circle. In many instances, however, the development of the crack is easier to follow, and in the set of magnified photographs from (c) to (i) is recorded a particularly marked case, much more pronounced than is usual. The series is intended to show how a horn-shaped crack, starting on the left, extends as the pressure is increased, finally finishing in a roughly-shaped complete ring-crack. The view of this crack from above, after removal of the ball, is figure (j). There follows, in plate 3, a number of magnified photographs of the surface cracks seen from above, varying from simple to highly complex, and formed, some by static pressure, some by the dropping of the ball from a height. No essential difference was observed in the two cases: but all the photographs show evidence of the development of the rings from one or more points, from which curved cracks have set out.

Inspection of a large number of "figures" suggested that their formation proceeded as follows. When the stress responsible for the fracture (almost certainly shear stress) has reached a value characteristic of the glass, a breakdown occurs at one or more points. The cracks thus formed will tend to be arcs of circles, since stresses are symmetrical about the area of contact, but the relaxation brought about by the fracture will mean a redistribution of stress. The tendency will now be for the crack to "run" along the line of maximum stress, and this line will depart from the circular from two causes: (i) the new distribution of stress due to the existence of the crack; (ii) the new position of the maximum stress as the ball presses into the glass. If therefore the crack is able to follow the maximum stress, it will not be circular. If, however, for any reason it is prevented from doing so, it may follow a more nearly circular outline for a short time, and then branch off so as to bridge the distance between its present position and that of the line of maximum stress. If fracture has begun at several places, a development of each crack in this manner is to be expected, giving rise to the complicated figures found in practice. The importance of this view derives from the fact that for one piece of glass fracture may be expected when and where the maximum stress reaches a definite characteristic value. If the process of development of the crack is that just described, the first cracks should approximate to arcs of circles with the same radius, no matter what the height of fall of the ball or the final static pressure applied to it.

On the other hand, the largest external diameter of the crack system would vary: and if the glass behaved in a perfectly elastic manner up to the time of fracture, we should anticipate—as others have anticipated—that this diameter would approximate to the diameter of the circle of contact calculable from Hertz's theory, for at the circumference of this circle the shear stresses are greatest. There is, however, little point in calculating these diameters of contact, since the elastic constants required are generally not known and are not easy to find. A more reliable test is obtained by plotting a graph to find whether the diameter varies as the $\frac{2}{3}$-power of the height of fall, as Hertz's theory predicts.

## §3. EXPERIMENTAL RESULTS

A series of observations was obtained where a 1-inch steel sphere was dropped on to a glass block from heights varying from 5 cm. to 45 cm. These observations are shown in figure 2, where the crosses represent the smallest diameters of the innermost cracks and the circles the largest external diameters. The line through the circles represents the variation required by Hertz's theory, on the assumption that the shear stress is greatest at the edge of the circle of contact.

The important fact emerges, that the smallest internal diameter is constant, and this no doubt measures the least stress required to produce fracture. The external cracks do roughly follow the law required by Hertz's theory.

The interest attaching to the constancy of the internal diameter is twofold. In the first place, we might use this method to test the "fragility" of specimens of glass. In the second place it affords a further means of investigating the process of compression. As a simple deduction from geometrical similarity, one would expect,
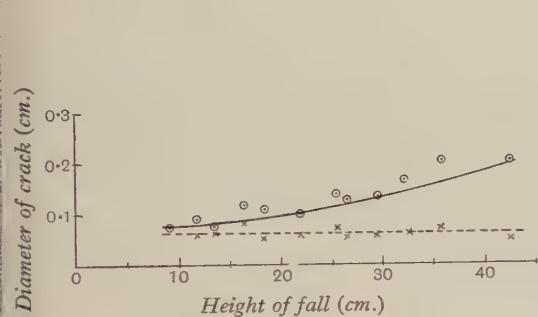


Fig. 2.
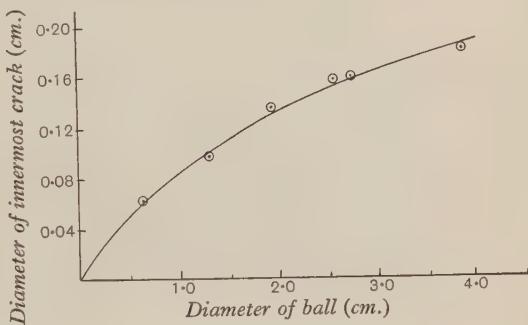


Fig. 3.

for example, the diameter of the smallest crack to be proportional to the diameter of the sphere used in producing it. Figure 3 shows the results of an experiment on these lines. For the larger balls, the crack is smaller than would be expected. The explanation probably depends on two factors: (1) since the first break-down probably occurs at a point where the glass is slightly weaker, the chance of the occurrence of the necessary flaw will be more nearly proportional to the area of contact, and hence to the square of the radius of the ball; (2) these cracks are associated with a rim formed just beyond, and due in an indirect way to, the volume of glass displaced inwards by the pressure of the ball. This volume is proportional to $R^3$, where $R$ is the radius of the ball. The circumference of the rim will be roughly proportional to $R$, so that we may consider the tendency to form a rim to depend on $R^2$. Large shear stresses are formed in the neighbourhood of the rim. We are thus led to suppose that the diameter of the crack should vary as some power of $R$, less than unity. A logarithmic plot shows the actual power to be 0·63 in this instance.

We return now to the other aspect, "fragility" or "brittleness"—terms which are preferable to "hardness," on account of the rather different phenomenon described. Five samples of optical glass were obtained from Messrs Chance. The

names of these glasses and their approximate chemical compositions, for which I am indebted to Messrs Chance, are given in table 1.

Table 1. List of chemical compositions of glass specimens

| | HC. | DBC. 5804 | DF. 5374 | EDF. 5909 | EDF. 5570 |
|---|---|---|---|---|---|
| | (%) | (%) | (%) | (%) | (%) |
| $SiO_2$ | 72·5 | 37·6 | 46·4 | 42·0 | 40·8 |
| $K_2O$ | 10·7 | 5·9 | 3·7 | 5·3 | 5·3 |
| $Na_2O$ | 6·0 | — | 2·5 | — | — |
| CaO | 10·8 | — | — | — | — |
| BaO | — | 44·7 | — | — | — |
| $Al_2O_3$ | — | 3·7 | — | 0·2 | 0·2 |
| ZnO | — | 6·8 | — | — | — |
| $Sb_2O_3$ | — | 1·3 | — | — | — |
| PbO | — | — | 47·4 | 52·3 | 53·5 |
| $As_2O_3$ | — | — | — | 0·2 | 0·2 |

Two kinds of experiment were performed on each block. Firstly, a $\frac{3}{4}$-in. ball was dropped from a number of different heights, each sufficiently great to cause a crack, and the smallest diameter of the innermost crack was measured microscopic- ally. For every sample, this diameter had no regular variation with height of fall of the sphere, but appeared nearly constant as in the case already described. The mean diameters are recorded in the second column of table 2 in scale divisions of the microscope (570 scale divisions = 1 cm.). It will be noticed that a considerable dif- ference exists between the different samples.

Table 2

| Glass | Diameter of innermost crack | Least height of fall to form crack |
|---|---|---|
| | (divs.) | (cm.) |
| DBC. | 89·7 | 21·1 |
| EDF. 5570 | 80·3 | 9·0 |
| HC. | 78·3 | 7·4 |
| EDF. 5909 | 77·3 | 6·58 |
| DF. | 75·3 | 5·3 |

Secondly, a steel ball was dropped from varying heights above the glass surface, until the height just sufficient to form a crack was found. In order to obtain greater distances to measure, a smaller ball, half an inch in diameter, was used. The ad- justment was found to be surprisingly sharp, and a critical distance of, say, 15 cm. could be estimated to within 2 mm. The cracks formed by a fall from a height just greater than this were naturally very small, and could rarely be detected from the upper surface of the specimen. The smallest cracks become visible as bright specks, however, when the block is held up to the light and the observer looks through one of the sides. Total reflection then occurs at the fissure, and the crack is observable. In the last column of table 2 these minimum heights are recorded. The table

emphasizes two points, namely (1) that both methods arrange the samples in the same order; (2) that the second method is much more sensitive.

We should anticipate this last fact from general considerations: for consider the cognate case where a number of spheres of different diameters are dropped upon a single sample of glass, the two experiments just described being performed for each sphere. Then, on the supposition that Hertz's theory may be applied, it may be shown that the innermost diameters vary as the $\frac{2}{5}$-power of the least height. We cannot predict what exact relation ought to hold in the case of the actual experiment, because the elastic constants will vary in an unknown manner. In figure 4 the two
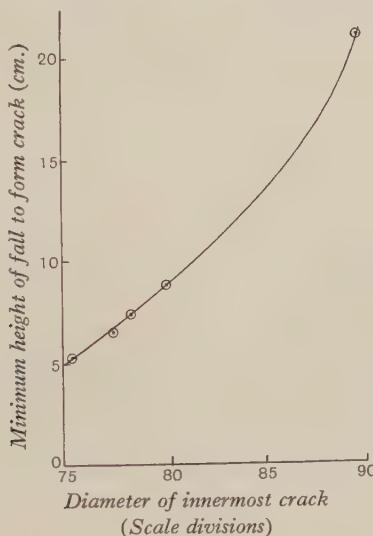


Fig. 4.

measurements are plotted one against the other, and are found to fall on a regular curve. If $F$ is the least height of fall and $d$ is the innermost diameter, in cm., the results are fairly well represented by the formula

$$F = 6\cdot83 \times 10^7 . d^{8.1}$$

which brings out the greater sensitivity of the minimum height method. The formula also gives an interesting item of new information about glasses in general. The maximum depth of penetration of the steel ball when falling from a given height is governed chiefly by Young's modulus for the glass. The critical depth of penetration at which the first crack appears probably depends on the shear strength of the glass: and there is no *a priori* reason for supposing that these two should vary together, at least in any simple fashion, in passing from one kind of glass to another. The formula indicates that they do so, nevertheless.

The reciprocal of $F$ or of $d$ might be employed as a measure of the "fragility" or "brittleness" of the glass. This is of practical interest, for according to J. W. French the action of abrasives is of the same character as that exerted by spheres when forming percussion figures. In optical glassworks measurements of the "hard-

ness" of the glass are sometimes made by measurement of the quantity of abrasive required to remove a measured quantity of glass. This operation could be profitably replaced by the much simpler measurement of $F$.

When the second object of the research was entered upon, close observation did not encourage much hope that percussion figures in glass would throw light on the formation of similar figures in metals. The following experiment was tried, nevertheless. A glass sphere about one inch in diameter was dropped, or thrown with force, on to a hardened steel anvil, in order to form percussion figures. The object was to simulate the case of two exactly similar glass spheres colliding, in which the surfaces of contact must be depressed to form planes during the collision. The very small yielding of the hardened steel ensures that the surface of contact shall be very nearly plane, and enables experiments to be performed much more easily. Examination of the figures revealed no new feature about the cracks. The curvature of the surface within the cracks was carefully compared with that outside in a number of cases: in each case these two were equal. It is known that the surface of a flat glass plate depressed by a spherical body is flat after the process. These two observations tend to show that the material remains elastic, in the sense that no permanent deformation is produced, up to the moment of fracture. This does afford a point of contact with the case of metal spheres colliding. There is reason to believe that up to the moment of definite breakdown, or flow, under pressure, the metal behaves as though perfectly elastic. Beyond this no further analogy was found. It is true that in a number of instances the metal percussion figures exhibited a rim and a central convex region. A magnified photograph, taken from an oblique direction, of two such deformations, both formed at the same collision, shows this convexity by the disposition of the shadows: see plate 3 (*g*) and (*h*). But whereas mainly the shear stresses are operative in the case of glass, it is almost certain that longitudinal or volume compressions are at the root of the phenomenon in the case of metals.

## §4. CONCLUSIONS

The results attained may now be summarized. We have shown that the diameter of the innermost crack remains constant for the same specimen of glass and the same ball. This constant diameter varies, however, according to the power 0·63 of the diameter of the ball. The distance between extreme external cracks, a measure of the diameter of the outer ring, justifies their association with the circumference of the greatest circle of contact of ball and block. When different specimens of glass are tested by this method and by the measurement of the minimum height of fall necessary to cause fracture the samples are graded in the same order of fragility or brittleness. Percussion figures upon glass spheres were unable to throw important new light on the problem of impact of metal spheres.

(a)

(b)

(c)

(d)

(e)

(f)

(g)

(h)

# DISCUSSION ON THE PRECEDING THREE PAPERS

Dr J. H. VINCENT. I congratulate the author on the great experimental skill which he has brought to bear on this subject, especially as regards the remarkably neat arrangement for determining the circumstances of impact for very small velocities of approach.

Mr T. B. VINYCOMB said that circular markings found in museum flints had at first been ascribed to organisms, in view of their definite minimum size. Some of them had, however, been found to be of recent origin and to have been caused by the impact of waves, the minimum diameter of the markings having different values for different materials. The fracture is conical, the section of the cone decreasing from the surface inwards down to a certain size, whereupon the angle of the cone undergoes an abrupt change.

Mr A. F. DUFTON. On reading the proofs of the first and third papers I was curious to know what Hertz wrote on the subject and found that the percussion figures were described by him in 1882. Hertz measured the hardness of a body by the normal pressure per unit area which must act at the centre of a circular surface of pressure in order that in some point of the body the stress may just reach the limit consistent with perfect elasticity. From the pressure necessary to produce the first crack and from the size of the crack he determined the hardness of glass, obtaining for mirror glass the value 130 to·140 kg./mm.[2].

In the first paper Mr Andrews determines for a practical case the pressure at the centre of the area of contact and states that the total force could be calculated by integration. As Hertz showed, the average pressure is two-thirds of the pressure at the centre; the integration need not be performed for individual cases.

Mr B. P. DUDDING. I wish to associate myself with Dr Vincent in congratulating Mr Andrews on the simplicity and accuracy of the method employed to determine the velocity of approach. I am sure that glass technologists will be interested to note the suggested relationship between the data given in the paper and the hardness tests usually employed in the glass industry. I suggest that the author should state whether the glass specimens were annealed or not, as that would be expected to affect profoundly any comparison of glasses having similar compositions. (See tables 1 and 2, p. 22.)

Mr T. SMITH suggested that the author might care to refer to some interesting photographs published by J. W. French in the *Journal of the Optical Society*.

AUTHOR'S reply. I should like to thank Dr Vincent and Mr Dudding for their appreciative remarks. The curious markings on pebbles mentioned by Mr Vinycomb are, from his description, percussion figures of the same kind as those I have dealt with. I am unable to state whether or not the blocks of glass were annealed; but since they were in a condition suitable for final polishing it seems probable that they were. I am grateful for Mr Dufton's reminder of Hertz's original work. Hertz says that he made a few experiments, but scarcely any detail is provided. Except therefore for the mention of that work, the present paper is an account of additional information about a phenomenon first brought prominently into notice by Sir C. V. Raman.

# THE ABSORPTION AND DISSOCIATIVE OR IONIZING EFFECT OF MONOCHROMATIC RADIATION IN AN ATMOSPHERE ON A ROTATING EARTH

## By S. CHAPMAN, M.A., D.Sc., F.R.S.

*ABSTRACT*. The absorption of monochromatic radiation from the sun in an atmosphere of which the density varies exponentially with height is considered; the energy of the radiation, or a definite fraction of it, is supposed to dissociate or ionize the air, and the dissociation products are supposed to recombine with one another only, and not to diffuse away from the element in which they were formed. The resulting distribution of density of the dissociation products is determined, a constant recombination coefficient being assumed, while account is taken of the variation in rate of dissociation due to the earth's rotation. The results are illustrated by numerous diagrams, showing the density of the dissociation-products as a function of height, time, latitude and season.

## § 1. INTRODUCTION

THE main object of this paper is to consider the following idealized problem:
(a) A uniform beam of monochromatic radiation from a sun falls upon a rotating earth, the rate of rotation of the earth and the changing declination of the sun being the same as for the actual earth and sun; the radiation is absorbed (before reaching the ground) in an atmosphere of uniform composition, in which the density varies exponentially with height. (b) The absorption of radiation at each point is proportional to the air-density and the intensity of the radiation reaching that point. (c) The energy of the absorbed radiation, or a constant fraction of it, is expended in dissociating some constituent $A$ of the air into two components $A_1$, $A_2$ which may be electrically neutral or not. (d) The two components recombine with one another (alone) to re-form $A$, at a rate $\alpha n^2$, where $\alpha$ is a constant independent of height and time, and $n$ is the number of $A_1$ or $A_2$ particles per unit volume. (e) The particles $A_1$, $A_2$ do not move from the element of volume in which they were formed.

The problem is to determine (f) the rate of absorption and dissociation or ionization at each point, as a function of height, time of day, season of year, and latitude, and (g) the value of $n$ at each point, as a function of the same variables.

This problem is easy to formulate in mathematical terms, and the differential equations can be partly, but not fully, integrated; at a certain point it is necessary to resort to numerical calculation. A feature of the present treatment is that, by suitable choice of units, the analysis and discussion are expressed in general terms, without the assumption of any special values for the numerical quantities involved, until the

latest possible stage; when this can no longer be avoided, particular numerical values are considered, but, even so, the differential equation is written so that only a single constant ($\sigma_0$, § 9) comes in question. This procedure makes it possible to apply the present analysis and results to different types of radiation (which may be absorbed at different levels in the atmosphere, and have different dissociative or ionizing effects) when the particular numerical data for each such case become available.

On the other hand, the problem is an ideal one which will scarcely represent adequately all the factors of importance in any actual case. It is thought likely, however, to be of value as an approximation, and as a starting point for further investigation into the influence of factors here neglected.

The number of independent variables involved is four, namely height, time of day, season of year, and latitude; this renders it difficult to gain a comprehensive view of the results. It has seemed most convenient to represent them graphically, rather than by numerical tables, though a considerable number of diagrams are required, each of which includes several curves. Figures 1–5 relate to the absorption and rate of dissociation or ionization; Figures 6–11 represent $n$ as a function of the time of day, for various heights, seasons, and latitudes (for the three adopted values of $\sigma_0$). The seasons considered are midsummer, midwinter, and the equinoxes; the latitudes are 0° (the equator) and 60°.

In § 14 the results are briefly considered in relation to the ionization of the upper atmosphere, though as regards the conditions (*d*) and (*e*) the present problem only approximately illustrates the ionization changes. But as this is the most interesting application of the results at the present time, the whole paper has been written as though the dissociated components $A_1$ and $A_2$ were ions and electrons; by merely verbal changes the discussion could be expressed relative to the corresponding dissociation phenomena in which $A_1$ and $A_2$ are neutral atoms or molecules.

## § 2. THE RATE OF ION-PRODUCTION

Consider a point $P$ at height $h$ above the ground at an angular distance $\theta$ (the colatitude) from the north pole. Let $t$, or $\phi$, denote the local time reckoned from noon, that is, the longitude of $P$ measured eastward from the noon meridian at the instant, $\phi$ being in angular measure (radians), and $t$ in time-measure (seconds). Clearly $h, \theta$ $t, \phi$

$$t = 86400\ \phi/2\pi = 1\cdot37 \cdot 10^4\ \phi, \qquad \ldots\ldots(1),$$

there being 86400 seconds in a day.

Over the range of level considered, the density of the atmosphere will be supposed to vary exponentially, i.e. $\rho = \rho_0 \exp(-h/H)$, where $\rho_0$ is the density that would exist at ground level if the formula were valid at all heights. In the actual atmosphere this formula is valid only if $H$ itself is a slowly varying function of height, but the probable variation over the range of level that is important in this investigation is not great, and may in a first approximation be neglected. Constancy of $H$ would result if the atmosphere were of uniform composition and temperature, but these conditions are only sufficient, not necessary. When they are fulfilled, $H = kT/mg$, $\rho_0, H$

$k, T, m, g$

where $k$, $T$, $m$ and $g$ denote respectively Boltzmann's constant $1 \cdot 37 \cdot 10^{-16}$, the absolute temperature, the mean molecular mass, and the acceleration of gravity; for example, if $T = 300°$ and the composition is the same as in the lower atmosphere (mainly nitrogen $N_2$ and oxygen $O_2$), $H = 8 \cdot 4$ km. This figure may be borne in mind in considering the following results, which, however, are independent of any particular numerical value of $H$, because heights will in general be expressed in terms of $H$ as unit. It is quite possible that, above 100 km., the value of $H$ differs from $8 \cdot 4$ km., but the value, when found, can at once be applied to the results of the general theory here given. The theory may also be relevant to different strata in the atmosphere, for which $H$ has different values.

$h'$

Thus, when $H$ is taken as the unit of height, $\rho = \rho_0 \exp(- h')$, where $h' (= h \, H)$ denotes height measured in this unit.

## § 3. THE INCIDENCE OF THE RADIATION

$\chi$

Since the sun is on the noon meridian, its zenith distance $\chi$ at $P$ is given by

$$\cos \chi = \sin \delta \cos \theta + \cos \delta \sin \theta \cos \phi \qquad \ldots\ldots(2),$$

$\delta$

where $\delta$ denotes the north declination of the sun.

At the equinoxes $\delta = 0$ and

$$\cos \chi = \sin \theta \cos \phi \text{ (equinox)} \qquad \ldots\ldots(3).$$

At noon ($\phi = 0$), denoting $\chi$ by $\chi_0$, we have

$$\chi_0 = \tfrac{1}{2}\pi - (\theta + \delta) \text{ (noon)} \qquad \ldots\ldots(4).$$

When it is desired to indicate the variables on which $\chi$ depends, it will be denoted by $\chi(\delta, \theta, \phi)$. Then, by (2),

$$\chi(\delta, \tfrac{1}{2}\pi, \phi) = \chi(0, \tfrac{1}{2}\pi - \delta, \phi) \qquad \ldots\ldots(5),$$

i.e. the sun's zenith distance, at any local time $\phi$, is the same for the equator at the season when the sun's declination is $\delta$, as at a point in latitude $\delta$ (or colatitude $\tfrac{1}{2}\pi - \delta$) at the equinoxes ($\delta = 0$).

## § 4. THE ABSORPTION OF RADIATION

Consider a beam of monochromatic ionizing solar radiation, of unit cross-section and of intensity $S_\infty$ outside the atmosphere, passing through the layer between $h$ and $h - dh$, above the point $\theta$, $\phi$, and therefore at the inclination $\chi$ to the vertical. Subject to the usual assumption that the absorption is proportional to the intensity $S$ at that height, and to the mass $\rho_0 \sec \chi \exp(- h \, H) . dh$ of air traversed, the change of intensity $dS$ after crossing the layer will be given by

$$dS = AS\rho_0 \sec \chi \exp(- h/H) \, dh \qquad \ldots\ldots(6),$$

where $A$ is the coefficient of absorption. The solution of this differential equation is*

$$S = S_\infty \exp\{- A\rho_0 H \sec \chi . \exp(- h/H)\} \qquad \ldots\ldots(7).$$

* P. Lenard, *Sitz. d. Heidelberger Ak. d. W.*, 12 Abh. (1911).

The absorption of radiation per cc. of atmosphere is $dS/(\sec \chi . dh)$, and if the number of ions produced by the absorption of unit quantity of the radiation is $\beta$, the rate of production of ions per cc. will be $\beta \cos \chi . dS/dh$; this, being a function of $h$ and $\chi$, will be denoted by $I(\chi, h)$. By (7),

$$I(\chi, h) = \beta \cos \chi \frac{dS}{dh} = \beta A S_\infty \rho_0 \exp \left\{ -\frac{h}{H} - A\rho_0 H \sec \chi \exp \left( -\frac{h}{H} \right) \right\} \quad \ldots\ldots(8).$$

The total number of ions produced in a square cm. column of air by the complete absorption of the radiation $(S_\infty)$ concerned is $\beta S_\infty \cos \chi$.

This rate of production of ions per c.c. has a maximum at the height $h(\chi)$ given by

$$\exp \frac{h(\chi)}{H} = A\rho_0 H \sec \chi \qquad \ldots\ldots(9),$$

and the corresponding maximum value $I(\chi)$ of $I(\chi, h)$ is given by

$$I(\chi) = \beta S_\infty \cos \chi / H \exp 1 \qquad (10),$$

where exp 1 is written instead of $e$ (or 2·718 ...) to avoid confusion with the usual symbol for the electronic charge. Let the values of $h(\chi)$ and $I(\chi)$ for $\chi = 0$ be denoted by $h_0$ and $I_0$. Then

$$\exp(h_0/H) = A\rho_0 H, \quad I_0 = \beta S_\infty / H \exp 1 \qquad (11);$$

consequently

$$h(\chi) = h_0 + H \ln \sec \chi \qquad \ldots\ldots(12),$$

where ln denotes the Napierian logarithm, and

$$I(\chi) = I_0 \cos \chi \qquad \ldots\ldots(13).$$

In terms of $I_0$ and $h_0$, (8) may be written

$$I(\chi, h) = I_0 \exp \left\{ \frac{h_0 + H - h}{H} - \sec \chi \exp \frac{h_0 - h}{H} \right\} \qquad \ldots\ldots(14).$$

It should be noted that these equations are not valid for very large values of $\sec \chi$ (corresponding to grazing incidence of the beam of radiation), because then the level surfaces traversed by the beam can no longer be treated as parallel planes, as they were when the distance along the beam between $h$ and $h - dh$ was taken as $\sec \chi . dh$. The approximation is probably sufficiently accurate up to $\sec \chi = 12$, or $\chi = 85°$, which along the equator corresponds to about 20 minutes after sunrise or before sunset. In a succeeding paper the special conditions existing near sunrise will be examined more accurately; it will be shown that at and near the level of maximum ion-content the results of the present paper are very nearly true except near dawn, at the equator; but that in higher latitudes, *in winter*, the necessary corrections are appreciable up to noon.

### § 5. THE DATUM UNIT FOR DIFFERENCES OF LEVEL

It is convenient (cf. § 2) to measure heights in terms of $H$ as unit, and reckoned from $h_0$ as datum; $H$ will have the value appropriate to the height $h_0$, and its change with height over the ionized layer, at and near the level $h_0$, will be assumed small and neglected. Thus, let

$$z = (h - h_0)/H \qquad \text{......(15).}$$

Then if $z(\chi)$ corresponds to the level $h(\chi)$, we have, by (12),

$$z(\chi) = \ln \sec \chi \qquad \text{......(16),}$$

and by (14),

$$I(\chi, h) = I_0 \exp\{1 - z - \sec\chi . \exp(-z)\} \equiv I(\delta, \theta, z, \phi) \qquad \text{......(17),}$$

where the notation $I(\delta, \theta, z, \phi)$ is used to indicate the independent variables of which $I(\chi, h)$ is a function.

### § 6. THE NOON DISTRIBUTION OF ABSORPTION

At any point $P$ the minimum value of $\chi$ and $\sec\chi$, and consequently the maximum value of $I(\chi, h)$ or $I(\delta, \theta, z, \phi)$, occur at noon ($\phi = 0$), when, by (4), $\chi = \frac{1}{2}\pi - (\theta + \delta)$. Hence, by (17),

$$I(\delta, \theta, z, 0) = I_0 \exp\{1 - z - \operatorname{cosec}(\theta + \delta)\exp(-z)\} \text{ (noon) ......(18).}$$

This has its maximum value, with respect to height, of amount

$$I(\delta, \theta) = I_0 \sin(\theta + \delta) \qquad \text{......(19),}$$

by (13), at the level

$$z(\delta, \theta) = \ln \operatorname{cosec}(\theta + \delta) \qquad \text{......(20),}$$

by (16).

These formulae are exemplified by the graphs in figure 1, which represent $I(\delta, \theta, z, 0)/I_0$ as a function of $z$; that is, they indicate, for a number of values of $\theta + \delta$, the ratio of the noon rate of ion-production at various heights, to the noon-rate at the equator at height $h_0$. The curves relate to the values (1) 6·5°, (2) 15°, (3) 30°, (4) 45°, (5) 53·5°, (6) 66·5° and (7) 90°.

At the equinoxes ($\delta = 0$) they refer to points having these colatitudes, or to latitudes varying from 83·5° (curve 1) to zero (the equator, curve 7). They show how the ion-production at noon decreases as we recede from the equator, while at the same time the level of maximum production rises, at first slowly, then more rapidly as the pole is approached.

The curve (6) shows the noon-rate of ion-production at the equator ($\theta = \frac{1}{2}\pi$) at the solstices ($\delta = \pm 23·5°$), and by comparison with the equinoctial curve (7) for the equator indicates how slight is the seasonal change in the height distribution of ion-production above the equator.

At latitude 60° ($\theta = 30°$), however, the seasonal change is very considerable, as is shown by curves (1), (3) and (5), which refer to this latitude at midwinter ($\delta = -23·5°$, $\theta + \delta = 6·5°$), the equinoxes ($\delta = 0$, $\theta + \delta = 30°$), and midsummer ($\delta = 23·5$, $\theta + \delta = 53·5°$) respectively. The level of maximum production varies
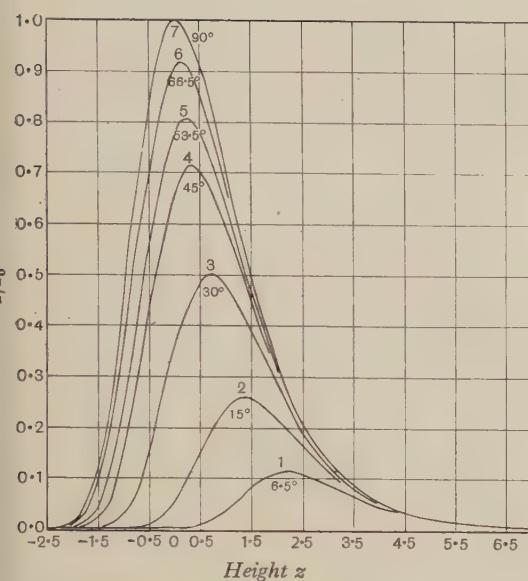
Fig. 1. Ion-production at noon for various values of $(\theta + \delta)$
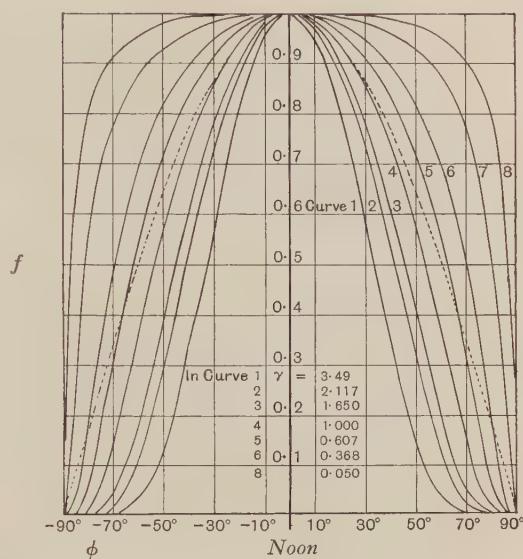


Fig. 2. Ion-production at the equinoxes
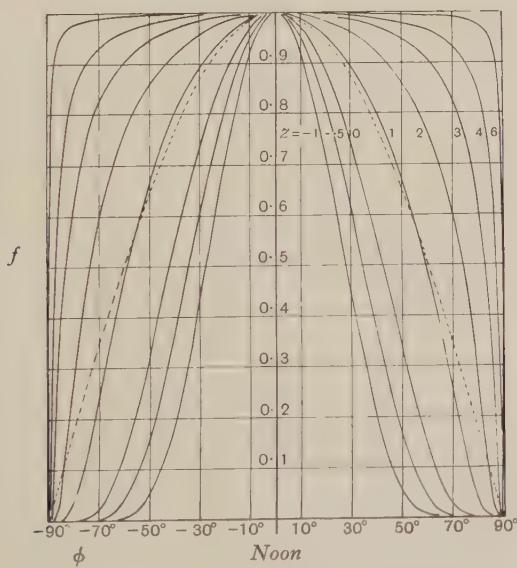


Fig. 3. Ion-production at the equinoxes in latitude 60°

from $z = 2\cdot2$ in midwinter to $z = 0\cdot2$ in midsummer (a change of 17 km. if $H = 8\cdot4$ km.), and the maximum rate of production is increased in the ratio $\sin 53\cdot5°/\sin 6\cdot5°$ or $7\cdot1$; the total rate of ion-production, integrated over all heights (i.e. $\beta S \cos \chi_0$, cf. § 4), is altered in the same ratio.

Considering curve (7) for the equator at the equinoxes, it may be seen that $I\,I_0$ falls from 1 at height $h_0$ ($z = 0$) to $\frac{1}{8}$ at approximately $z = 1\cdot5$ and $z = 3\cdot0$; thus the greater part of the ion-production occurs in a layer of thickness $4\cdot5\,H^*$ (or about 39 km. if $H = 8\cdot4$ km.). Here, and at other latitudes and seasons, the rate of ion-production at noon decreases much more rapidly in passing downwards than in *ascending* from the level of maximum production.

The higher the level above $h_0$, the more uniform is the noon rate of ion-production at nearly all latitudes and seasons; this is already marked at $z = 3$, where $I\,I_0$ is approximately $\frac{1}{8}$ for all values of $\theta + \delta$ between $15°$ and $165°$. Over this range the term $\operatorname{cosec}(\theta + \delta)\exp(-z)$ in the exponential formula (18) is very small when $z > 3$, and $I$ then becomes approximately $I_0 \exp(1 - z)$.

The variation of $z(\delta, \theta)$ is also shown in table 1 for various values of $\chi_0$ or $\frac{1}{2}\pi - (\theta + \delta)$; the corresponding values in km. are also given, $H$ being taken as $8\cdot4$ km.

Table 1.

| $\chi_0 = \frac{1}{2}\pi - (\theta + \delta)$ | $0°$ | $30°$ | $45°$ | $60°$ | $75°$ | $80°$ | $82\cdot5°$ | $85°$ |
|---|---|---|---|---|---|---|---|---|
| $z(\delta, \theta)$ | 0 | 0·062 | 0·151 | 0·301 | 0·587 | 0·760 | 0·884 | 1·060 |
| $z$ (km.) | 0 | 1·2 | 2·9 | 5·8 | 11·3 | 14·7 | 17·1 | 20·5 |

## §7. THE PROPORTIONATE DAILY VARIATION OF ABSORPTION

It is of interest to indicate also how the rate of ion-production varies with respect to $\phi$, that is, throughout the day at different heights, seasons and latitudes. This can conveniently be done by representing graphically, as a function of $\phi$, the ratio of the rate at time $\phi$ to that at noon ($\phi = 0$), i.e.

$f$
$$f(\delta, \theta, z, \phi) = I(\delta, \theta, z, \phi)/I(\delta, \theta, z, 0)$$
$$= \exp\{(\sec \chi_0 - \sec \chi).\exp(-z)\}$$
$$= \exp[\{\operatorname{cosec}(\theta + \delta) - \sec \chi\}.\exp(-z)] \qquad \ldots\ldots(21).$$

The range of $\phi$ is that for which $\cos \chi > 0$, so that the limiting values of $\phi$ are given by
$$\cos \phi = -\tan \delta \cot \theta \qquad \ldots\ldots(22).$$

At the equinoxes $\delta = 0$ and $\phi$ ranges between $\pm \frac{1}{2}\pi$, while (21) takes the form
$$f(0, \theta, z, \phi) = \exp\{-\operatorname{cosec}\theta \exp(-z)(\sec \phi - 1)\} \qquad \ldots\ldots(23),$$
in which the dependence on each variable is specially simple; $z$ and $\theta$ are involved together in the factor $\gamma$ where

$\gamma$
$$\gamma = \operatorname{cosec}\theta \exp(-z) \qquad \ldots\ldots(24),$$
in terms of which
$$f(0, \theta, z, \phi) = \exp\{-\gamma(\sec \phi - 1)\} \qquad \ldots\ldots(25).$$

\* $H$ itself is assumed to have a negligible variation throughout a layer of thickness about $5H$.

The values of $\gamma$ for various values of $z$ and $\theta$ are given in table 2.

Table 2

$$\gamma = \operatorname{cosec} \theta \cdot \exp(-z)$$

| $z$ | $\theta$ | | | | | | | |
|---|---|---|---|---|---|---|---|---|
| | 6·5° | 15° | 30° | 45° | 53·5° | 60° | 66·5° | 90° (eqr.) |
| 4·0 | 0·162 | 0·071 | 0·037 | 0·026 | 0·023 | 0·021 | 0·020 | 0·018 |
| 3·0 | 0·440 | 0·192 | 0·100 | 0·070 | 0·062 | 0·057 | 0·054 | 0·050 |
| 2·0 | 1·196 | 0·523 | 0·271 | 0·191 | 0·168 | 0·156 | 0·148 | 0·135 |
| 1·5 | 1·971 | 0·862 | 0·446 | 0·316 | 0·278 | 0·258 | 0·243 | 0·223 |
| 1·0 | 3·250 | 1·421 | 0·736 | 0·520 | 0·458 | 0·425 | 0·401 | 0·368 |
| 0·5 | 5·358 | 2·343 | 1·213 | 0·858 | 0·755 | 0·700 | 0·661 | 0·607 |
| 0 | 8·834 | 3·864 | 2·000 | 1·414 | 1·244 | 1·155 | 1·090 | 1·000 |
| −0·5 | 14·56 | 6·37 | 3·297 | 2·332 | 2·051 | 1·904 | 1·798 | 1·649 |
| −0·75 | 18·70 | 8·18 | 4·23 | 2·99 | 2·63 | 2·445 | 2·308 | 2·117 |
| −1·0 | 24·01 | 10·50 | 5·44 | 3·84 | 3·38 | 3·14 | 2·96 | 2·72 |
| −1·25 | 30·83 | 13·49 | 6·98 | 4·94 | 4·34 | 4·03 | 3·81 | 3·49 |
| −1·5 | 39·59 | 17·32 | 8·96 | 6·34 | 5·58 | 5·18 | 4·89 | 4·48 |

In figure 2, curves representing $f(0, \theta, z, \phi)$ as a function of $\phi$, equation (25), are drawn for various values of $\gamma$. They indicate the proportionate diurnal variation in the rate of ion-production, *at the equinoxes* ($\delta = 0$), for any point at height $z$ (above or below $h_0$) in any colatitude $\theta$; the value of $\gamma$ corresponding to $\theta$ and $z$ may be found by interpolation from table 2, and the corresponding curve can then be obtained from figure 2 by interpolation.

At the level $h_0$ ($z = 0$), at the equator ($\theta = \frac{1}{2}\pi$), $\gamma = 1$; the curve $\gamma = 1$ in figure 2 resembles, though except at $\phi = 0$ it is below, the curve of $\cos \phi$ (shown by a dotted line for comparison). For $\gamma > 1$, corresponding, *inter alia*, to levels below $h_0$ at the equator, or to levels extending somewhat above $h_0$ at higher latitudes (cf. table 2), the excess of $\cos \phi$ over $f(0, \theta, z, \phi)$ is greater, indicating that the part of the day during which these levels absorb the radiation is more and more concentrated round the hour of noon. Conversely, for $\gamma < 1$, $f(0, \theta, z, \phi)$ approaches unity the more rapidly and over a wider range of $\phi$, the smaller the value of $\gamma$, indicating that in the higher levels of the atmosphere the rate of ion-production is near its maximum and varies little, from near sunrise to near sunset, the rise and fall near these epochs being rapid.

## § 8. THE SEASONAL CHANGES IN THE PROPORTIONATE DAILY VARIATION

At times other than the equinoxes the curves showing $f(\delta, \theta, z, \phi)$ as a function of $\phi$ differ from those of figure 2, except for the equator ($\theta = \frac{1}{2}\pi$). There, by virtue of (5),

$$f(\delta, \tfrac{1}{2}\pi, z, \phi) = f(0, \tfrac{1}{2}\pi - \delta, z, \phi),$$

indicating that the equatorial curve for the season $\delta$ and for any height $z$ is the same as the *equinoctial* curve for the same height in latitude $\delta$. The slightness of the seasonal change in the proportionate diurnal variation of ion-production at any

height above the equator is indicated by the small difference between the values of $\gamma$ in the two last columns of table 2, which refer respectively, for any height $z$, to the solstices and equinoxes.

At latitudes far from the equator the proportionate daily variation in the rate of ion-production at any height changes considerably with the season, as also does the duration of ion-production. This is illustrated by the curves in figures 3, 4, 5, which refer to latitude $60°$ $(\theta - 30°)$ at the equinoxes, the summer solstice, and the winter solstice $(\delta = 23\cdot5\cdot0, - 23\cdot5)$, for a series of heights between $z = -2$ and $z = 7$; the curve representing $\cos \chi$ is also shown on each diagram by a dotted line.

The different base-lengths in the three diagrams refer, of course, to the different periods of daylight at the three seasons. In summer, when the sun's rays are most direct, the rate of ion-production at the level $z = 0$ exceeds half its maximum (noon) value for about half the period of daylight; this is nearly true at the same level at the equinoxes also, but in winter the absorption of radiation at this level increases more slowly, and it exceeds half the noon value only for about a quarter of the period of daylight. At $z = 6$ at all seasons the absorption is nearly at its full value throughout almost the whole day.

To obtain a comprehensive idea of the variation of ion-production with respect to season, height, latitude and local time the curves in figure 1 should be considered in conjunction with those of figures 2–5.

### § 9. THE DISTRIBUTION AND VARIATIONS OF ION-DENSITY

$n, n_e, n_-$       Let $n$, $n_e$, $n_-$ denote the number per c.c. of positive ions, electrons, and negative ions, at a point $\phi$, $\theta$, $z$. The ions of either kind are, for simplicity, supposed to be all alike and simply charged; hence, the air being electrically neutral,

$$n = n_e + n_- \qquad \qquad \ldots\ldots(26).$$

The number of positive ions produced per c.c. per second is denoted, as in the preceding sections, by $I$ $(\delta, \theta, z, \phi)$. The equation of variation for $n$, due to new formation of positive ions, and their disappearance by recombination, is

$$dn/dt = I\,(\delta,\,\theta,\,z,\,\phi) - \alpha_e nn_e - \alpha_- nn_- \qquad \ldots\ldots(27),$$

$\alpha_e, \alpha_-$       where $\alpha_e$, $\alpha_-$ denote coefficients of recombination. Their values are not known with any certainty, at the low pressures which obtain in the atmospheric region under consideration; for simplicity it will be assumed that they are equal, though this is a pure assumption. Thus we take

$\alpha$                
$$\alpha_e = \alpha_- = \alpha \qquad \qquad \ldots\ldots(28),$$

so that, by virtue also of (26), (27) reduces to

$$dn/dt = I - \alpha n^2 \qquad \qquad \ldots\ldots(29).$$

This is the equation that expresses the condition ($d$) of § 1.

Here, as has been shown in §§ 2–8, $I$ is a function of $\delta$, $\theta$, $z$ (or $h$) and $\phi$, so that $n$ also will depend on these variables; $\alpha$ may be a function of $z$, but will be supposed independent of $\delta$, $\theta$, and $\phi$; the solutions of (29) which are obtained here will, however, only be discussed for values of $\alpha$ independent also of $z$.
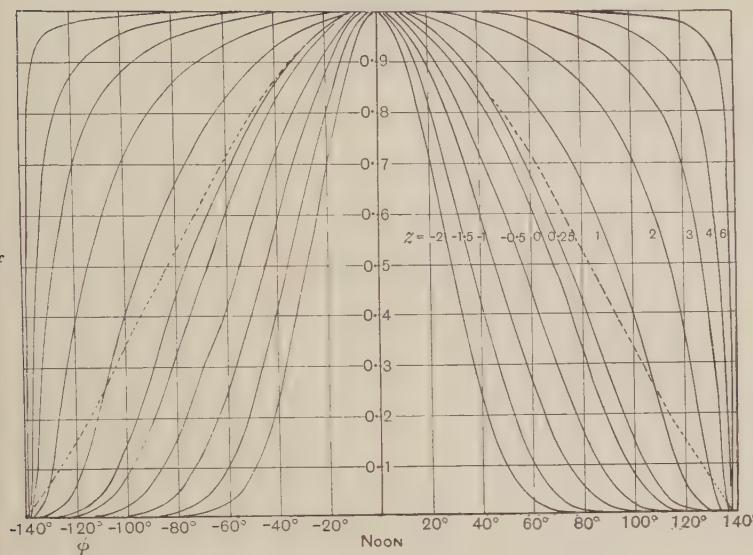
Fig. 4. Ion-production at the summer solstice in latitude 60°.
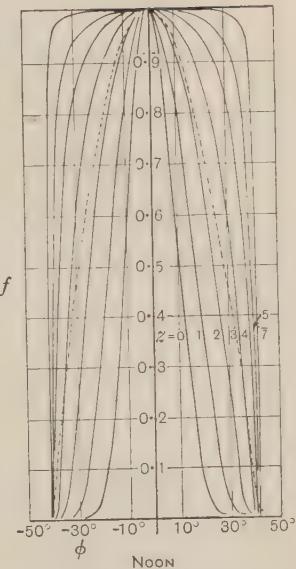


Fig. 5. Ion-production at the winter solstice in latitude 60°.
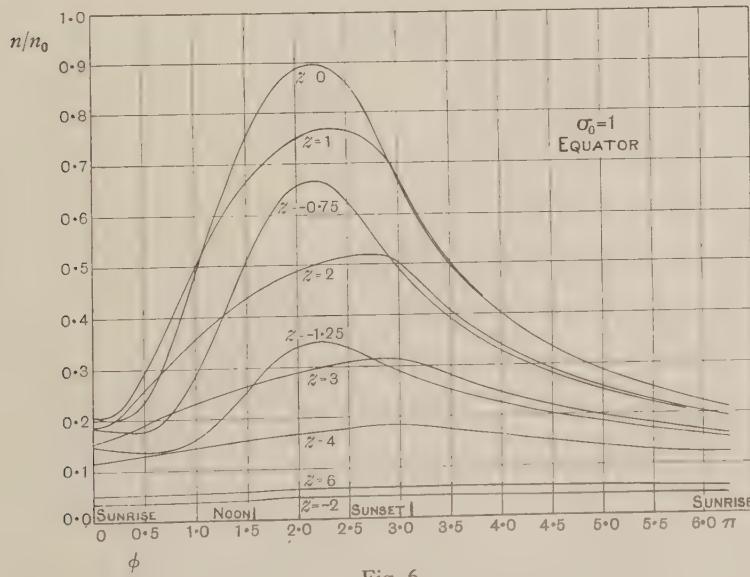


Fig. 6.

*t*      It is convenient to express the local time $t$ in (29) in terms of $\phi$, by (1). Then (29) becomes, using (17):

$$(1/1\cdot37.10^4).dn/d\phi = I_0 \exp \{1 - z - \sec \chi . \exp (- z)\} - \alpha n^2 \quad \ldots\ldots(30),$$

where $\chi$ depends on $\phi$, $\theta$ and $\delta$ according to (2).

$n_0$      Let    .           $n_0 = (I_0/\alpha)^{\frac{1}{2}}$          $\ldots\ldots(31)$,

$\sigma_0$                       $1/\sigma_0 = 1\cdot37.10^4 (I_0\alpha)^{\frac{1}{2}}$       $\ldots\ldots(32)$,

so that $n_0$ is the steady value which $n$ would attain at the level $h_0$ ($z = 0$) at the equator at midday (when $z = 0$, $\chi - 0$) if the earth did not revolve. Then $n_0$, $\sigma_0$ are alternative modes of specifying $\alpha$ and $I_0$, i.e.

$$1/\alpha = 1\cdot37.10^4 \sigma_0 n_0 \qquad \ldots\ldots(33),$$
$$I_0 = n_0/(1\cdot37.10^4 \sigma_0) \qquad \ldots\ldots(34).$$

In terms of $n_0$, $\sigma_0$, and $\nu$, defined by

$$\nu \equiv n/n_0 \qquad \ldots\ldots(35),$$

(30) may be written in the form

$$\sigma_0 . d\nu/d\phi + \nu^2 = \exp \{1 - z - \sec \chi \exp (-z)\} \quad \text{(day)}$$
$$= F (z, \chi) \qquad \ldots\ldots(36).$$

*F*      This represents the variation of $\nu$, or $n/n_0$, during the hours of daylight; during the hours of darkness the right-hand side must be replaced by zero, i.e.

$$\sigma_0 . d\nu/d\phi + \nu^2 = 0 \quad \text{(night)} \qquad \ldots\ldots(37).$$

The solution of this equation is

$$\nu = \sigma_0/(\phi + C) \quad \text{(night)} \qquad \ldots\ldots(38),$$

*C*      where $C$ is an arbitrary constant.

*r, s*      Distinguishing the values of $\nu$ and $\phi$ at sunrise and sunset by the suffixes $r$ and $s$, we have

$$\frac{1}{\nu_r} - \frac{1}{\nu_s} = \frac{\phi_r - \phi_s}{\sigma_0} \qquad \ldots\ldots(39).$$

The solution of (36) has to be found subject to this condition, which determines the arbitrary parameter involved in the general solution of (36).

It does not seem possible to solve the non-linear equation (36) in terms of elementary functions, and numerical methods must be adopted. If one solution of (36) has been found numerically, not satisfying (39), the true solution can be obtained from it by a process of quadratures, but the latter is not appreciably easier than finding the correct solution of (36), subject to (39), by successive direct trials; it is therefore unnecessary to explain the method referred to.

### § 10. SOLUTIONS FOR THREE VALUES OF $\sigma_0$

The equation (36) has been solved, subject to the condition (39), for three values of $\sigma_0$, namely $1$, $\frac{1}{5}$ and $\frac{1}{25}$, for various heights (at distances $z$ above and below $h_0$) at the equator ($\theta = \frac{1}{2}\pi$) at the equinoxes ($\delta = 0$); and also, for $\sigma_0 = \frac{1}{25}$, at various
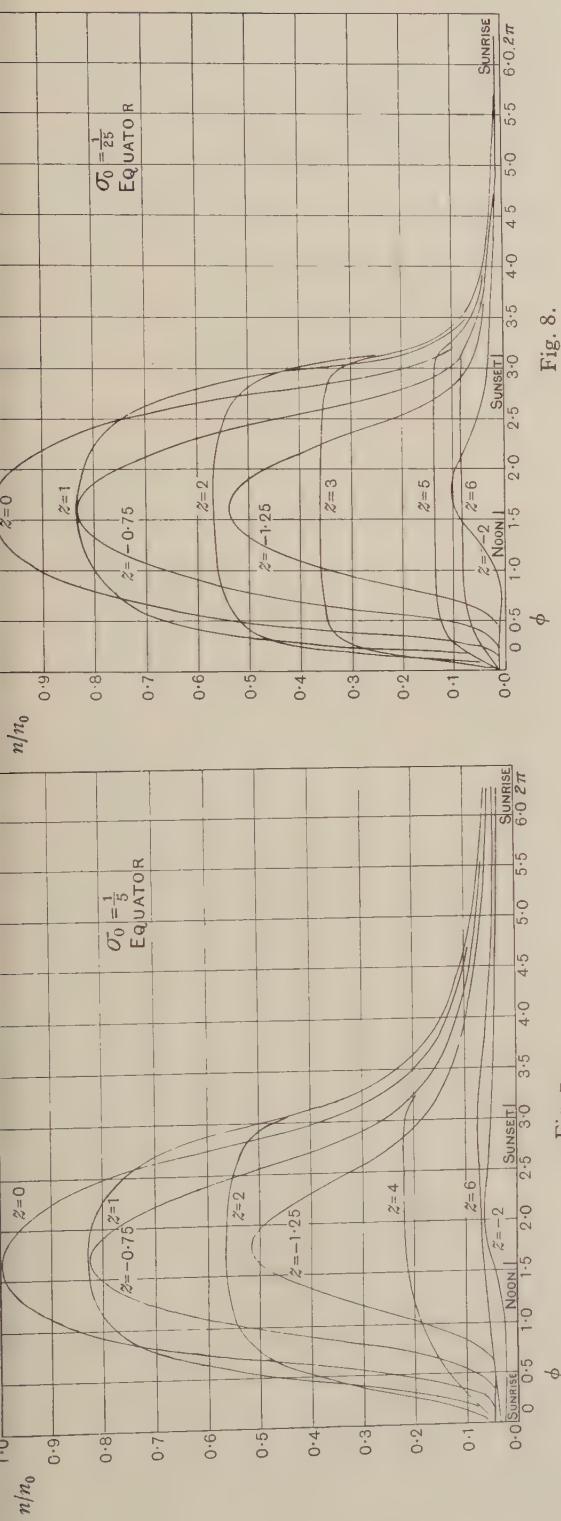
Fig. 8.

Fig. 7.
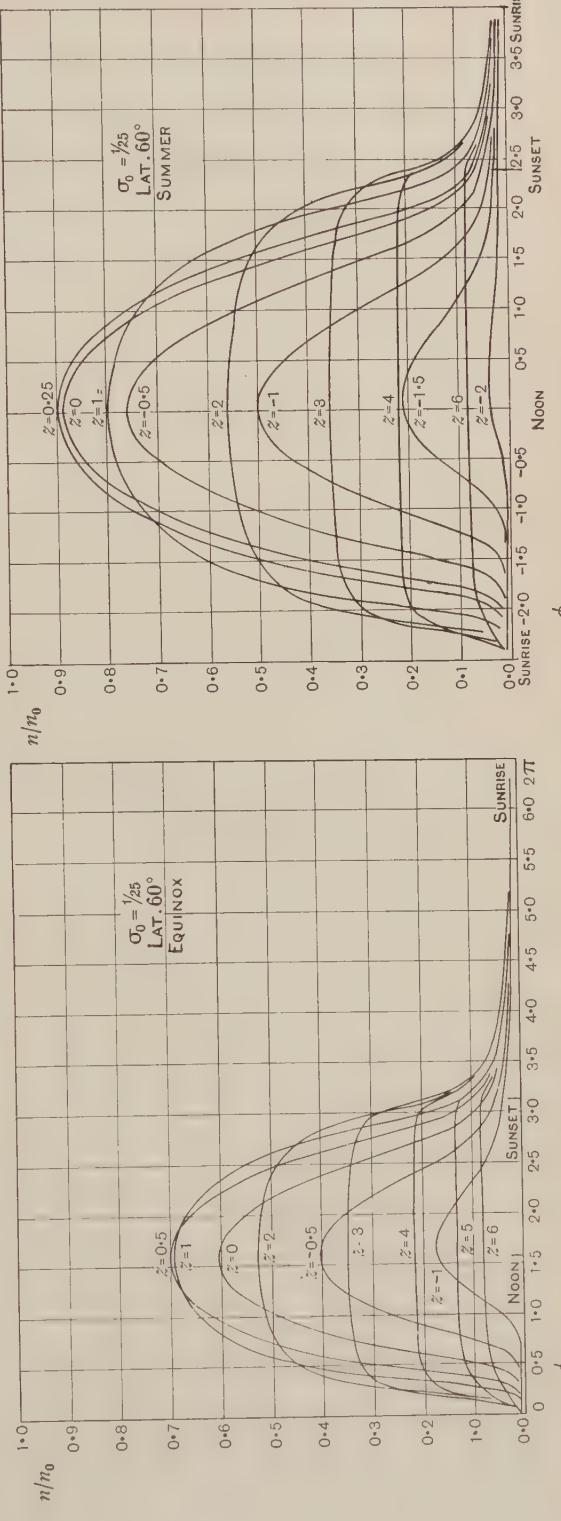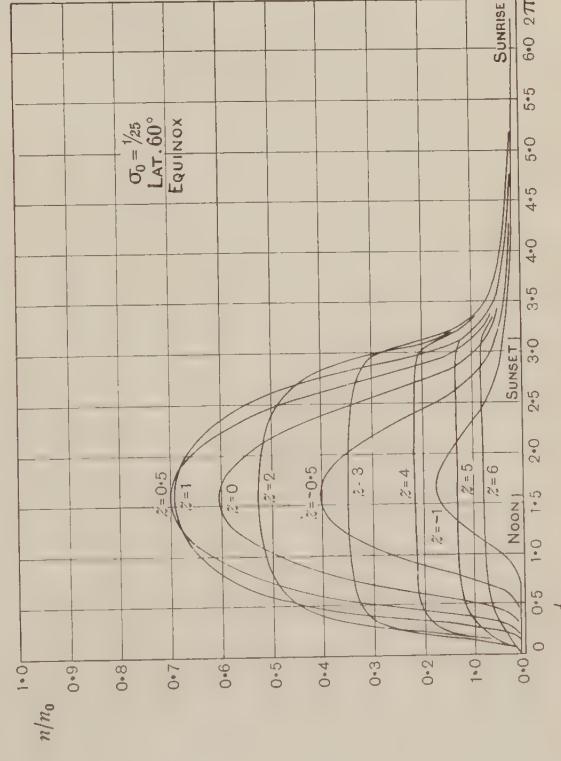
Fig. 10.

Fig. 9.

heights in latitude $60°$ ($\theta = 30°$), at the equinoxes ($\delta = 0$) and the solstices ($\delta = \pm 23\cdot5$). The corresponding values of $v$ or $n/n_0$ as a function of $\phi$ (in circular measure) are shown by series of graphs in figures 6–11. Further graphs have been derived from these, showing, in figures 12–17, the values of $n/n_0$ as a function of height at various local times, for the equator ($\sigma_0 = 1, \frac{1}{5}, \frac{1}{25}$) and latitude $60°$ ($\sigma_0 = \frac{1}{25}$). In the "equinoctial" figures 6–9 and 12–15, $\phi$ is reckoned from *sunrise*, not from *noon* as in figures 2–5, 10, 11, 16, 17, and elsewhere in this paper. These curves, and further general conclusions which can be inferred from them, or from the differential equations (36), (37), will now be discussed.

## § 11. THE ION-DENSITY AS A FUNCTION OF TIME

At and between sunset and sunrise $v$ varies according to (37), i.e.

$$dv/d\phi = -\, v^2/\sigma_0;$$

thus $v$ is decreasing at and between these epochs. Between sunrise and sunset $v$ varies according to (36), the right-hand side of which is essentially positive, and has its maximum at noon (when $\chi - \frac{1}{2}\pi - \theta - \delta$); during part of the hours of sunlight

must increase, and the reversal from the decreasing rate $v_r^2 \sigma_0$ at sunrise occurs after an interval of time which is shorter, the smaller the value of $\sigma_0$. In many of the graphs in figures 6–10 this interval is too small to be shown, though for heights *below* $h_0$ ($z$ negative) a considerable time elapses after sunrise before the increase in $v$ becomes noteworthy.

At the equator, for $\sigma_0 = 1$ the maximum value of $n/n_0$ occurs distinctly after noon at heights adjacent to $h_0$, and at greater heights the maximum is deferred till near sunset. But for $\sigma_0 = \frac{1}{5}$ and $\sigma_0 = \frac{1}{25}$ the value of $n/n_0$ at noon is very near the maximum value; this is true likewise for $\sigma_0 = \frac{1}{25}$, at $60°$ latitude, and therefore also at intermediate latitudes. For such values of $\sigma_0$ it is possible to deduce a close approximation to $v_{max}$; for if, at noon, when $\sec \chi = \operatorname{cosec}(\theta + \delta)$, $dv/d\phi$ is small or zero, then by (36)

$$v^2 = F(z, \chi) = \exp\{1 - z - \operatorname{cosec}(\theta + \delta)\exp(-z)\},$$

or

$$n_{max}/n_0 = \exp\tfrac{1}{2}\{1 - z - \operatorname{cosec}(\theta + \delta).\exp(-z)\}$$
$$= \sqrt{(I/I_0)} \text{ (noon)} \qquad\qquad ......(40)$$

by (18). At height $h_0$ ($z = c$) at the equator ($\theta = \frac{1}{2}\pi$) at the equinoxes ($\delta = 0$), the value of $I/I_0$ is unity (cf. figure 1), so that $n_{max} = n_0$ almost exactly. At the solstices at the equator $(I/I_0)_{noon, max} = 0\cdot938$ (curve 6, figure 1), so that $n_{max} = 0\cdot968\, n_0$; the maximum value occurs very shortly after noon, at the height $z = -0\cdot1$. At the equinox in $60°$ latitude $(I/I_0)_{noon, max} = 0\cdot5$ (curve 3, figure 1) so that $n_{max}/n_0 = 0\cdot707$, occurring at $z = 0\cdot7$; at the same latitude the values of $n_{max}/n_0$ at midsummer and midwinter (cf. curves 5 and 1, figure 1) are $0\cdot90$ and $0\cdot33$, occurring nearly at noon at $z = 0\cdot2$ and $z = 2\cdot2$ respectively. At this latitude the seasonal change in $n_{max}$ is very great, though less than that of $(I/I_0)_{noon, max}$.

Before attaining its maximum, $v$ must be less than $\sqrt{F(x, \chi_0)}$, because $v^2 = F(z, \chi) - \sigma dv/d\phi$, and $dv/d\phi$ is positive; similarly $v > \sqrt{F(z, \chi)}$ after attaining
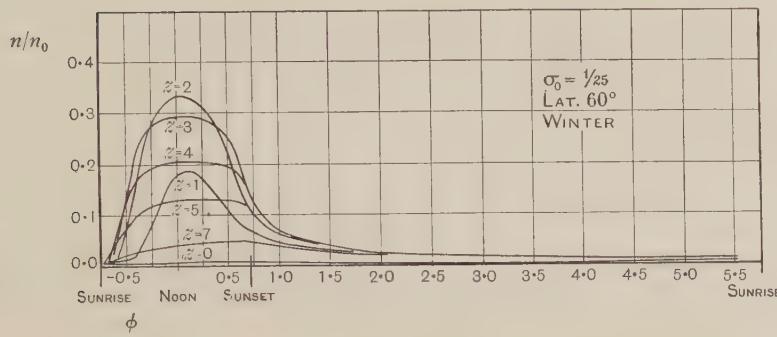
Fig. 11.
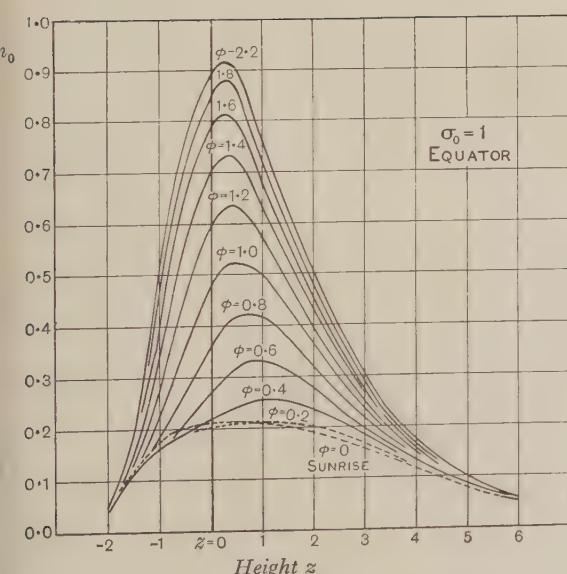


Fig. 12a.
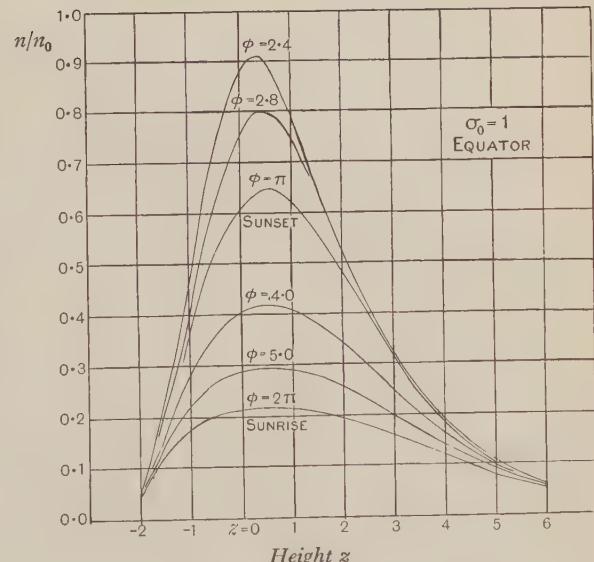


Fig. 12b.

its maximum. But there appears to be no easy general way of finding the amount of the difference.

At heights above the level of maximum noon ionization the graphs of $n/n_0$ as a function of $\phi$ (for $\sigma < \frac{1}{5}$) become increasingly flat; at the greater heights considered $n/n_0$ rises nearly to its maximum soon after sunrise, and varies little until near sunset; this is because $\sqrt{(I/I_0)}$ varies in a similar way (figures 2–5). At heights below the level of maximum noon $(n/n_0)$, the graphs become increasingly narrow, the maximum ion density at such levels being approximated to over a short time only, near noon.

The seasonal variation of $n/n_0$, in latitude $60°$, is much less for the upper levels than for the lower; for example for $\sigma_0 = \frac{1}{25}$ at $z = 6$, $n_{max} n_0$ lies between $0.8$ and $0.9$ all through the year, while for $z = -1$ it is $0.6$ in summer, $0.5$ at the equinoxes, and less than $0.1$ in winter. The seasonal variation of $n/n_0$ at the equator is so small that no graphs have been drawn to illustrate it.

### § 12. THE ION-DENSITY AS A FUNCTION OF HEIGHT

The curves in figures 12–17, giving $n/n_0$ as a function of height at various local times, will next be considered.

Figures 12 $a, b$, for $\sigma_0 = 1$ at the equator, show that in this case $n$ has its maximum, at all heights, at about $2\frac{1}{2}$ hours after noon $(\phi = 2.2)$; the maximum value of $n$ occurs at about $z = \frac{1}{4}$, or about 2 km. (if $H = 8.4$ km.) above $h_0$, the level of maximum ion-production at midday; moreover the maximum value of $n$ is distinctly less than $n_0$, being about $0.92\, n_0$. Before and after the epoch of maximum ionization, $n$ varies fairly rapidly with respect both to height and time; at sunset $(\phi = \pi)$ the ion-distribution has fallen from its maximum only by about one-third, and a considerable decrease of ionization proceeds during the night. But even at sunrise $(\phi = 0$ or $2\pi)$ there is a well-marked distribution of ionization, with maximum ion-density at about $z = \frac{1}{2}$. The level of maximum ion-density falls while $n$ is rising, and *vice versa*.

Figures 13 $a, b$, for $\sigma_0 = \frac{1}{5}$ at the equator, show that in this case $n/n_0$ has a maximum value of almost exactly unity at or very near to the height $h_0$, and that the maximum ion-density, at all heights considered, is attained very shortly after noon. Before and after noon the level of maximum ion-density is above $h_0$, the value of $z$ for maximum $n$, near sunrise or sunset, being about 2. The maximum ion-density at sunset occurs at about the level $z = 1.5$, and is approximately $0.4\, n_0$; the further reduction in $n$ during the night is considerable, and at sunrise the ion-distribution consists of a thick layer of nearly uniform ion-density with a maximum of about $\frac{1}{20}\, n_0$ at about $z = 2$.

Figures 14 $a, b$, for $\sigma_0 = \frac{1}{25}$ at the equator, show that in this case $n$ attains the maximum value $n_0$ at the level $h_0$ at noon, almost exactly. At sunset the maximum ion-density is reduced to about $0.23\, n_0$ and occurs at the level $z = 2.5$ (about 21 km. above $h_0$, if $H = 8.4$ km.). During the night the ion-density decreases still further to about $\frac{1}{100}\, n_0$ at sunrise, when $n$ is nearly uniform throughout a thick layer extending from about $z = -2.5$ to $z > 6$. These remarks apply to the equinoxes, but the reduction, and changes of distribution, of the ionization at the solstices are very slight.

Fig. 13b.

Fig. 13a.

Fig. 14b.

Fig. 14a.

## S. Chapman
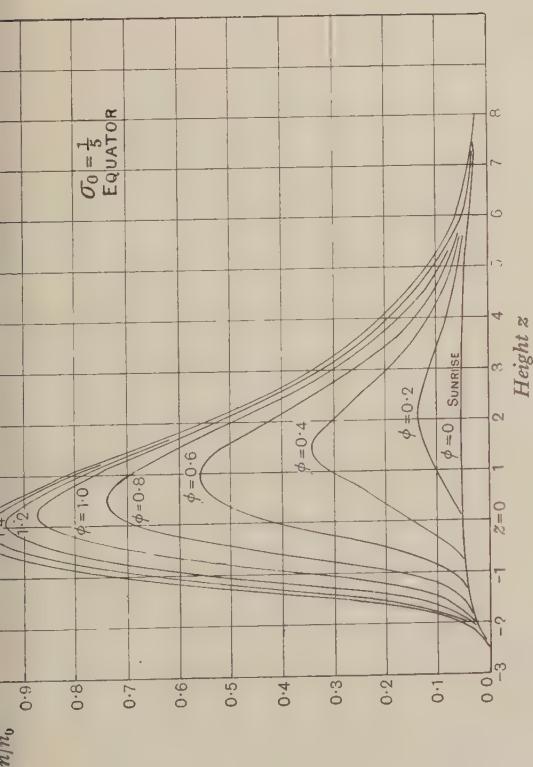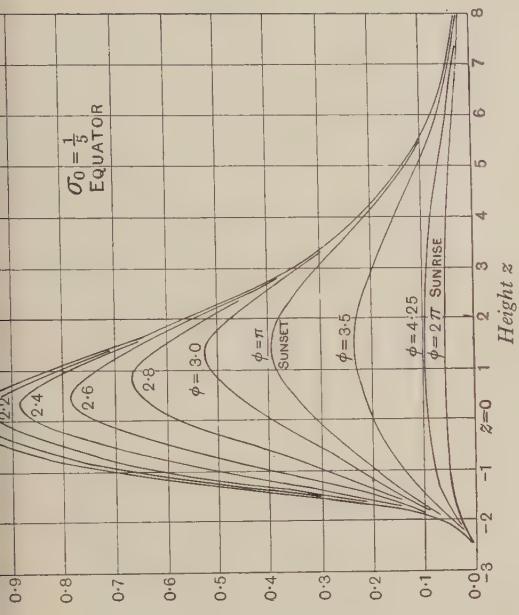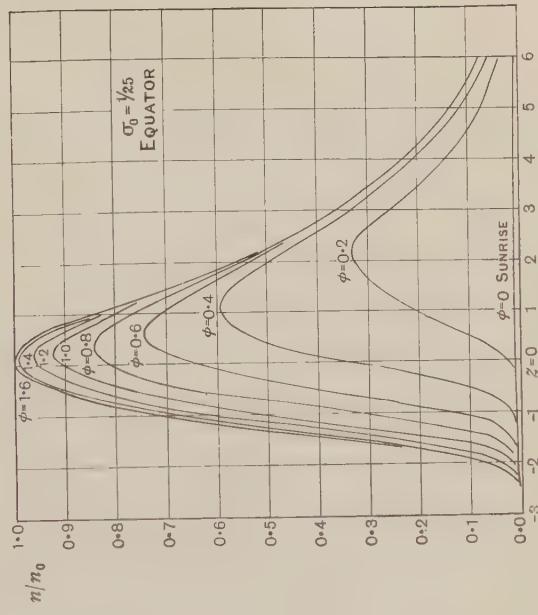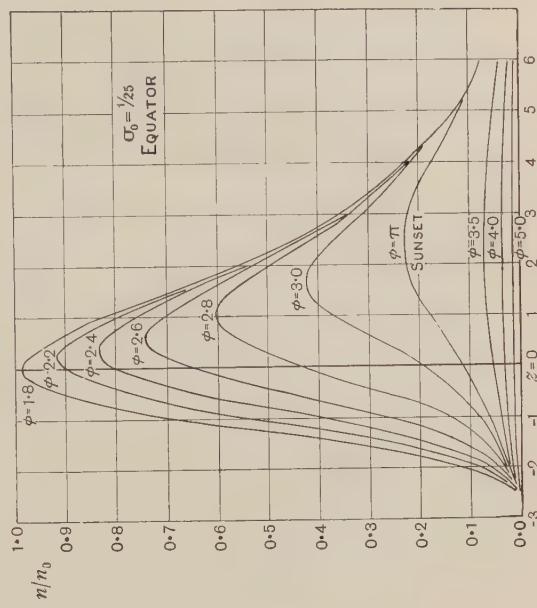
Figures 17–18 for $\sigma_0 = \frac{1}{25}$ at latitude $60°$ show that at the equinox here, as at the equator, $n$ has its maximum nearly at noon, but the maximum is less than at the equator, being about $0.71\ n_0$ instead of $n_0$; moreover it occurs at a somewhat higher level, where $z = 0.7$ or about 6 km. above $h_0$. Allowing for an all-round reduction in $n$ at all times and heights, and for a rather higher level of $n_{max}$ at any time (by about $0.5$ to $0.7$, or 4 to 6 km.) the features of this case resemble those for the equator ($\sigma_0 = \frac{1}{25}$).

Figures 16 and 17 show the height-distribution of $n'n_0$ at $60°$ latitude at midsummer and midwinter, for $\sigma_0 = \frac{1}{25}$; at midsummer the sunrise curve is a little above the sunrise curve for the equator (figure 14$a$), owing to the long day and short night in summer at $60°$ latitude; in midwinter the converse is true. In midsummer the noon maximum value of $n$ is nearly as great at latitude $60°$ as at the equator; the sunset ionization at $60°$ latitude is greatest at about $z = 3.3$, and is about $0.16\ n_0$, as compared with $0.23\ n_0$ at $z = 2.5$ at the equator. At $60°$ latitude the sunset ionization in midwinter is very little less than in midsummer, though at noon the difference of ionization between the two seasons is large.

For still smaller values of $\sigma_0$ it is evident that the main changes from the curves of figures 14–17 would be as follows: the ion-density at sunrise and sunset, and throughout the night, would be reduced; the noon distribution of ion-density would scarcely be affected, but the rise to it would be initially less rapid, mainly taking place in a shorter interval before noon; similarly most of the fall from the noon maximum would be completed in a shorter interval, the period of high ion-density thus being concentrated more towards the middle of the day.

### § 13. UPPER ATMOSPHERIC IONIZATION

The preceding results will be briefly considered in relation to the ionization in the upper atmosphere; for further information, as regards both observational data and more detailed theory, reference may be made to the works of Pedersen[*], Appleton[†], Eckersley[‡], Hulburt[§] and other writers.

At present our knowledge of the actual values and variation of $n$ as a function of height and time, at high levels in the atmosphere, is uncertain, though there is hope that it will later become possible to obtain detailed information of the kind by radio methods. There can scarcely be any doubt, however, that at least one strongly ionized layer exists in the atmosphere, at a height of the order 100 km., in which the ion-density undergoes a considerable daily variation; the evidence for this consists of various kinds of radio measurements, together with the daily, especially the lunar-diurnal, variations of the earth's magnetism. These suggest that the ion-density is greater by day than by night, rising from sunrise to about noon, and decreasing towards sunset, but still leaving at sunset a considerable distribution of ion-density,

[*] P. O. Pedersen, *The Propagation of Radio Waves* (Copenhagen, 1927).

[†] E. V. Appleton and collaborators, *Proc. R.S.* A, **128**, 133, 159 (1930) and earlier papers there cited.

[‡] T. L. Eckersley, *Proc. Inst. Rad. Eng.* **18**, 106 (1930), and earlier references.

[§] E. O. Hulburt, *Phys. Rev.* **31**, 1028 (1928); **34**, 1167 (1929); **35**, 240 (1930).
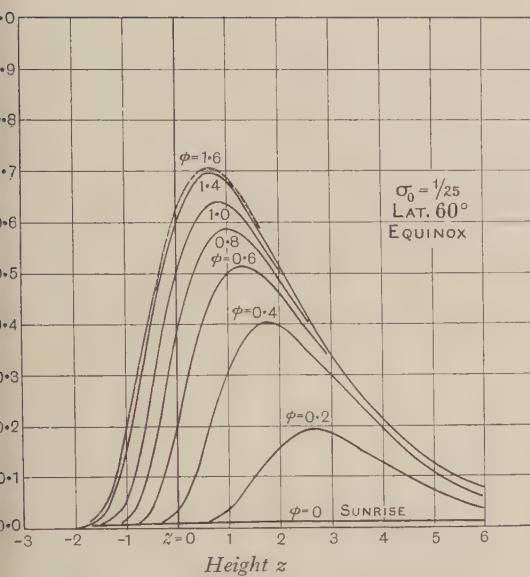
Fig. 15a.
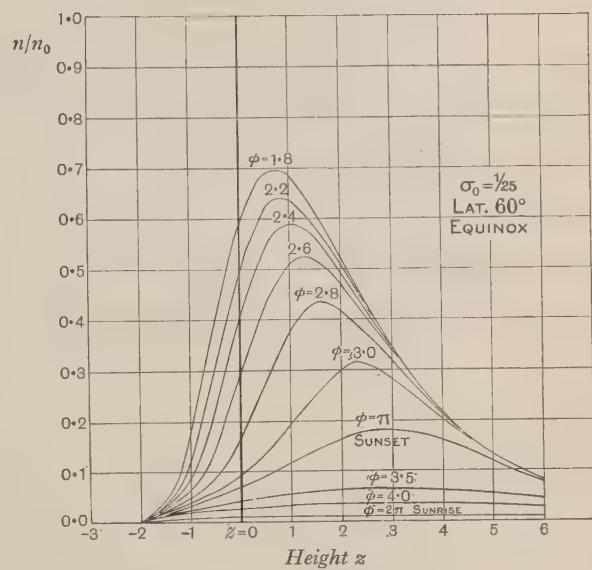


Fig. 15b.



Fig. 16a.



Fig. 16b.

## S. Chapman
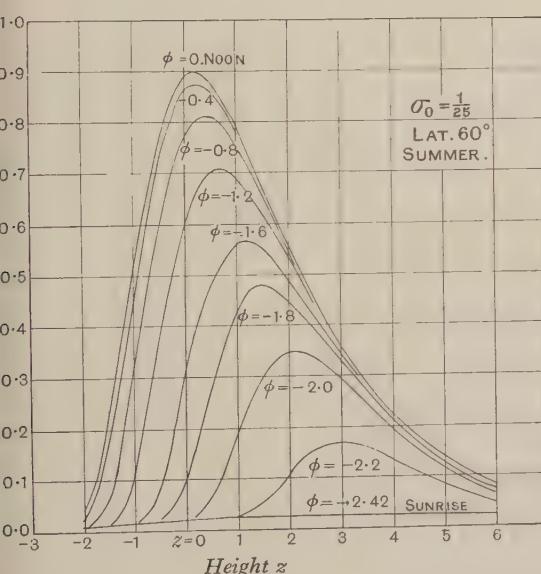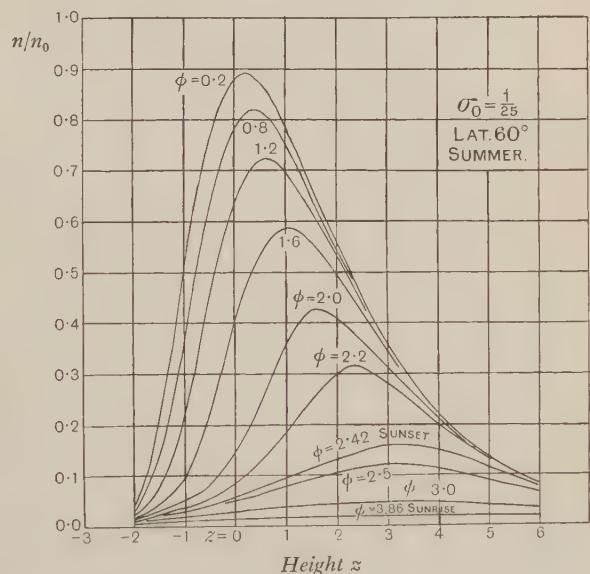
which slowly decreases throughout the night. The theory of the lunar daily magnetic variations is not sufficiently well established to justify any safe estimate of the ratio of the values of $n$ at noon, sunset and sunrise, but a guess may be hazarded, which is perhaps not likely to be wholly wrong as regards order of magnitude, that $n_{noon}/n_{sunset}$ is about 5. This, and the apparent absence of any appreciable lag in the maximum ion-density after noon, suggests, on the basis of figures 12 to 17, that the value of $\sigma_0$ lies between $\frac{1}{5}$ and $\frac{1}{25}$, being definitely less than 1, and probably not less, or at least not much less, than $\frac{1}{25}$.

$n_0$

The value of $n_0$, the maximum (noon) equatorial value of $n$ for the positive ions, is uncertain, but such indications as exist (based on radio measures) suggest that the order of magnitude is $10^6$ or $10^7$.

By (33) or (34) it is possible from these very rough estimates of $n_0$ and $\sigma_0$ to derive corresponding estimates of $\alpha$ and $I_0$, as follows:

| $\sigma_0$ | $n_0$ | $a$ | $I_0$ |
|---|---|---|---|
| $\frac{1}{25}$ | $10^6$ | $2 \cdot 10^{-9}$ | $2 \cdot 10^3$ |
| $\frac{1}{25}$ | $10^7$ | $2 \cdot 10^{-10}$ | $2 \cdot 10^4$ |

The corresponding total rate of production of ions in a cm.$^2$ column of air at the equator at noon is (cf. § 3) $\beta S_\alpha$ or, by (8), $HI_0 \exp 1$; if $H = 8 \cdot 4$ km., the values of $\beta S_\infty$ corresponding to the above two values of $I_0$ are about $5 \cdot 10^9$ and $5 \cdot 10^{10}$.

These estimates of $\alpha$, $I_0$ and $\beta S_\alpha$ are in general accordance with those of the same quantities (there denoted by $\alpha$, $q$, and $\int q dh$) which I made in an earlier discussion of upper atmospheric ionization[*]; this discussion was based on data rather different in kind from those here considered. They seem also to be in general accordance with the observations of the effects of eclipses on radio transmission, which indicate a rapid change in at least the lower part of the ionized layer due to the temporary (total or partial) interception of solar radiation; if, at time $t = 0$, the ion-density at the point considered being $n$, the ion-producing agent is entirely removed, $n$ will at later time be given by $n (1 - \alpha nt)$, so that it will be halved in a time $1/\alpha n$. If $\alpha = 2 \cdot 10^{-9}$ and $n = 10^6$, this time is 500 seconds, or about 8 minutes, which is of the right order of magnitude; similarly if $\alpha = 2 \cdot 10^{-10}$ and $n = 10^7$.

The main purpose of the present paper, however, is not to discuss the actual state of ionization of the atmosphere on the basis of the scanty available data; it is intended to afford a means of discussing the value and variations of the ion-content of the upper atmosphere when reliable data become available. Its results are applicable not only to the ionized layer near 100 km., but also to the higher layer, at about 250 km., discovered by Appleton[†]; the values of the constants $H$, $\beta$, $S_\alpha$, $\alpha$, ... for the two layers may, and probably will, be different. The present analysis is applicable also to the absorption of non-ionizing radiation, such as that which, by dissociating oxygen molecules, leads to the formation of ozone; but the work of §§ 9 et seq. is valid for dissociating-radiation only if the products of dissociation recombine according to the simple law (29), which may not be the case for ozone.

[*] Q.J.R. Met. Soc. **52**, 229 (1926).　　　　　　　　　[†] Loc. cit.

$n/n_0$

$\sigma_0 = 1/25$
LAT. 60°
WINTER

$\phi = 0$ NOON
$\phi = -0.2$
$\phi = -0.3$
$\phi = -0.4$
$\phi = -0.5$
$\phi = -0.6$
$\phi = -0.72$ SUNRISE

$z = 0$ 1 2 3 4 5 6 7

*Height z*

Fig. 17a.

$n/n_0$

$\sigma_0 = 1/25$
LAT. 60°
WINTER

$\phi = 0.1$
$0.3$
$0.5$
$\phi = 0.6$
$\phi = 0.72$ SUNSET
$\phi = 0.8$
$\phi = 1.0$ $\phi = 2.0$ $\phi = 5.56$ SUNRISE

$z = 0$ 1 2 3 4 5 6 7

*Height z*
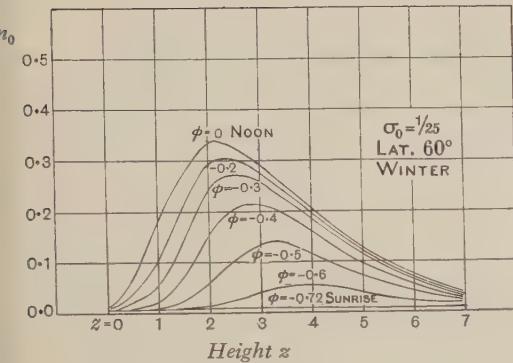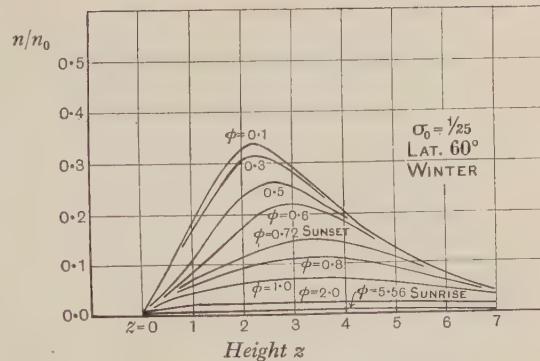
Fig. 17b.

## § 14. ACKNOWLEDGMENTS

# TURBULENT FLOW THROUGH TUBES

By W. N. BOND, M.A., D.Sc., F.Inst.P.,

Lecturer in Physics in the University of Reading

ABSTRACT. The flow of fluid through long straight tubes of circular section was experimented on, at speeds in the neighbourhood of the lower critical velocity, in an attempt to detect any trace of periodicity in the turbulent motion. The experimental methods included (*a*) an aural method; (*b*) photography of the motion of a deflected vane; and (*c*) injection of colour-streamers about halfway along the tube. Intermittent turbulence was investigated at speeds near the critical speed, and measurements of the critical speed were made. It was shown that the velocity parallel to the tube-axis is sometimes almost uniform momentarily over the transverse section.

No trace was found of a simple frequency, but evidence was obtained of a predominant wave-length in the turbulent motion at the critical speed. Both these observations seem to agree with the approximate theory for flow between a pair of parallel planes given by Heisenberg.

## § 1. INTRODUCTION

THE primary aim of this investigation was to search for any evidence of regular periodicity in the motion of fluid that is flowing turbulently in a long straight tube.

The subject of turbulent flow through tubes was first treated systematically by Osborne Reynolds[*]; extensive accurate experiments were subsequently performed by Stanton and Pannell[†]; and a theoretical basis was finally given by Heisenberg[‡]. Heisenberg's paper contains extensive references to prior papers on the subject.

Heisenberg gives a detailed approximate theory for the flow between a pair of *parallel planes*. He concludes that all turbulence will ultimately get suppressed when the "Reynolds' number" $vd\rho/\mu$ is less than a critical value of the order $10^3$; here $v$, $d$, $\rho$, $\mu$, denote the mean velocity, distance between planes or tube diameter, fluid density and viscosity respectively. At greater speeds turbulence will not be suppressed if its "wave-length" is between maximum and minimum values, which are functions of $vd\rho/\mu$. When $vd\rho/\mu$ has the critical value, only turbulence of a certain critical wave-length will persist. Heisenberg suggests a critical wave-length equal to about $\pi$ times the distance between the planes; this is only an approximate estimate, and he says a more exact calculation is not feasible. Though Heisenberg suggests a single critical wave-length at the critical rate of flow, yet there is not supposed to be a single frequency; the velocity, and consequently the frequency, vary across the transverse section of the system.

$v, d, \rho, \mu$

[*] *Phil. Trans. R.S.* **174**, 935 (1883).

[†] *Proc. R.S.* A, **85**, 366 (1911); *Phil. Trans. R.S.* A, **214**, 199 (1914).

[‡] *Ann. der Physik*, **74**, **7**, 577 (1924).

## § 2. AURAL EXPERIMENTS

As the ear is known to be an excellent harmonic analyser, the first experiments were made by an aural method. A small hole was drilled in the side of a long tube and a stethoscope was connected to the hole. When air was blown through the long tube, the only sound heard in the stethoscope was like that of a wind. Next the stethoscope was connected to a small glass Pitot-tube, which was inserted in the exit end of the long tube. It was then found that, as the air speed was increased, a speed was reached at which pronounced crackling, like pistol shots, was heard. At still higher speeds a continuous roar was heard, but no trace of a musical note, except for æolian tones due to the presence of the Pitot-tube itself. The result of the experiment was the same if the Pitot-tube was placed in or near the jet of air emerging from the end of the long tube, except that in the latter position æolian tones were avoided. The failure to detect any trace of a musical note by this very sensitive method is in agreement with Heisenberg's theory.

In the tube, near its entrance, the flow was turbulent over the whole range of speeds considered above: the crackles heard near the exit therefore represent the first turbulence that has persisted throughout the length of the tube, which is from 500 to 550 diameters. It is thus the *lower* critical velocity that is detected. For tubes shorter than about 25 diameters no abrupt transition to turbulence is found: the tube is then so short that the eddies have not time to get damped down or to develop fully.

The transition to turbulence could also be detected by ear or eye by letting the emergent jet impinge on a long luminous gas flame. Or even the unaided ear placed near the air jet could detect the effects.

Table 1

| Fluid and method | Tube diameter (cm.) | Distance from entrance (in tube-diameters) | Lower critical velocity. Values of Reynolds' number, $vd\rho/\mu$ | | |
|---|---|---|---|---|---|
| | | | (i) | (ii) | (iii) |
| Air, stethoscope | $0 \cdot 199_8$ | 500 | 1950 | 2060 | 2130 |
| Air, stethoscope | $0 \cdot 178_5$ | 550 | 1890 | 1990 | 2060 |
| Water, deflected vane | $0 \cdot 178_5$ | 550 | — | 2260 | — |
| Water, deflected vane | $0 \cdot 74$ | 150 | 1980 | — | 2200 |
| Water, colour-band | $0 \cdot 77_9$ | 130 | — | 2250 | — |

Quantitative experiments were next performed, the results of which are given in the upper part of table 1. Though the crackling was very precise, yet the velocity

# W. N. Bond

for which it just started was not sharply defined. The crackles appeared to be distributed at random in time, becoming much more frequent as the rate of air flow was slightly increased. For convenience of measurement three stages were distinguished: (i) crackles every few seconds, (ii) 8 or 10 crackles a second, (iii) a roar with momentary lulls every few seconds.

## § 3. DEFLECTED VANE EXPERIMENTS

In order to find in more detail the nature of the turbulence and the transition, the air jet emerging from the long tube was allowed to impinge on a mica flake clamped at one edge, and measuring 1·5 · 1·5 · 0·005 cm. The mica vane carried a very small mirror, from which a beam of light could be reflected to a moving photographic film: and the vane was placed a few tube diameters away from the end of the tube, so as neither to affect the flow in the tube appreciably nor to be so far along the jet that the instability of the long jet itself should complicate the results.
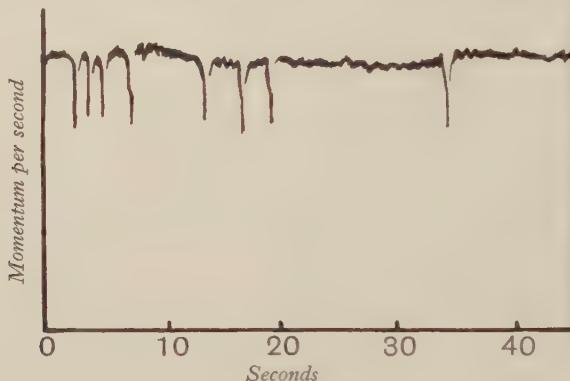


Fig. 1. Results for water ($d=0·74$ cm., $vd\rho/\mu=1980$).

In the case of air flow through the 0·178 cm.-diameter tube, the photographic records showed the intermittent turbulence at the transition stage (the crackling in the aural method), and indicated that each such burst of turbulence had occupied a length of tube of between 12 and 25 diameters.

The same mica vane was next used with water flowing through wider tubes. The change to wider tubes results in smaller speeds, and the change to water leads to smaller speeds, larger forces and more damping of the vane's free oscillations, all of which are desirable; the only disadvantage is the increase in the vane's free period. Below the critical speed the reflection was found to be proportional to the square of the rate of flow, as was to be expected. The first traces of turbulence are shown in figure 1, where the ordinates represent the force exerted by the jet on the vane, or the momentum per second of the emergent liquid. In figure 2 various results are collected together with a larger time-scale so as to show the transition to turbulence in more detail. The natural period and damping of the vane are also shown at the bottom of the diagram.

In the curves of figure 2, and in others obtained with yet wider tubes, no regular periodicity could be detected, apart from that due to the vane itself. This is in agreement with Heisenberg's theory which suggests* a single wave-length at the critical stage, but velocities and frequencies that vary across the transverse section of the tube†.

The noticeable features of the transition stage are the alternate periods of stable and turbulent flow, and the gradual commencement but rapid termination of each period of turbulence. The ratio of the extreme values of the ordinates (corresponding to maximum turbulence and stable flow) was estimated for each curve, allowance being made for errors due to the free oscillation of the vane. The mean of the values so obtained was 0·73 ± 0·006. This number may have been affected by constant errors. But it is significant to note that for a transition from parabolic velocity-distribution to uniform velocity across the whole transverse
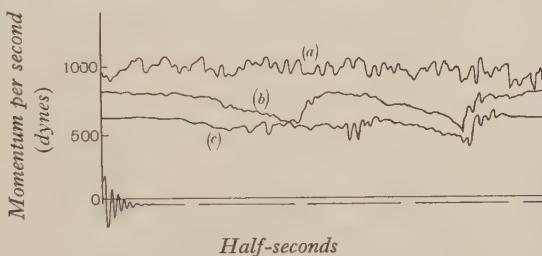


Fig. 2. Results for water (tube diameter 0·74 cm.); $v d\rho/\mu = (a)$ 2900; $(b)$ 2150; $(c)$ 2250.

section, the ratio should be 0·75: and a change from parabolic to a velocity distribution typical of that supposed to exist when there is turbulence should correspond to a ratio of ordinates of about 0·79. We are driven to the conclusion that during the transition stage and probably also during full turbulence, there are times when the velocity parallel to the tube-axis is appreciably more uniform over the transverse section than is indicated by the curves of *average* velocity distribution‡ as determined by Pitot-tubes.

Finally we may note the results of some measurements of the critical speeds made by this vane method (table 1). All the values fall within the range obtained by other observers, but the different lines in the table cannot be compared simply. The frequency of the eddy groups varies as $vd\rho/\mu$ varies: but for a fixed value of $vd\rho/\mu$ the frequency is probably proportional to $\mu/\rho d^2$, and changes with the fluid and tube-diameter.

## §4. COLOUR-BAND EXPERIMENTS

The colour-band method has (by some workers) been considered inapplicable to the determination of the *lower* critical velocity, as the motion near the entrance of the tube is then turbulent, and any colour injected there will have become more or less uniformly distributed across the tube before it reaches the later parts of the

* *Loc. cit.* 605 and 608.　　　　† *Loc. cit.* 609 and 616.
‡ T. E. Stanton, *Proc. R.S.* A, 85, 366 (1911).

tube where the motion may be in stable stream-lines. This difficulty was avoided by injection of the colour through holes in the wall of the tube, at a considerable distance from the tube entrance. At the transition stage intermittent turbulence was again observed, and each turbulent portion could be watched as it moved rapidly along the tube. Each was more abrupt and regular at its end than at its front, the appearance being approximately as indicated in figure 3.

The tubes for the above experiments were arranged almost horizontally, and water was passed through them. Small air-bubbles, that moved along the upper side of the tube, gave some further indication as to the effect of the turbulence. They
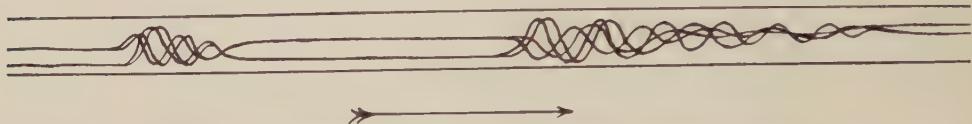


Fig. 3. Intermittent turbulence. (Colour-bands observed visually.)



Fig. 4. Distortion of colour-band due to abrupt stoppage of flow (the speed being initially slightly less than the critical).
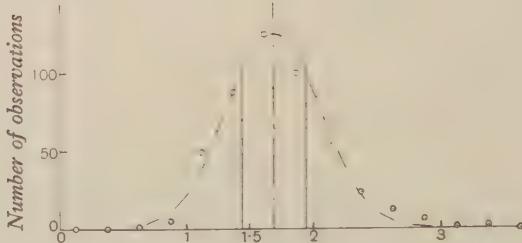


Fig. 5. Values of $\lambda$ expressed as multiples of the tube diameter.

no longer moved uniformly, but jumped forward rapidly, with a tendency to move sideways also, when any group of eddies passed, and then resumed their uniform motion. Even for quite small and slowly moving air-bubbles near the wall, the ratio of the two velocities was considerably greater than 2 : 1. This momentary increase in the velocity near the walls, and decrease near the axis, are more marked than we might have deduced by taking the ratio of the pressure-gradients for speeds just greater than and just less than the critical, as given by Stanton and Pannell*. The apparent discrepancy is explained (as we saw in the previous section of this paper) when we remember that only time-average values of the pressure-gradient were measured. The observations of the motion of air-bubbles show that, though the flow near the walls may remain in stable stream-lines whilst the flow in the

central parts of the tube is turbulent, yet the stream-lines will be distorted and the velocities will vary when the eddies are passing.

Let water be flowing through a long straight tube with abrupt entrance, so that in the earlier part of the tube the flow is turbulent but in the later part stable, as indicated by a colour-band injected part-way along. Then if the flow of liquid be abruptly stopped, it is found that the colour-band along the bottom side will remain unchanged if the speed has been appreciably below the critical: but if the speed has been nearly equal to the critical, the colour-band develops a sinuous form or becomes broken up into a series of approximately equal lengths, $\lambda$, as illustrated in figure 4. The details of the distortion of the colour-band vary with the initial speed and rapidity of stoppage, and the spacing is apt to be rather irregular: but the phenomenon proved sufficiently distinct to enable measurements to be made. $\lambda$

460 measurements of this "wave-length," $\lambda$, from 30 experiments with each of two tubes, are collected statistically in figure 5. I conclude that this "wave-length," of about 1·7 times the diameter of the tube, corresponds to the critical value suggested by Heisenberg, and estimated by him to be of the order $\pi$ times the distance between a pair of parallel planes. (We may compare the ratio 1·7 : $\pi$ with the ratio of the "hydraulic mean depths," which is 1 : 2.)

Thus, no regular frequency was detected in the turbulent motion in the tube: but at the critical speed a more or less definite wave-length $\lambda$ equal to 1·7 $\times$ $d$ was found. These two results appear to be in agreement with the theoretical work of Heisenberg, who suggests a critical wave-length of the order stated above, but a wave-velocity that varies across the transverse section of the system.

## § 5. ACKNOWLEDGMENTS

## DISCUSSION

Dr E. G. Richardson. I should like to know whether Dr Bond traversed the Pitot tube across the end of the pipe from side to side. At lower velocities the turbulence will persist to the end of the pipe at the axis though not at the edges, so that the radial distance of the Pitot tube from the axis seems to me to be an important factor in measurements of critical velocity by the aural method. It is interesting to compare these results with the attempt made by Prof. Burgers in 1926 to detect, by means of a couple of hot wires, a definite wave-length in disturbances propagated along the floor of his large wind channel at Delft. As far as I know, a negative result was obtained.

\* *Loc. cit.*

*W. N. Bond*

AUTHOR'S REPLY. I did try the effect of traversing the Pitot tube across the end of the pipe, but merely observed that the aeolian tones were most noticeable when there was only a small gap between the Pitot tube and the wall of the pipe. The crackling was heard for all positions of the Pitot tube, even when it was not actually in the air-jet. Hence this experiment gave no evidence as to whether the turbulence was near the axis only of the pipe or was distributed more or less over the whole of the transverse section. The results given in the first two lines of table 1 were obtained with the stethoscope connected to a tube near to, but not in, the air-jet.

On the other hand, the experiments, especially the measurements of the decrease in momentum per second (see figures 1 and 2), indicated that during intermittent turbulence the end of each body of turbulence consists of a disturbance extending almost completely over the transverse section of the tube.

# THE SPECTRUM OF TREBLY-IONIZED CERIUM
## (Ce IV)

By J. S. BADAMI, Imperial College, South Kensington

*ABSTRACT*. The spectrum of the condensed spark of cerium has been investigated in the ultra-violet, and doublet combinations in Ce IV, in addition to those given by Gibbs and White, have been found. The $6^2P - 6^2D$ combination of La III also has been identified. Term values and ionization potentials of La III and Ce IV are calculated.

THE spectrum of Ce IV is very simple, as is evident from the term scheme given in table 1. It is similar in electronic structure to the spectra of Cs I, Ba II and La III. Some of its combinations can be identified by extrapolation from Cs I, etc. by means of the irregular and regular doublet laws, and of the

Table 1. Predicted terms of Ce IV.

| Orbits of outer electrons | | | | | | | | | | | Terms |
|---|---|---|---|---|---|---|---|---|---|---|---|
| $4_1$ | $4_2$ | $4_3$ | $4_4$ | $5_1$ | $5_2$ | $5_3$ | $6_1$ | $6_2$ | $6_3$ | $7_1$ | |
| 2 | 6 | 10 | | 2 | 6 | 1 | | | | | $5^2D$ |
| 2 | 6 | 10 | | 2 | 6 | | 1 | | | | $6^2S$ |
| 2 | 6 | 10 | | 2 | 6 | | | 1 | | | $6^2P$ |
| 2 | 6 | 10 | 1 | 2 | 6 | | | | | | $4^2F$ |
| 2 | 6 | 10 | | 2 | 6 | | | | | 1 | $7^2S$ |
| 2 | 6 | 10 | | 2 | 6 | | | | 1 | | $6^2D$ |

irregular doublet law modified so as to be applicable to transitions between two orbits of different total quantum numbers. The various transitions are considered below.

$6^2S_{\frac{1}{2}} - 6^2P_{\frac{1}{2}, \frac{3}{2}}$: For the identification of this pair of lines good guidance is provided by comparison with the behaviour of NaI-, KI- and RbI-like spectra, the details for which are shown in table 2.

These give a good idea of how the irregular doublet law, according to which the second differences should be very small, will be obeyed in CsI-like spectra, and roughly extrapolated values for $6S_{\frac{1}{2}} - 6P_{\frac{1}{2}}$ are shown below in brackets.

# J. S. Badami

$$6^2S_{\frac{1}{2}} - 6^2P_{\frac{1}{2}}$$

| | $\nu$ | $\Delta\nu$ | $\Delta^2\nu$ |
|---|---|---|---|
| Cs I | 11178 | | |
| | | 9084 | |
| Ba II | 20262 | | [970] |
| | | [8114] | |
| La III | [28376]* | | [430] |
| | | [7684] | |
| Ce IV | [36060] | | |

Table 2.  $^2S - {}^2P$ lines of Na-, K- and Rb-like spectra.

| $3^2S_{\frac{1}{2}} - 3^2P_{\frac{1}{2}}$ | | | $4^2S_{\frac{1}{2}} - 4^2P_{\frac{1}{2}}$ | | | $5^2S_{\frac{1}{2}} - 5^2P_{\frac{1}{2}}$ | | |
|---|---|---|---|---|---|---|---|---|
| $\nu$ | $\Delta\nu$ | $\Delta^2\nu$ | $\nu$ | $\Delta\nu$ | $\Delta^2\nu$ | $\nu$ | $\Delta\nu$ | $\Delta^2\nu$ |
| Na I  16956 | | | K I  12985 | | | Rb I  12579 | | |
| | 18713 | | | 12207 | | | 11136 | |
| Mg II 35669 | | 702 | Ca II 25192 | | 835 | Sr II 23715 | | 917 |
| | 18011 | | | 11372 | | | 10219 | |
| Al III 53680 | | 411 | Sc III 36564 | | 402 | Y III 33934 | | 435 |
| | 17600 | | | 10970 | | | 9784 | |
| Si IV  71280 | | | Ti IV 47534 | | | Zr IV 43718 | | |

By application of Sommerfeld's† regular doublet law

$$\Delta\nu = K\,(Z - S)^4,$$

$\Delta\nu$ the $(6^2P_{\frac{1}{2}} - 6^2P_{\frac{3}{2}})$ separation can be approximately calculated. $\Delta\nu$ is the required
$Z, S$ separation, $Z$ is the atomic number and $S$ is the screening constant. The constant
$K$ $K = 0{\cdot}0135$ for $6P$. Table 3 gives the values of the screening constant $S$ for NaI-,

Table 3.  Screening constants for $^2P_{\frac{1}{2}} - {}^2P_{\frac{3}{2}}$ separations in Na-, K-, Rb-
and Cs-like spectra.

| $3^2P_{\frac{1}{2}} - 3^2P_{\frac{3}{2}}$ | | $4^2P_{\frac{1}{2}} - 4^2P_{\frac{3}{2}}$ | | $5^2P_{\frac{1}{2}} - 5^2P_{\frac{3}{2}}$ | | $6^2P_{\frac{1}{2}} - 6^2P_{\frac{3}{2}}$ | |
|---|---|---|---|---|---|---|---|
| $S$ | $\Delta S$ | $S$ | $\Delta S$ | $S$ | $\Delta S$ | $S$ | $\Delta S$ |
| Na I  7·450 | | K I  13·036 | | Rb I  26·96 | | Cs I  40·77 | |
| | 0·844 | | 1·396 | | 2·56 | | 3·58 |
| Mg II 6·606 | | Ca II 11·640 | | Sr II  24·40 | | Ba II  37·19 | |
| | 0·455 | | 0·73 | | 1·45 | | [1·90] |
| Al III 6·151 | | Sc III 10·91 | | Y III  22·95 | | La III [35·29] | |
| | 0·227 | | 0·48 | | 1·00 | | [1·30] |
| Si IV  5·924 | | Ti IV 10·43 | | Zr IV 21·95 | | Ce IV [33·99] | |

KI- and RbI-like spectra, and the extrapolated values for La III and Ce IV, for
purposes of comparison. Taking the extrapolated value of $S$ for Ce IV we get
$(6^2P_{\frac{1}{2}} - 6^2P_{\frac{3}{2}}) \eqsim$ (approx.   ) 4500. The line $6^2S_{\frac{1}{2}}$    $6^2P_{\frac{3}{2}}$ would thus be located
near $\nu = (36060 + 4500) = 40560$, i.e. at about $\lambda 2465$, and this line should be the
stronger one of the pair. A line at $\lambda 2456{\cdot}81$ even by its appearance on one of the
plates was marked out from other lines. It was intense only at the tips and could

---

\* The observed value as given by Gibbs and White is 28424·3. This was not known to the author
when this extrapolation was made. See footnote † on p. 55.

† A. Sommerfeld, *Atomic Structure and Spectral Lines*, Engl. Trans. p. 496 (Methuen and Co.
1923).

be unmistakably identified as $6^2S_{\frac{1}{2}} - 6^2P_{\frac{3}{2}}$. Simultaneously Gibbs and White* corrected their previous† identifications for this doublet of Ce IV and gave:

| $\lambda$ vac. | $\nu$ | $\Delta\nu$ | |
|---|---|---|---|
| 2779·07 | 35983·3 | | $6^2S_{\frac{1}{2}} - 6^2P_{\frac{1}{2}}$ |
| | | 4706·9 | |
| 2457·59 | 40690·2 | | $6^2S_{\frac{1}{2}} - 6^2P_{\frac{3}{2}}$ |

$6^2P_{\frac{1}{2},\frac{3}{2}} - 7^2S_{\frac{1}{2}}$: This combination involves a change in the total quantum number and the irregular doublet law cannot be applied directly. Millikan and Bowen‡ give the following formula:

$$\nu' = \nu - \{R\,(Z-A)^2\,(n_2{}^2 - n_1{}^2)\}/n_1{}^2\,n_2{}^2,$$

where $\nu$ is the observed frequency, $R$ the Rydberg constant, $Z$ the atomic number, $n_2$ and $n_1$ the total quantum numbers involved, and $A$ any suitable constant. To this $\nu'$, or modified $\nu$, the irregular doublet law can be applied. For Cs the atomic number is 55, so we choose $A$ equal to 54. We obtain the following values for $\nu - \nu'$: 808·3 for Cs I, 3233·1 for Ba II, 7274·5 for La III and 12932·5 for Ce IV. For the $6^2P_{\frac{3}{2}} - 7^2S_{\frac{1}{2}}$ transition the values of $\nu$ and $\nu'$ for Cs I and Ba II are as follows:

Cs I, $\nu = 6803·3$, $\nu' = 5995·0$; Ba II, $\nu = 20402·6$, $\nu' = 17169·5$.

$$\Delta\nu' = 17169·5 - 5995·0 = 11174·5.$$

Taking a progressive variation with atomic number in the value of $\nu'$ we predict for La III $\nu' = 17169·5 + 11174·5 = [28344]$ and $\nu = 28344 + 7274 = [35618]$ and similarly for Ce IV $\nu' = [39518]$ and $\nu = [52451]$. For Ce IV the difference $6^2P_{\frac{1}{2}} - 6^2P_{\frac{3}{2}}$ being already known to be $\Delta\nu = 4707·0$ we can locate the other line $6^2P_{\frac{1}{2}} - 7^2S_{\frac{1}{2}}$ at about $\nu = 52451 + 4707 = [57158]$.

There are two lines of cerium observed in the condensed spark at $\lambda 2009·98$ and $\lambda 1836·19$ with $\Delta\nu = 4706·5$, $\lambda 2009·98$ being the stronger of the two. From their behaviour and appearance, especially of $\lambda 2009·98$, we can classify them as:

| | | |
|---|---|---|
| $\lambda 2009·98$; | $\nu = 49735·7$; | $6^2P_{\frac{3}{2}} - 7^2S_{\frac{1}{2}}$: |
| $\lambda 1836·19$; | $\nu = 54442·2$; | $6^2P_{\frac{1}{2}} - 7^2S_{\frac{1}{2}}$. |

From the available data for La it was not possible to pick out the corresponding doublet.

$6^2P_{\frac{1}{2},\frac{3}{2}} - 6^2D_{\frac{3}{2},\frac{5}{2}}$: From data for Cs I and Ba II, by application of the irregular and regular doublet laws as before, we obtain the following approximate values for this combination:

| | $6^2P_{\frac{1}{2}} - 6^2D_{\frac{3}{2}}$ | $6^2P_{\frac{3}{2}} - 6^2D_{\frac{5}{2}}$ | $6^2P_{\frac{3}{2}} - 6^2D_{\frac{3}{2}}$ |
|---|---|---|---|
| La III | [40170] | [37505] | [37075] |
| Ce IV | [55287] | [51300] | [50580] |

* R. C. Gibbs and H. E. White, *Phys. Rev.* 33, 157 (1929).
† R. C. Gibbs and H. E. White, *Proc. Nat. Acad. Sc.* 12, 551 (1926). This paper had escaped notice. Both La III and Ce IV, $6^2S - 6^2P$, doublets were identified; for Ce IV the values given were $\lambda$ vac. 2769·2 and $\lambda$ vac. 2455·1 with $\Delta\nu = 4619·8$.
‡ R. A. Millikan and I. S. Bowen, *Phys. Rev.* 26, 313 (1925).

The following three lines (La III) of the lanthanum spark spectrum satisfy the conditions regarding the differences and intensities:

| $\lambda$ | $\nu$ | |
|---|---|---|
| 2476·71 | 40363·9 | $6^2P_{\frac{1}{2}} - 6^2D_{\frac{3}{2}}$ |
| 2651·68 | 37700·7 ⌐ 3095·0 | $6^2P_{\frac{3}{2}} - 6^2D_{\frac{5}{2}}$ |
| | 431·8 | |
| 2682·4 | 37268·9 | $6^2P_{\frac{3}{2}} - 6^2D_{\frac{3}{2}}$ |

The value obtained for the difference $6^2D_{\frac{3}{2}} - 6^2D_{\frac{5}{2}}$ is very near that predicted.

In the cerium spectrum there is a faint line at $\lambda 1949·85$, $\nu = 51269·2$, which, from its appearance at tips on some plates and its position, may be classified as the $6^2P_{\frac{3}{2}} - 6^2D_{\frac{5}{2}}$ combination of Ce IV; but the other two lines are not observed, being perhaps very faint, so this finding cannot be confirmed.

Knowing the values of $6S - 6P$ and $6P - 7S$ for Ce IV, we can calculate approximately the term values for $6P$ and $6S$; and if the tentative location of $6P - 6D$ is correct the term value of $6D$ also can be calculated. Knowing $6D$, we can get an idea of the $5D$ term from Rydberg's tables. Thus we find

$$6^2P_{\frac{1}{2}} = 167810, \quad 6^2S_{\frac{1}{2}} = 203794, \quad 6^2D_{\frac{5}{2}} = 11834 \text{ and } 5^2D_{\frac{5}{2}} = 20012.$$

The $5D$ term in La III is considerably deeper than $6S$. The above estimated values show however that in Ce IV the $5D$ if not less than $6S$ cannot be very far above it.

$5^2D_{\frac{3}{2}, \frac{5}{2}} - 6^2P_{\frac{1}{2}, \frac{3}{2}}$: From the values of $\Delta\nu - 5^2D_{\frac{3}{2}} - 5^2D_{\frac{5}{2}}$ for Cs I, etc. the value of $\Delta\nu$ for Ce IV can be predicted, by means of the regular doublet law, to be about 3340. The following three lines of Ce IV, owing to their frequency differences and positions, are classified as the $5D - 6P$ multiplet:

| $\lambda$ | $\nu$ | |
|---|---|---|
| 2430·25 | 41135·5 | $5^2D_{\frac{3}{2}} - 6^2P_{\frac{1}{2}}$ |
| 2350·16 | 42537·3 ⌐ 4706·7 | $5^2D_{\frac{5}{2}} - 6^2P_{\frac{3}{2}}$ |
| | 3304·9 | |
| 2180·71 | 45842·2 | $5^2D_{\frac{3}{2}} - 6^2P_{\frac{3}{2}}$ |

The appearance and intensities of these lines are entirely appropriate for this combination.

From $5D - 6P$ and $6P - 6D$ by means of the Rydberg formula the term value of $6P$ can be calculated. Table 4 gives the term values for La III and Ce IV. For Ce IV a mean of the two values of $6P$, calculated from the $S$ series and the $D$ series respectively, is given. All the other terms are based on $6P$.

The behaviour of the $5D$ term is somewhat anomalous. For Cs I, Ba II, La III and Ce IV the term values for $5^2D_{\frac{3}{2}}$, $6^2S_{\frac{1}{2}}$ and $6^2P_{\frac{1}{2}}$ are given in table 5. They show that for Cs I, $6S$ is the deepest term and $6P$ is deeper than $5D$; for Ba II, $6S$ is still the deepest term but $5D$ is deeper than $6P$; for La III, $5D$ is the deepest term, $6S$ being of course deeper than $6P$; while for Ce IV also $5D$ is the deepest term

Table 4. Term values for La III and Ce IV.

| Terms | La III | | Ce IV | |
|-------|--------|--|-------|--|
| $5^2D_{\frac{3}{2}}$ | 165574·3 ⌐ | | 210895·3 ⌐ | |
| | | 1603·8 | | 3304·9 |
| $5^2D_{\frac{5}{2}}$ | 163970·5 ⌐ | | 207590·4 ⌐ | |
| $6^2S_{\frac{1}{2}}$ | 151984·3 | | 205743·7 | |
| $6^2P_{\frac{1}{2}}$ | 123560·0 ⌐ | | 169760·0 ⌐ | |
| | | 3095·4 | | 4706·9 |
| $6^2P_{\frac{3}{2}}$ | 120464·6 ⌐ | | 165053·1 ⌐ | |
| $7^2S_{\frac{1}{2}}$ | — | | 115317·6 | |
| $6^2D_{\frac{3}{2}}$ | 83195·7 ⌐ | | [114504] ⌐ | |
| | | 431·8 | | [720] |
| $6^2D_{\frac{5}{2}}$ | 82763·9 ⌐ | | 113783·9 ⌐ | |

but not so much deeper than $6S$ as in La III. Table 5 also gives the ionization potentials calculated from the deepest levels*, which are underlined.

Table 5. Deep terms and ionization potentials in Cs-like spectra.

| Terms | $5^2D_{\frac{3}{2}}$ | $6^2S_{\frac{1}{2}}$ | $6^2P_{\frac{1}{2}}$ | Ionization potential |
|-------|-----------|-----------|-----------|-----------|
| Cs I | 16905·0 | 31404·6 | 20226·3 | 3·88 |
| Ba II | 68674·3 | 80664·9 | 60403·4 | 9·96 |
| La III | 165574·3 | 151984·3 | 123560·0 | 20·4 |
| Ce IV | 210895·3 | 205743·7 | 169760·0 | 26·0 |

Tables 6 and 7 give lists of the classified lines of La III and Ce IV respectively. The wave-length measures for lanthanum are taken from Eder and Valenta's *Atlas Typischer Spektren*, corrected to I.A.; for cerium they are by the author.

Table 6. La III; classified lines.

| λ air | (Int.) | ν | Classification | |
|-------|--------|---|----------------|--|
| 3517·11 | (20) | 28424·3 | $6^2S_{\frac{1}{2}} - 6^2P_{\frac{1}{2}}$ ⎫ | Gibbs and |
| 3171·66 | (15) | 31520·2 | $6^2S_{\frac{1}{2}} - 6^2P_{\frac{3}{2}}$ ⎭ | White |
| 2682·4 | (2) | 37268·9 | $6^2P_{\frac{3}{2}} - 6^2D_{\frac{3}{2}}$ ⎫ | |
| 2651·68 | (10) | 37700·7 | $6^2P_{\frac{3}{2}} - 6^2D_{\frac{5}{2}}$ ⎬ | Present |
| 2476·71 | (8) | 40363·9 | $6^2P_{\frac{1}{2}} - 6^2D_{\frac{3}{2}}$ ⎭ | investigation |
| 2379·41 | (10) | 42014·3 | $5^2D_{\frac{3}{2}} - 6^2P_{\frac{1}{2}}$ ⎫ | |
| 2297·83 | (6) | 43505·9 | $5^2D_{\frac{5}{2}} - 6^2P_{\frac{3}{2}}$ ⎬ | Gibbs and |
| 2216·13 | (2) | 45109·7 | $5^2D_{\frac{3}{2}} - 6^2P_{\frac{3}{2}}$ ⎭ | White |

* It is assumed here, as suggested by Gibbs and White, *loc. cit.*, that the $4^2F$ term is not the deepest. The suggestion depends on the correctness of the assignment of term values of the $4^2F_{\frac{5}{2},\frac{7}{2}}$ levels for Ba II by Paschen and Götze.

Table 7. Ce IV; classified lines.

| λ air | (Int.) | ν | Classification | |
|---|---|---|---|---|
| 2778·23 | (4) | 35983·5 | $6^2S_{\frac{1}{2}} - 6^2P_{\frac{1}{2}}$ } | Gibbs and |
| 2456·81* | (6) | 40690·9 | $6^2S_{\frac{1}{2}} - 6^2P_{\frac{3}{2}}$ } | White |
| 2430·25 | (6) | 41135·5 | $5^2D_{\frac{3}{2}} - 6^2P_{\frac{1}{2}}$ | |
| 2350·16 | (5) | 42537·3 | $5^2D_{\frac{5}{2}} - 6^2P_{\frac{3}{2}}$ } | Present |
| 2180·71 | (4) | 45842·2 | $5^2D_{\frac{3}{2}} - 6^2P_{\frac{3}{2}}$ } | investigation |
| 2009·98 | (3) | 49735·7 | $6^2P_{\frac{3}{2}} - 7^2S_{\frac{1}{2}}$ } | Present |
| 1836·19 | (2) | 54442·2 | $6^2P_{\frac{1}{2}} - 7^2S_{\frac{1}{2}}$ } | investigation |
| 1949·85 | (1) | 51269·2 | $6^2P_{\frac{3}{2}} - 6^2D_{\frac{5}{2}}$ | Ditto |

\* This line was classified independently in the present investigation.

# THE PHOTOGRAPHIC EFFECTS OF GAMMA-RAYS

## By J. S. ROGERS, B.A., M.Sc., F.Inst.P.,

### Senior Lecturer in Natural Philosophy, University of Melbourne

*ABSTRACT.* The photographic action of $\gamma$-rays from radium and radon in equilibrium with their short-lived products has been investigated, the rays being filtered with lead screens of thicknesses 0, 0·19, 1·42, 2·61 and 4·03 cm. The variations of photographic density both with time and with intensity have been examined. The shape of the characteristic ($C$) curves ($D - \log I$) have been found to be independent of the filtering, and the same holds for the Hurter-Driffield (H.D.) curves ($D - \log t$), except when no lead filter is used. The value of $p$ in the Schwarzschild relation, $D = f(It^p)$, has been found to be unity for all the lead filters. The absorption coefficient of lead for $\gamma$-rays from the sources used has been found to be 0·533 cm$^{-1}$ for thicknesses of lead from 1 to 7 cm.

---

## § 1. INTRODUCTION

ALTHOUGH there have been several systematic investigations of the photographic effects of X-rays*, no experiments appear to have been carried out on the photographic action of $\gamma$-rays. This is no doubt due to the smallness of the action of these rays, which suffer very little absorption in the photographic emulsion. Generally, therefore, investigations of $\gamma$-rays have been carried out with ionization chambers designed to absorb an appreciable fraction of the rays. The photographic method has, however, one advantage, for although the instantaneous effect may be small this effect is additive with time, and with sufficiently long exposures even the smallest $\gamma$-ray intensities can be measured. Experiments in this laboratory have shown the convenience of the photographic method of measuring X-ray intensities†.

Experiments have been undertaken to examine the variation of photographic density with time of exposure (constant intensity) and the variation of density with intensity (constant time) for $\gamma$-rays filtered through various thicknesses of lead. From the curves so obtained the absorption-coefficient of $\gamma$-rays in lead has been obtained. A method has been developed for determining absorption-coefficients by a photographic method in which these curves need not be drawn.

* E.g. W. Friederich and P. P. Koch, *Ann. der Phys.* **45**, 399 (1914); R. Glocker and W. Traub, *Phys. Zeit.* **22**, 345 (1921); A. Bouwers, *Dissertation* (Utrecht 1924); *Zeit. für. Phys.* **14**, 374 (1923).
† Miss Allen and T. H. Laby, *Proc. R.S. Vict.* **31**, 421 (1919); H. C. Webster, *Proc. Phys. Soc.* **41**, 181 (1929); C. E. Eddy and T. H. Laby, *Proc. R.S.* **127**, 20 (1930).

## § 2. APPARATUS

Gamma-rays from a source $R$, figure 1, were confined to a narrow vertical channel by two rectangular lead blocks $B$, 15·3 cm. long, 2·3 cm. wide, and 7·5 cm. high, standing on a wooden base. The distance apart of these at the source end was 4 mm. and they opened to a distance of 8 mm. at the film end. The film, Agfa duplitized*, was held in a special holder $H$ constructed as follows. A groove was milled in a piece of aluminium sheet 10 cm. by 6 cm. and approximately 4 mm. thick so that a piece of film 6 cm. by 1·8 cm. could just be accommodated, the depth of the groove being equal to the thickness of the film. The piece of film was backed with a thin sheet of aluminium the inside face of which was covered with velvet, and the latter sheet was clamped to the former by two screws, so that the film-holder was perfectly light tight. The film was exposed so that the long edge was
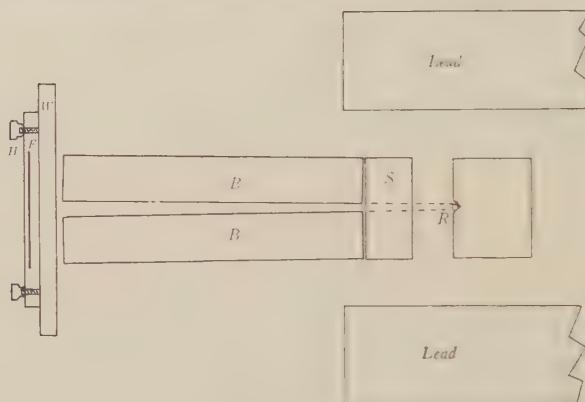


Fig. 1. Sketch of apparatus.

horizontal. During exposures the film-holder was carried by a vertical soft wood frame $W$ the centre of which was cut away. This frame carried two aluminium bolts and two holes in $H$ permitted it to be slipped over these bolts. The film-holder was then clamped by two aluminium nuts the ends of which fitted geo-metrically into the countersunk holes in $H$. By this means the film was always placed in the same position relative to the source. The $\gamma$-rays after passing through the absorbing screens passed through 17 cm. of air and 0·38 cm. of aluminium before striking the film.

The sources of $\gamma$-radiation used were radium and radon contained in equilibrium with their short-lived products, in glass tubes 4·8 cm. long and 0·35 mm. in diameter. The source was supported vertically in a shallow recess in a wooden block lined with cotton wool and was held in position with the minimum quantity of fine copper wire. At the sides of the source, and distant approximately 5 cm. from it,

---

* Duplitized film was used to reduce the time of exposure. The double layer of emulsion pro-duced no uncertainty as the same value of the photographic density was obtained whichever side of the film was facing the photometer lamp.

were lead blocks 5 cm. wide. Over the top of the source were 10 cm. of lead. For the Hurter-Driffield curves (*HD* curves)—i.e. those in which density is plotted against the logarithm of time—a tube of radium carbonate was used, the radium content of this being 103·6 mg. For the characteristic curves (*C* curves), in which density is plotted against the logarithm of the intensity, a tube containing radon was used which had a $\gamma$-ray activity equal to 400 mg. of radium three hours after sealing off.

In some of the later absorption experiments, four tubes containing radium carbonate were employed and these were kept in the brass cases supplied by the Radium Belge. These tubes of radium content 94·8, 99·0, 90·6, and 89·8 mg. respectively were placed as closely together as possible in vertical holes in a wooden block so that their axes were in line with the centre of the channel formed by the lead blocks *BB*. The tubes were always placed in the same order in the wooden block. The distance of the source *R* was 21·6 cm. from the film when radium in glass alone was used, but was several centimetres more when the four tubes were used together.

The lead absorbing screens were placed at *S* and were sufficiently wide to cover the whole width of the blocks *B*. These were rectangular and were carefully machined. They were cut from a pig of Broken Hill Associated Smelters lead which is very nearly pure metal, being 99·9915 per cent. pure as estimated by difference; the most prevalent impurity is antimony (0·004 per cent.).

## § 3. EXPERIMENTAL

*Development of films.* The films were developed with a metol-hydroquinone developer for 5 minutes at 18° C. In order to ensure uniformity of development the films of any one series were all developed together. A holder was constructed capable of holding twelve pieces of film vertically and for development a litre of developer was used and was placed in a two litre beaker. This volume of developer was brought to 18° C. and the temperature remained sensibly constant during the period of development. During the whole five minutes of development the film holder was moved up and down, so that the liquid surfaces at the film were continually being renewed. During fixing the same vertical agitation of the film was maintained.

*Density measurement.* The density was measured with a Moll microphotometer. During photometry the current through the heating-lamp was maintained constant at 3·9 amp. As photographic density is given by $\log_{10}$ [(galvanometer deflection produced by the heat energy transmitted by the unexposed portion of the film)/(that for energy transmitted by the exposed portion)], two readings would be necessary for each film, provided that the readings in the exposed and unexposed portions were constant among themselves. Owing, however, to irregularities in the photographic emulsion and in the thickness of the gelatine, and to non-uniformity of development, readings in any one portion were never quite constant, though, with the film used and the precautions taken during development, variations in the

readings were small. Figure 2, a photometer curve obtained by movement of the film through a definite distance between consecutive readings, shows the magnitude of the variations. In obtaining the actual densities, however, curves similar to figure 2 were not drawn for each film, but the mean galvanometer deflections were obtained. For the unexposed portion this averaging was done over a distance of approximately 0·7 to 1·7 cm. from the apparent edge of the exposed portion on one side, this side being determined by a mark on the film placed there before exposure.
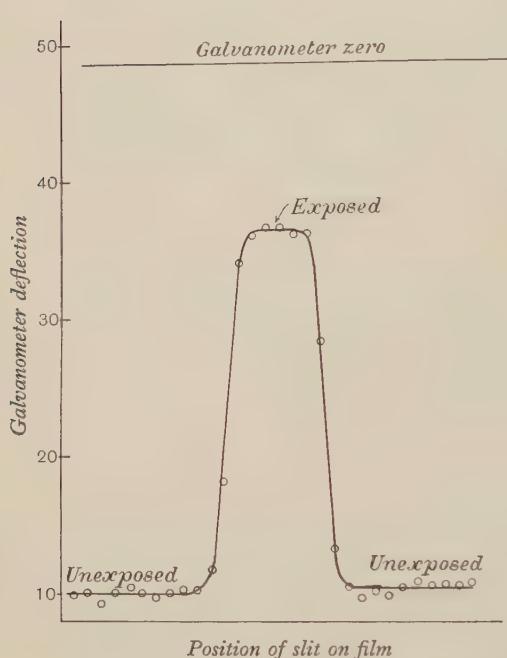


Fig. 2. Photometry of film exposed for 60 min.
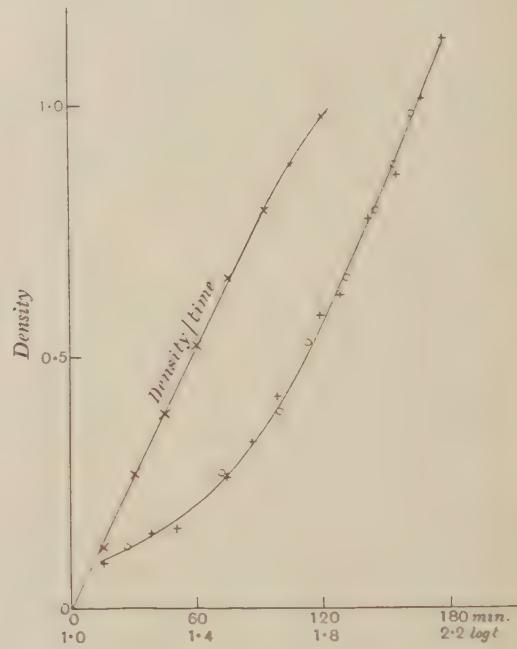


Fig. 3. Curves obtained with γ-rays filtered through 1·42 cm. of lead. o, *HD* curve; +, *C* curve.

The accuracy of the whole method—i.e. uniformity of conditions of exposure, uniformity of film, uniformity of development and accuracy in photometry—can be checked by exposure of a number of films in turn under exactly the same conditions; they are developed together and their densities are then measured. Table 1 represents a series of such determinations. It will be seen that the greatest accuracy is obtained with densities in the vicinity of 0·7, where the average departure from the mean is just over 1 per cent.

Table 1. Reproducibility of density determinations.

| Individual readings | Mean |
|---|---|
| 1·06, 1·10, 1·11 | 1·09 ± 0·02 |
| 1·16, 1·17, 1·22 | 1·18 ± 0·02 |
| 0·741, 0·760, 0·778, 0·769 | 0·76 ± 0·01 |
| 0·31, 0·35, 0·34, 0·31, 0·30, 0·34, 0·35 | 0·33 ± 0·02 |

In general, densities greater than 1 were not employed, for, with the method used for photometering, the accuracy with which densities greater than 1 can be measured decreases with density. Thus, for density 2 the galvanometer deflection for the exposed portion would be 0·01 of that for the unexposed portion, and it is questionable whether a 10 per cent. accuracy could be attained.

*The curves.* HD and C curves were obtained for γ-rays after they had passed through the following thicknesses of lead: 0, 0·19, 1·42, 2·61, 4·03 cm. The number of points for each curve varied between 8 and 12.
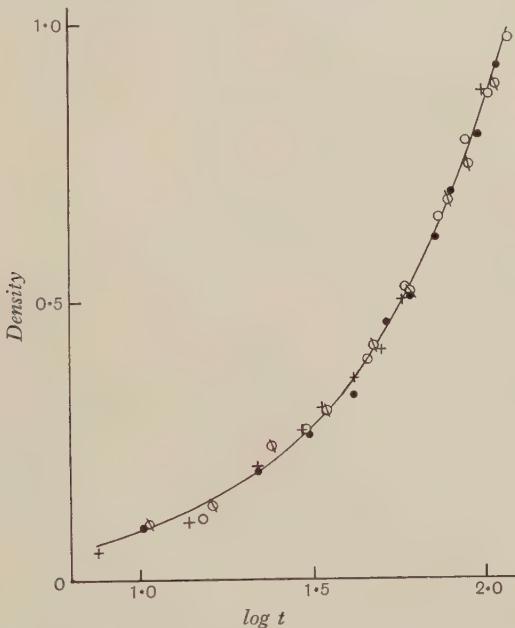


Fig. 4. *HD* curves obtained for γ-rays filtered through various thicknesses of lead. *HD* curves: •, 0·19 cm. lead; ○, 1·42 cm. lead; +, 2·61 cm. lead; ◌, 4·03 cm. lead.

(a) *Variation of density with time.* Figure 3 shows the results of readings obtained with 1·42 cm. of lead, the density $D$ has been plotted both against the time of exposure $t$ and against log $t$. It will be seen that $D$ is proportional to $t$ in the region extending from $D = 0$ to $D = 0·8$, while $D$ is proportional to log $t$ at densities greater than 0·8. The same remarks apply to the curves obtained with the other four thicknesses of lead. Figure 4 shows a combined curve formed from the four *HD* curves corresponding to γ-rays filtered through 0·19, 1·42, 2·61, 4·03 cm. of lead; the scale for log $t$ is the same for all four, but those for the first, third and fourth have been laterally displaced*. The single curve represents the four sets of readings equally well, so that the variation of density with log $t$ is unaffected by the

* To produce density 0·9 exposures of approximately 60, 110, 210 and 420 minutes were required with the different filters.

range of filters used. This statement does not hold for the curve obtained without lead, for which the slope of that part of the curve where $D$ is proportional to $\log t$ is less than that for the common curve. The numerical value of the slope $\gamma$ for the common curve is 2·0, while that for no lead-filtering is 1·5.

$D, I$

  (b) *Variation of density D with intensity I.* Twelve exposures for each of the five filterings were obtained over a period of a fortnight, the times of exposure being 10, 15, 45, 60 and 120 minutes for 0, 0·19, 1·42, 2·61 and 4·03 cm. of lead respectively. For the calculation of the intensities the half-value-period of radon was taken as 3·85 days. As for the $HD$ curves, $D$ is proportional to $I$ for values of $D$ up to
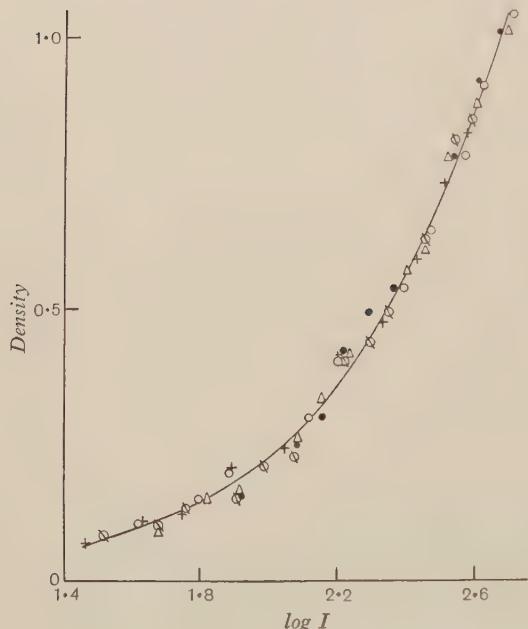


Fig. 5. Characteristic curves obtained with $\gamma$-rays with different filtering. $C$ curves: o, no lead; •, 0·19 cm. lead; △, 1·42 cm. lead; ◌, 2·61 cm. lead; +, 4·03 cm. lead.
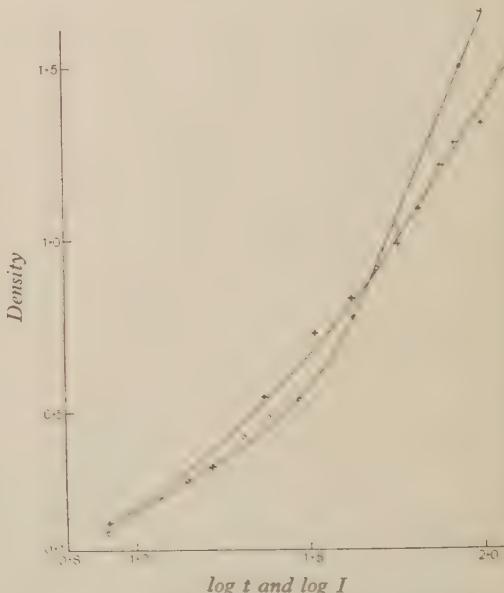
Fig. 6. Curves obtained with no lead filtering. o, $HD$ curve; +, $C$ curve.

0·8; and for higher densities $D$ is proportional to $\log I$. In figure 5 all the readings for the $C$ curves with the five different filterings are represented on one graph, the scale for $\log I$ being the same throughout, though the numerical values differ for the various sets of points. The conclusion is therefore drawn that the variation of density with $\log I$ is independent of the filtering of the $\gamma$-rays.

  The readings for the $C$ curve for $\gamma$-rays filtered by 1·42 cm. of lead are represented on figure 3, the points being indicated by . It will be seen that the $HD$ and $C$ curves are identical. This statement holds also for the other three filterings of lead but does not hold when no lead filter was used. Figure 6 shows both the $HD$ and $C$ curves obtained with no lead filter. These have been taken to higher densities than the remainder of the curves in the attempt to separate them with greater certainty.

## §4. DISCUSSION OF THE DENSITY CURVES

(i) As the *HD* and *C* curves for all filterings (except those obtained with no lead screen) coincide, the conclusion is drawn that, for $\gamma$-rays, the variation of density with time is of exactly the same nature as the variation of density with intensity, and hence the Bunsen-Roscoe reciprocity law holds, and the value of the exponent $p$ in Schwarzschild's law ($D \propto It^p$) is unity. Various experiments have determined values of $p$ for X-rays, and the values found have been in the vicinity of unity*. Bouwers has stated that this value may be due to the emission of X-rays being an intermittent process, as intermittent sources of ordinary light produce high values of $p$. In these experiments, however, the sources either have been constant—radium produces the most constant radiation that could affect a photographic plate—or else have decreased in a regular manner, so that the resulting value of $p$ cannot be attributed to any intermittence of the source. The curves obtained without lead cannot be discussed in this connexion, as, in the absence of a magnetic field, $\beta$-rays from the sources were able to affect the photographic film, whereas with the other filterings these were all absorbed before reaching the film. The question whether or not the value of 0·7 of $p$, given by the curves obtained without lead, is due to $\beta$-rays has not been investigated, as the experiments have been performed in the strong room of the Commonwealth Radium Laboratory, where there is no direct current supply for an electromagnet.

(ii) As the curves for all thicknesses of lead are identical there are two possible conclusions. The first is that the $\gamma$-rays incident on the film are of the same quality for each filter, and the second that the shape of the density-curves representing the photographic action of $\gamma$-rays is independent of the wave-length of the rays. It will be shown later that, although the $\gamma$-rays emerging from the three thickest filters have the same absorption-coefficient, those through 0·19 cm. have a different value, and hence, if constancy of absorption-coefficient indicates constancy of wave-length, the effective wave-length of the rays from the thinnest filter differs from that from the others. Hence even if the quality of the $\gamma$-rays from the three thickest filters is the same, the second conclusion appears to be the correct one, and it is in agreement with the results found for X-rays by Glocker and Traub, who showed that this independence holds for wave-lengths from 1·1 to 0·4 A.U., and by Bouwers who obtained similar results in the range 1·54 to 0·18 A.U.

(iii) The direct proportionality between density and time or intensity up to $D = 0·8$ is comparable with the result found by Glocker and Traub, who showed that the proportionality held for X-rays up to $D = 0·6$ whatever development conditions (time and temperature) were used. These authors found that $D$ varied as log $t$ between densities 1·3 and 4. Such high densities have not been examined here, but the proportionality appears to begin at about $D = 0·8$.

* See, for instance, R. Glocker and W. Traub, *loc. cit.* and A. Bouwers, *loc. cit.*

*J. S. Rogers*

## § 5. DETERMINATION OF THE ABSORPTION COEFFICIENT OF LEAD FROM THE DENSITY CURVES

As the value of $p$ has been shown to be unity, the photographic density is proportional to the product $It$ when $D$ has the value 0·8 or less. Suppose now that we consider within this range, some constant value of $D$, taken from each of the $C$ curves obtained through 0·19, 1·42, 2·61 and 4·03 cm. of lead. To produce this density there must be emergent from each filter the same value of the product $It$, but the value of $I_1 t_1$ incident on the filter will depend on the thickness $d_1$ of the

$I_1, t_1^1, d_1$
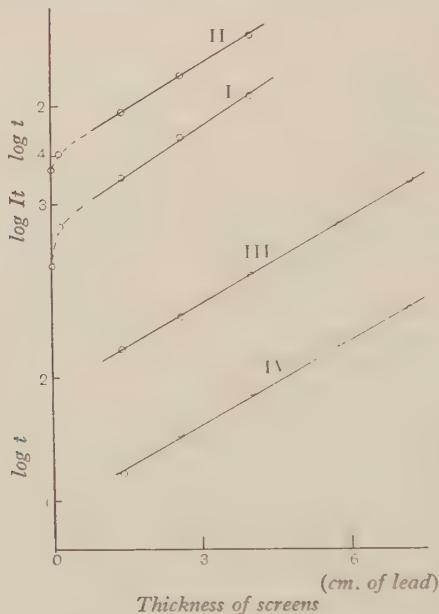


Fig. 7. Absorption curves for lead.

$\mu$

$J, J_0$

filter. The general equation, $J = J_0 e^{-\mu d}$ for $\mu$, the absorption-coefficient, where $J_1, J_0$ are the intensities of the emergent and incident beams respectively, can therefore be replaced by

$$It = I_1 t_1 e^{-\mu d_1},$$

and for a second filter of thickness $d_2$,

$$It = I_2 t_2 e^{-\mu d_2}.$$

Thus equating these two values of $It$ we have

$$I_1 t_1 e^{-\mu d_1} = I_2 t_2 e^{-\mu d_2},$$

and hence
$$\mu = (\log I_1 t_1 - \log I_2 t_2)/(d_1 - d_2) \qquad \ldots\ldots(1).$$

If the source is of constant intensity,

$$I_1 = I_2,$$

and
$$\mu = (\log t_1 - \log t_2)/(d_1 - d_2) \qquad \ldots\ldots(2).$$

By use of (1) a series of values of $\mu$ for different densities can be obtained from the $C$ curves, and by (2) a series of values of $\mu$ from the $HD$ curves.

Curve I, figure 7, shows the values of log $It$ plotted against $D$ for $D = 0.8$. Three such determinations for different densities gave the value of $\mu = 0.560 \pm 0.007$ cm$^{-1}$, for $d = 1.4$ to $d = 4.0$ cm. Between 0.19 cm. and 1.4 cm. the value of $\mu$ is higher.

Curve II of the same figure shows log $t$ plotted against $d$ for values obtained from the $HD$ curves. Four determinations gave the value $\mu = 0.532 \pm 0.008$ cm$^{-1}$. Although the agreement between the two values is not very good, it is to be noted that values obtained from the curves depend on films which have been developed at quite different times; and although the greatest care has been exercised in reproducing the same conditions of development, there is, no doubt, some uncertainty introduced on this account.

### § 6. PHOTOGRAPHIC DETERMINATION OF ABSORPTION-COEFFICIENTS

The photographic method can however be used in a manner in which this uncertainty of development is eliminated. In this method a source of constant intensity (374 mg. of radium) was employed and exposures were obtained with a series of absorbers of different thicknesses. The time of exposure for each absorber was so chosen that approximately the same density was produced, the densities always being less than 0.8, i.e. in the range where density is proportional to time of exposure. All the films obtained in any one series were then developed and fixed together. From the densities so obtained the times of exposure to produce some standard density were calculated. Then log $t$ could be plotted against $d$, and $\mu$ could be evaluated. The value of $\mu$ so obtained was 0.528 cm$^{-1}$. Another series obtained with densities of the order 0.3 is represented in Curve IV and gave the value 0.524 cm$^{-1}$ for $\mu$.

The mean value of $\mu$ from all the determinations is 0.533 $\pm$ 0.008 cm$^{-1}$, if half weight is given to the values obtained from the $C$ and $HD$ curves for reasons which have been previously discussed, and this value holds for thicknesses of lead ranging from 7 cm. down to about 1 cm. This is exactly the same value as that obtained by Kohlrausch* for the harder rays from RaC but is considerably less than the value 0.721 obtained by Ahmad† with a filter of 1 cm. of lead.

The absorption experiments are being extended to a large range of elements.

### § 7. ACKNOWLEDGMENTS

* K. W. F. Kohlrausch, *Wien. Ber.* **126**, 893 (1917).

† N. Ahmad, *Proc. R.S.* **109**, 206 (1925).

# THE SPECTRUM OF DOUBLY-IONIZED ARSENIC

By K. R. RAO, D.Sc., Madras Government Research Scholar,
University of Upsala

*ABSTRACT.* The doublet system of As III published by R. J. Lang has been amended and extended in the light of fresh observations which have been made, and a scheme of terms has been evaluated.

## § 1. INTRODUCTORY

THE spectrum of arsenic has been under investigation by the writer for a considerable time. In a previous paper[*] some regularities among the arc lines of arsenic have been published. Evidence of a doublet system of As III was obtained very early in the course of the work and the chief separation 723 cm.$^{-1}$ of the $5p$ $^2P$ term and the doublets of the secondary series were obtained by extrapolation from Ge II by the writer and Prof. A. L. Narayan[†]. Our present knowledge of the series of doublets in this spectrum is due, however, chiefly to an investigation by R. J. Lang[‡]. Independently P. Pattabhiramiah and A. S. Rao[§] have published an analysis of As III where the separation $4p$ $^2P_{\frac{1}{2}} - 4p_{\frac{1}{2}}$ $^2P_{1\frac{1}{2}} = 2940$ cm.$^{-1}$ is correctly identified.

In the present paper the doublet system published by Lang is considered in detail and, in the light of the present experimental observations, it has been altered in some respects and slightly extended. It is now possible to evaluate a reliable scheme of terms of As III by assuming a probable value for the term $5g$ $^2G$.

## § 2. EXPERIMENTAL

Several sources were employed for the excitation of the spectrum. From $\lambda$ 8000 to $\lambda$ 1300, they were the arc *in vacuo*, the spark between arsenic poles in air or hydrogen, and discharges through capillary tubes containing vapour of metallic arsenic. This part of the investigation was carried out in Prof. Fowler's laboratory at the Imperial College of Science, with various instruments. Below $\lambda$ 1400 photographs were taken at Upsala, of the spark between aluminium electrodes containing arsenic, with a vacuum grating spectrograph designed by Prof. Siegbahn. The grating is of radius 150 cm. and is mounted at tangential incidence; the dispersion varies from about 3·5 A.U. per mm. at $\lambda$ 1400 to about 2·0 A.U. per mm. at

[*] K. R. Rao, *Proc. R.S.* A, **125**, 238 (1929).
[†] K. R. Rao and A. L. Narayan, *Proc. R.S.* A, **119**, 611 (1928).
[‡] R. J. Lang, *Phys. Rev.* **32**, 737 (1928).
[§] P. Pattabhiramiah and A. S. Rao, *Ind. J. of Phys.* **3**, 437 (1929).

$\lambda$ 400. The author is indebted to Dr J. E. Mack and Mr D. Borg for permitting him to see some plates taken by them of the spectrum of arsenic by the use of a highly condensed and violent vacuum spark in which lines of As VI are obtained with ease. The wave-lengths in the table which follows are from the author's measurements and the intensities are estimated on a scale having 10 for maximum.

### §3. RESULTS

The analysis of As III published by Lang, while being quite correct in its essential features, appears to be defective in some details. The first member of the diffuse series, $4p\ ^2P - 4d\ ^2D$, is too weak and even fainter than the second member. Even if its correctness were assumed, no satisfactory pair could be found for the combination $4d\ ^2D - 4f\ ^2F$ which, at the same time, would give the other strong pair $4s\ 4p^2\ ^2D - 4f\ ^2F$. These latter two doublets are very prominent in spectra of this type, e.g. Ge II, Si II, etc. There are strong lines in the spectrum of arsenic which could be definitely ascribed to As III in the region where $4d\ ^2D - 4f\ ^2F$ may be expected, but no proper choice was found possible with Lang's classification.

Lang has drawn attention to the doubtful identification of the term $cP$ of the configuration of three $4p$ electrons. Of the combinations of this term with $4s\ 4p^2\ ^2P$, while $\lambda$ 2151 and $\lambda$ 2053 are lines of As III, $\lambda$ 2144 belongs to the arc spectrum and has been classified as such*. The group $bD - cP$ (in Lang's notation) shows abnormal intensities on Lang's plates. The line $\lambda$ 1266 is certainly due to As II.

In view of the above considerations, the analysis has been slightly modified. The details of the new scheme are set forth in table 1, in which Lang's classification also is given in order to indicate clearly the modification that has been made in it by the writer. The wave-lengths above $\lambda$ 2000 are in air; the others are *in vacuo*. The notation is that proposed by Russell, Shenstone and Turner†, the symbol $\circ$ which distinguishes the odd terms being omitted for convenience.

By alteration of the diffuse series member, the combinations of the $4f\ ^2F$ term with $4d\ ^2D$ and $4s\ 4p^2\ ^2D$ have been identified with certainty. The satellites $\lambda\lambda$ 2155·78 and 1274·13 are calculated and could not be observed. They are probably too faint and close to be resolved from the respective main lines, which are strong and diffuse. The pair at $\lambda$ 4031, which is prominent and belongs to As III, has suggested the present assignment. Further, there would otherwise be a slight discrepancy in the agreement of the $D$ separations, which is somewhat higher than the probable error in measurement. Two lines $\lambda$ 7240 and $\lambda$ 6923, photographed on a krypto-cyanine plate in the arsenic spark in hydrogen, are found in the calculated position of the inverted member $4d\ ^2D - 5p\ ^2P$.

Lang refers to a pair and satellite $\lambda\lambda$ 3319, 3122, 3091 which occur exactly in the calculated position of $bD - bP$ (according to his scheme). In the present classification, the last two lines correspond to the forbidden transition $4s^2\ 4d\ ^2D - 4s\ 4p^2\ ^2D$; the coincidence is believed to be only accidental and the origin of the lines also seems doubtful.

---

\* *Loc. cit.*   † Russell, Shenstone and Turner, *Phys. Rev.* **33**, 900 (1929).

## K. R. Rao

### Table 1

| Classification | | | | λ I.A. (int.) | | ν (vac.) | Δν |
|---|---|---|---|---|---|---|---|
| Lang | | Rao | | | | | |
| — | | $4d\,^2D_{1\frac{1}{2}}$ — | $5p\,^2P_{\frac{1}{2}}$ | 7240 | (3) | 13808 | — |
| — | | $^2D_{2\frac{1}{2}}$ — | $^2P_{1\frac{1}{2}}$ | 6923 | (1) | 14441 | — |
| — | | $^2D_{1\frac{1}{2}}$ — | $^2P_{1\frac{1}{2}}$ | — | | — | — |
| $4s\,4p^2\,^2S_{\frac{1}{2}}$ — | $5p\,^2P_{\frac{1}{2}}$ | Same as Lang's | | 4226·74 | (6) | 23652·3 | 723·0 |
| $^2S_{\frac{1}{2}}$ — | $^2P_{1\frac{1}{2}}$ | | | 4101·37 | (7) | 24375·3 | |
| $5s\,^2S_{\frac{1}{2}}$ — | $5p\,^2P_{\frac{1}{2}}$ | Same as Lang's | | *4037·01 | (9) | 24763·8 | 723·2 |
| $^2S_{\frac{1}{2}}$ — | $^2P_{1\frac{1}{2}}$ | | | *3922·46 | (10) | 25487·0 | |
| $5p\,^2P_{1\frac{1}{2}}$ — | $6s\,^2S_{\frac{1}{2}}$ | Same as Lang's | | *3255·55 | (5) | 30708·0 | 723·2 |
| $^2P_{\frac{1}{2}}$ — | $^2S_{\frac{1}{2}}$ | | | *3180·64 | (4) | 31431·2 | |
| $5p\,^2P_{1\frac{1}{2}}$ — | $5d\,^2D_{1\frac{1}{2}}$ | Same as Lang's | | *2989·42 | (3) | 33441·6 | 84·5 |
| $^2P_{1\frac{1}{2}}$ — | $^2D_{2\frac{1}{2}}$ | | | *2981·88 | (10) | 33526·1 | 723·0 |
| $^2P_{\frac{1}{2}}$ — | $^2D_{1\frac{1}{2}}$ | | | *2926·15 | (10) | 34164·6 | |
| $4s\,4p^2\,^2D_{1\frac{1}{2}}$ — | $5p\,^2P_{1\frac{1}{2}}$ | Same as Lang's | | 2132·76 | (3) | 46872·7 | 320·8 |
| $^2D_{2\frac{1}{2}}$ — | $^2P_{1\frac{1}{2}}$ | | | 2147·46 | (7) | 46551·9 | 723·7 |
| $^2D_{1\frac{1}{2}}$ — | $^2P_{\frac{1}{2}}$ | | | 2166·21 | (5) | 46149·0 | |
| — | | $4d\,^2D_{2\frac{1}{2}}$ — | $4f\,^2F_{3\frac{1}{2}}$ | 2156·20 | (9) | 46363·3 | − 8·9 |
| — | | $^2D_{2\frac{1}{2}}$ — | $^2F_{2\frac{1}{2}}$ | [2155·78] | | 46372·2 | 91·2 |
| $4s\,4p^2\,^2P_{1\frac{1}{2}}$ — | $4p^3\,^2P_{1\frac{1}{2}}$ | $^2D_{1\frac{1}{2}}$ — | $^2F_{2\frac{1}{2}}$ | 2151·55 | (8) | 46463·4 | |
| — | | $4f\,^2F_{2\frac{1}{2}}$ — | $5g\,^2G$ | 4032·45 | (10) | 24791·8 | − 8·9 |
| — | | $^2F_{3\frac{1}{2}}$ — | $^2G$ | 4031·01 | (10) | 24800·7 | |
| $4s\,4p^2\,^2P_{\frac{1}{2}}$ — | $4p^3\,^2P_{1\frac{1}{2}}$ | $4s\,4p^2\,^2P_{1\frac{1}{2}}$ — | $4f\,^2F_{2\frac{1}{2}}$ | 2053·37 | (5) | 48684·8 | — |
| $4s\,4p^2\,^2D_{2\frac{1}{2}}$ — | $4p^3\,^2P_{1\frac{1}{2}}$ | $4s\,4p^2\,^2D_{2\frac{1}{2}}$ — | $4f\,^2F_{3\frac{1}{2}}$ | 1274·27 | (9) | 78476 | − 9 |
| — | | $^2D_{2\frac{1}{2}}$ — | $^2F_{2\frac{1}{2}}$ | [1274·13] | | 78485 | 321 |
| $^2D_{1\frac{1}{2}}$ — | $^2P_{1\frac{1}{2}}$ | $^2D_{1\frac{1}{2}}$ — | $^2F_{2\frac{1}{2}}$ | 1268·95 | (6) | 78805 | |
| $4p\,^2P_{1\frac{1}{2}}$ — $4s\,4p^2\,^2D_{1\frac{1}{2}}$ | | Same as Lang's | | 1214·00 | (2) | 82372 | 321 |
| $^2P_{1\frac{1}{2}}$ — | $^2D_{2\frac{1}{2}}$ | | | 1209·29 | (10) | 82693 | 2941 |
| $^2P_{\frac{1}{2}}$ — | $^2D_{1\frac{1}{2}}$ | | | 1172·16 | (10) | 85313 | |
| $4p\,^2P_{1\frac{1}{2}}$ — | $5s\,^2S_{\frac{1}{2}}$ | Same as Lang's | | 963·80 | (8) | 103756 | 2938 |
| $^2P_{\frac{1}{2}}$ — | $^2S_{\frac{1}{2}}$ | | | 937·26 | (6) | 106694 | |
| $4p\,^2P_{1\frac{1}{2}}$ — $4s\,4p^2\,^2S_{\frac{1}{2}}$ | | Same as Lang's | | 953·55 | (4) | 104871 | 2938 |
| $^2P_{\frac{1}{2}}$ — | $^2S_{\frac{1}{2}}$ | | | 927·57 | (4) | 107809 | |
| $4p\,^2P_{1\frac{1}{2}}$ — $4s\,4p^2\,^2P_{1\frac{1}{2}}$ | | $4p\,^2P_{1\frac{1}{2}}$ — | $4d\,^2D_{1\frac{1}{2}}$ | †871·79 | (8) | 114707 | 94 |
| — | | $^2P_{1\frac{1}{2}}$ — | $^2D_{2\frac{1}{2}}$ | 871·07 | (10) | 114801 | 2941 |
| $4p\,^2P_{\frac{1}{2}}$ — $4s\,4p^2\,^2P_{1\frac{1}{2}}$ | | $^2P_{\frac{1}{2}}$ — | $^2D_{1\frac{1}{2}}$ | 849·99 | (9) | 117648 | |
| — | | $4p\,^2P_{1\frac{1}{2}}$ — $4s\,4p^2\,^2P_{\frac{1}{2}}$ | | 900·94 | (6) | 110995 | 1487 |
| $4p\,^2P_{1\frac{1}{2}}$ — $4s\,4p^2\,^2P_{\frac{1}{2}}$ | | $^2P_{1\frac{1}{2}}$ — | $^2P_{1\frac{1}{2}}$ | 889·03 | (8) | 112482 | 2943 |
| — | | $^2P_{\frac{1}{2}}$ — | $^2P_{\frac{1}{2}}$ | 877·67 | (7) | 113938 | |
| $4p\,^2P_{\frac{1}{2}}$ — $4s\,4p^2\,^2P_{\frac{1}{2}}$ | | $^2P_{\frac{1}{2}}$ — | $^2P_{1\frac{1}{2}}$ | 866·36 | (7) | 115425 | |
| $4p\,^2P_{1\frac{1}{2}}$ — | $5d\,^2D_{1\frac{1}{2}}$ | Same as Lang's | | 614·70 | (1) | 162681 | 85 |
| $^2P_{1\frac{1}{2}}$ — | $^2D_{2\frac{1}{2}}$ | | | 614·38 | (3) | 162766 | 2939 |
| $^2P_{\frac{1}{2}}$ — | $^2D_{1\frac{1}{2}}$ | | | 603·79 | (2) | 165620 | |

\* These were identified independently by the writer.

† For this group Lang has λλ 849·34 (1), 845·86 (2), 828·65 (2). This and the lines λ 2144·13 (4) and λ 1266·39 (30), Lang's $bP_2 - cP_1$, and $bD_2 - cP_1$, have been omitted from the above table, as incorrectly identified.

## §4. TERM VALUES

As some combinations are now available which involve the $F$ and $G$ levels, the terms can be evaluated as usual by assumption of a probable value for the term $5g\ ^2G$. In table 2 they are based on the value 39500 cm.$^{-1}$. The ionization potential corresponding to $4p\ ^2P_{\frac{1}{2}}$ is about 28·19 volts.

Table 2

| Term | Term value | Term | Term value |
|------|-----------|------|-----------|
| $4p\ ^2P_{\frac{1}{2}}$ | 228406 | $4f\ ^2F_{2\frac{1}{2}}$ | 64292 |
| $^2P_{1\frac{1}{2}}$ | 225466 | $^2F_{3\frac{1}{2}}$ | 64301 |
| $5s\ ^2S_{\frac{1}{2}}$ | 121712 | $5d\ ^2D_{1\frac{1}{2}}$ | 62783 |
| $4d\ ^2D_{1\frac{1}{2}}$ | 110755 | $^2D_{2\frac{1}{2}}$ | 62698 |
| $^2D_{2\frac{1}{2}}$ | 110664 | $5g\ ^2G$ | [39500] |
| $5p\ ^2P_{\frac{1}{2}}$ | 96948 | $4s\ 4p^2\ ^2D_{1\frac{1}{2}}$ | 143097 |
| $^2P_{1\frac{1}{2}}$ | 96225 | $^2D_{2\frac{1}{2}}$ | 142776 |
| $6s\ ^2S_{\frac{1}{2}}$ | 65517 | $^2S_{\frac{1}{2}}$ | 120600 |
|  |  | $^2P_{\frac{1}{2}}$ | 114468 |
|  |  | $^2P_{1\frac{1}{2}}$ | 112981 |

The results of the application of the regular and irregular doublet laws to GaI-like spectra are set out by Lang. Table 3 shows the progressive variation of only the term values in these spectra—those of GeII having been divided by 4 and those of AsIII by 9, as is usual in such comparisons.

Table 3

|  | $4p\ ^2P_{\frac{1}{2}}$ | $5p\ ^2P_{\frac{1}{2}}$ | $5s\ ^2S_{\frac{1}{2}}$ | $6s\ ^2S_{\frac{1}{2}}$ | $4d\ ^2D_{1\frac{1}{2}}$ | $5d\ ^2D_{1\frac{1}{2}}$ |
|------|------|------|------|------|------|------|
| GaI | 48380 | [15326] | 23592 | 10795 | 13598 | 7577 |
| GeII | 32159 | 12408 | 16559 | 8464 | 11950 | 7138 |
| AsIII | 25378 | 10772 | 13524 | 7280 | 12306 | 6976 |

|  | $4f\ ^2F_{2\frac{1}{2}}$ | $4s\ 4p^2\ ^2P_{\frac{1}{2}}$ | $4s\ 4p^2\ ^2S_{\frac{1}{2}}$ | $4s\ 4p^2\ \frac{1}{2}D_{1\frac{1}{2}}$ | $5g\ ^2G$ |
|------|------|------|------|------|------|
| GaI | — | — | 8115 | — | — |
| GeII | [7080] | 9406 | 13586 | 15906 | — |
| AsIII | 7144 | 12719 | 13400 | 15900 | [4389] |

## §5. ACKNOWLEDGMENT

# THE DETERMINATION OF THE ACOUSTICAL CHARACTERISTICS OF SINGLY-RESONANT HOT-WIRE MICROPHONES

## By E. T. PARIS, D.Sc., F.Inst.P.

*ABSTRACT.* A method is described for measuring the damping-coefficients and conductances of the orifices of the small resonators used in the construction of hot-wire microphones. Observations show that resonant microphones with cylindrical necks of diameter between 0·5 and 0·64 cm. and length between 1·2 and 2·25 cm. have damping-coefficients which are about 23 per cent. greater than the values indicated by theory. The observed conductances of the necks agree very closely with those calculated from a formula in which allowance is made for the added inertia due to viscosity.

## §1. INTRODUCTORY REMARKS

A SINGLY resonant hot-wire microphone consists of a Helmholtz resonator in the neck of which is mounted an electrically heated grid of fine platinum wire. The resistance of the hot-wire grid is a function of the magnitude of the aerial vibrations in the neck of the resonator.

The equation of motion of the air in the neck of the resonator is

$$\frac{\rho}{c}\frac{d^2q}{dt^2} + \frac{2h\rho}{c}\frac{dq}{dt} + \frac{a^2\rho}{Q}\,q = \rho\,\frac{d\phi}{dt} \qquad \text{......(1)},$$

$q$

$t, \rho, c$

$h$

$a, Q$

$\phi$

where $q$ is the volume of air in cc. which has entered the resonator at any instant, so that $dq/dt$ is the current of air into the resonator; $\rho$ is the density of air; $c$ is a linear quantity, the 'conductance' of the neck, which is inversely proportional to the inertia of the air in the neck of the resonator; $h$ is the damping coefficient (the reciprocal of the modulus of decay); $a$ is the velocity of sound in air; $Q$ is the internal volume of the resonator; and $\phi$ is the primary velocity-potential at the opening of the neck due to an external source of sound: that is, $\phi$ is the velocity-potential which the source would produce at that position if the resonator were not there.

Second-order effects due to differences in $\rho$ at positions just outside the resonator, in the neck, and inside the body of the resonator are ignored. The velocity of sound, $a$, is the velocity in the air inside the resonator.

The acoustical characteristics of the resonator are the three quantities $c$, $h$ and $Q$. If these three quantities are known, then, by integration of (1) $\phi$ may be deduced from observed values of $q$, or conversely $q$ may be forecasted for specified values of $\phi$. The measurement of $Q$ presents no difficulty and the remainder of this note is

devoted to a discussion of the experimental determination of $c$ and $h$ and a comparison of observed and calculated values.

A method of determining $h$ has already been described in an appendix to a paper on the measurement of sound-absorption*. The method consists in exposing the microphone to sound of constant amplitude and frequency $\omega/2\pi$ and then varying $\quad\omega$ the tuning by altering the volume of the resonator. A series of pairs of values of volume $Q$ and resistance-change $\delta R$, in the hot-wire grid is recorded, and the $\quad\delta R$ relative amplitude of oscillation of the air in the neck of the resonator, corresponding to each observed resistance change, is found by a calibration with stationary wave apparatus. The relative amplitude appears as a circular function $\sin ky$ $(ky \not> \pi/2)$, where $k = \omega/a$ and $y$ is the distance which the microphone must be displaced from $\quad k, y$ a loop position in a stationary wave in order that the grid may suffer the resistance-change $\delta R$. The process of calibration is fully described in the paper referred to.

The damping coefficient was calculated from the observations by means of the formula

$$h = \pm \tfrac{1}{2} \triangle \left/ \left\{ \left( \frac{\sin ky_m}{\sin ky} \right)^2 - 1 \right\}^{\frac{1}{2}} \right. \qquad \dots\dots(2),$$

where $\triangle = \omega_0 \,(\omega_0/\omega - \omega/\omega_0)$ and $\omega_0{}^2 = a^2 c/Q\dagger$. $\sin ky_m$ is the relative amplitude $\quad \triangle, \omega_0, y_m$ when $\triangle = 0$.

The use of the formula (2) is not satisfactory when the tuning of the resonator is such that its frequency is near to that of the sound, for then $\sin ky_m/\sin ky$ is near to unity, and both the numerator and denominator of the right-hand side of (2) tend to zero as the resonance frequency is approached.

The observations can be more satisfactorily dealt with by an application of the "circle and straight line" construction described by Mallett‡ for the analysis of resonance curves. The theory of the method as applied to the Helmholtz resonator is given in the next section.

### §2. THEORY

The equation (1) can be written in the form

$$\frac{d^2q}{dt^2} + 2h \frac{dq}{dt} + \omega_0{}^2 q = c \frac{d\phi}{dt} \qquad \dots\dots(3).$$

If $\phi \propto \epsilon^{\iota\omega t}$ we may put
$$q = \Omega\phi \qquad \dots\dots(4),$$

where
$$\Omega = \frac{c}{2h - \iota\triangle} \qquad \dots\dots(5), \qquad \Omega$$

so that
$$|q| = \frac{c}{(4h^2 + \triangle^2)^{\frac{1}{2}}} |\phi| \qquad \dots\dots(6).$$

In the experiment $\omega$ remains constant and $\triangle$ is varied by making changes in $\omega_0$.

* *Proc. Phys. Soc.* **39**, 287–288 (1927).
† The conductance $c$ varies with frequency owing to the effects of viscosity. $\omega_0/2\pi$ is therefore only approximately the frequency of the resonator when its volume is $Q$ since $c$ is the conductance when the frequency is $\omega/2\pi$.
‡ E. Mallett, *J.I.E.E.* **62**, 517–525 (1924).

Let $\triangle/2h = \tan \alpha$. Then from (6)

$$|q| = \frac{c}{2h} \cos \alpha \cdot |\phi| \qquad \qquad \ldots\ldots(7).$$

$q_m$

Now $(c/2h) \cdot |\phi|$ is the maximum value of $|q|$, that is, the value it attains when $\triangle = 0$ and the resonator is in unison with the sound. Denoting this value by $|q|_m$ we have

$$|q| = |q|_m \cdot \cos \alpha \qquad \qquad \ldots\ldots(8).$$

$\alpha$

So that if a circle be drawn on a diameter $|q|_m$ and a chord of length $|q|$ be drawn from one end of a diameter the angle included between the chord and the diameter is the angle $\alpha$. This is the circle construction for finding $\alpha$ from a resonance curve.

$Q_m$

Suppose that in the experiment a series of corresponding values of $|q|$ and $\phi$ has been recorded, and let $Q_m$ be the value of $Q$ for which the greatest value of $|q|$ occurs. Since by Rayleigh's formula for the frequency of a Helmholtz resonator,

$$\omega^2 = a^2 c Q_m^{-1} \qquad \qquad \ldots\ldots(9a),$$

and since

$$\omega_0{}^2 = a^2 c Q^{-1} \qquad \qquad \ldots\ldots(9b),$$

we have

$$= (Q^{-1} - Q_m{}^{-1}) \, a^2 c/\omega$$
$$= (Q^{-1} - Q_m{}^{-1}) \, 2\pi n / Q_m{}^{-1} \qquad \qquad \ldots\ldots(10),$$

$n$

where $n$ is the frequency of the sound. Now $\tan \alpha = \triangle/2h$ and therefore

$$\tan \alpha = (Q^{-1} - Q_m{}^{-1}) \, \pi n / h Q_m{}^{-1} \qquad \qquad \ldots\ldots(11),$$

or

$$Q^{-1} = Q_m{}^{-1} + (h Q_m{}^{-1}/\pi n) \tan \alpha \qquad \qquad \ldots\ldots(12),$$

so that $Q^{-1}$ and $\tan \alpha$ are linearly related, and if $Q^{-1}$ is plotted against $\tan \alpha$ we obtain a straight line the slope of which is $dQ^{-1}/d \tan \alpha$ where

$$dQ^{-1}/d \tan \alpha = h Q_m{}^{-1}/\pi n \qquad \qquad \ldots\ldots(13).$$

If the slope is measured $h$ may be calculated from the equation

$$h = \frac{\pi n}{Q_m{}^{-1}} \cdot \frac{dQ^{-1}}{d \tan \alpha} \qquad \qquad \ldots\ldots(14).$$

In the method as described by Mallett, $\tan \alpha$ is plotted against frequency and the linear relation is only approximate, but the relation given in (12) is exact.

Examples of the application of the method to the determination of the damping factors of hot-wire microphones are given in the following two sections.

## §3. THE DETERMINATION OF THE DAMPING COEFFICIENT OF A MICROPHONE TUNED TO 30·66 ∼

The microphone used in this experiment was one designed for recording the low-frequency sound emitted by an airscrew. The neck was cylindrical and made as shown in the section in figure 1. The dimensions of the cylindrical neck above the grid at $M$ were: length 22·5 mm., diameter 6·4 mm. The grid was supported in the usual way on a porcelain bridge in a circular hole, 6·5 mm. in diameter, in a mica disc. The grid was about 1 mm. below the lower end of the neck.

For the determination of the damping coefficient the resonator was fitted with a side tube and tap so that water could be run in or out in order to vary the internal volume. A glass gauge was also fitted on one side of the resonator so that the level of the water could be read off, and the gauge was calibrated by the running of water into a measuring cylinder and observation of the gauge readings, allowance being made for the volume of water from the gauge. Sound of constant amplitude and frequency was provided by a moving-coil loud-speaker driven by a thermionic valve-oscillator, the microphone being placed about 2 ft. in front of the loud-speaker. The experiment was performed in a room, but the observer was at some distance from the microphone and was careful to make only small movements so as not to cause any sensible disturbance of the acoustic field round the microphone. The experiment was begun with the volume of the container small and the change in the resistance of the hot-wire grid also small, and the volume was increased step
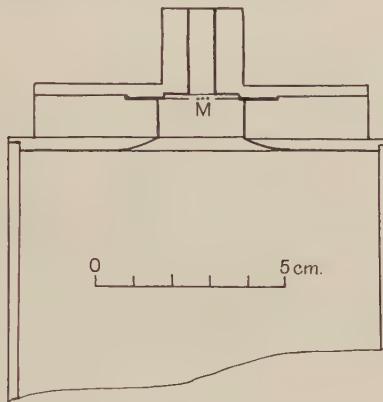


Fig. 1. Section through neck of resonator ($n = 30\cdot66 \sim$).

by step until the change in resistance had just passed through its maximum value. The microphone was then calibrated by the stationary-wave method. The apparatus employed for this purpose was the same in principle as that already described*; but in order to cope with the long wave-length the pipe in which the stationary wave was produced was 21 ft. long and 2 ft. 6 in. in diameter, made up of concrete sections cemented together. The pipe was sealed at one end with a heavy concrete disc in a circular iron frame held by bolts and nuts against a compressed cork washer. The other end of the pipe was covered with a three-ply baffle-board at the middle of which was mounted a moving-coil loud-speaker. This pipe was one that had been constructed at the Air Defence Experimental Establishment for the purpose of calibrating microphones at the low frequencies which occur in airscrew sound.

The stationary wave in the pipe could be made very strong at about 30 $\sim$ and the loops were always very perfect. The change in resistance when the microphone was at a loop was only about 0·01 ohm when the sound was turned on or off (except

* *Proc. Phys. Soc.* **39**, 274–275 (1927).

for a transient effect which was of no importance so far as calibration was concerned) although the change in resistance at a node was about 50 ohms.
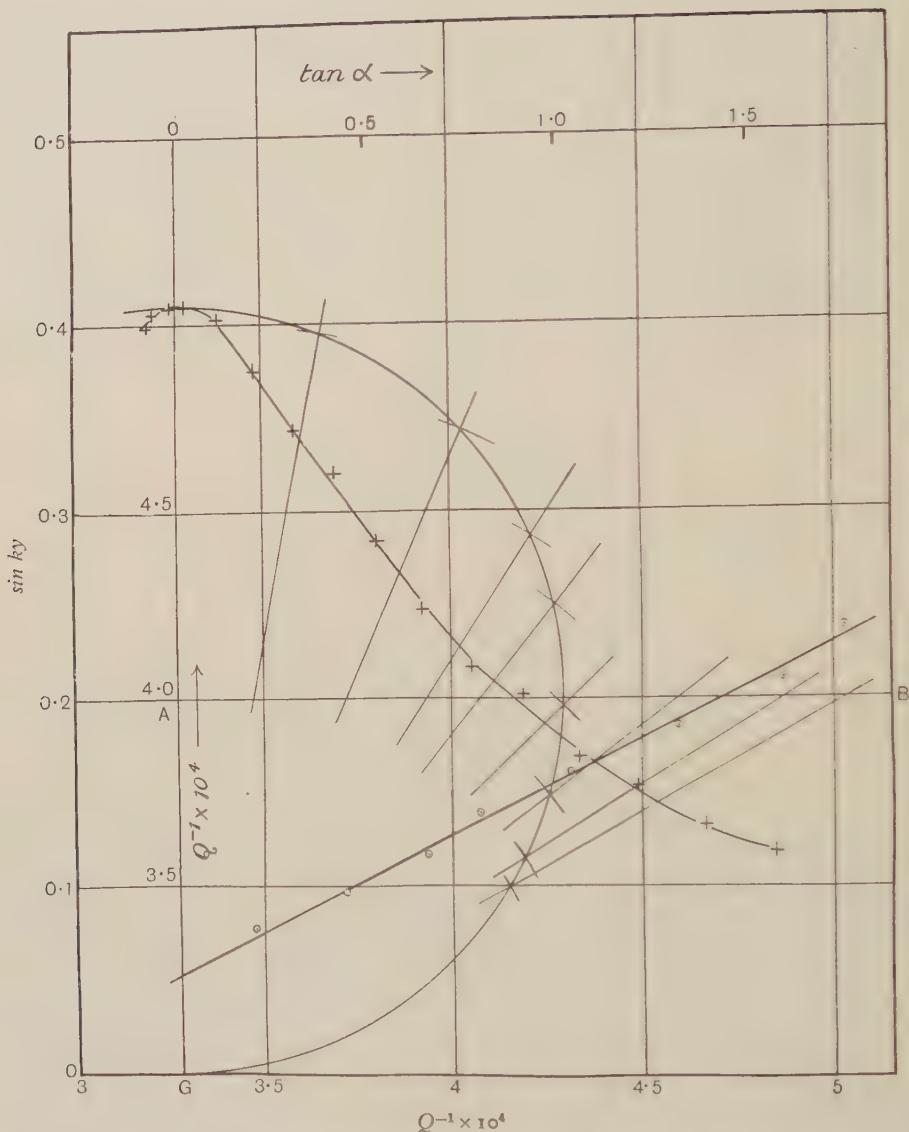


Fig. 2. Determination of damping coefficient and conductance by circle and straight line method $(n = 30.66 \sim)$.

In both parts of the experiment the frequency of the sound was found by a stroboscopic method, the primary of a transformer being placed in series with the moving-coil loud-speaker and the secondary connected to a neon lamp which illuminated intermittently (with the frequency of the sound) a rotating white disc

on which was drawn a black triangle. The disc was driven by a phonic motor at 10·17 rev./sec. The frequency was calculated from the observed slip of the triangle.

The set of figures shown in table 1 was obtained. The values of sin $ky$ are of course proportional to $|q|$ in the theory given in § 2.

From these figures a resonance curve was drawn, sin $ky$ being plotted against $Q^{-1}$ (figure 2), and a set of values of tan $\alpha$ was determined from the curve by the circle construction. The intercept on $AB$ between the chord drawn from $G$ and the vertical diameter of the circle, $GA$ being taken as unity, is, of course, equal to

Table 1. Determination of damping-coefficient at 30·66 $\sim$ and 13° C.

| $Q^{-1} \times 10^4$ | sin $ky$ | $Q^{-1} \times 10^4$ | sin $ky$ |
|---|---|---|---|
| c.c. | | c.c. | |
| 4·84 | 0·118 | 3·69 | 0·320 |
| 4·66 | 132 | 3·58 | 344 |
| 4·49 | 154 | 3·48 | 375 |
| 4·34 | 169 | 3·39 | 403 |
| 4·19 | 202 | 3·30 | 410 |
| 4·05 | 216 | 3·26 | 410 |
| 3·92 | 248 | 3·21 | 404 |
| 3·80 | 284 | 3·20 | 399 |

tan $\alpha$. Finally tan $\alpha$ was plotted against $Q^{-1}$ and a straight line was drawn as nearly as possible through the points. From measurement of the figure it was found that

$$dQ^{-1}/d \tan \alpha = 0.88 \times 10^{-4}/1.70,$$

and also that

$$Q_m^{-1} = 3.26 \times 10^{-4},$$

so that by (13)

$$h = 15.3 \text{ sec.}^{-1}.$$

The air-temperature being 13° C. we have $a = 33960$ cm./sec., and therefore

$$c = 0.0989 \text{ cm.}$$

The accuracy with which $c$ can be determined depends mainly upon the accuracy with which $Q_m^{-1}$ can be found. The error in the value of $c$ given above is probably not more than 4 parts in 1000—a much smaller error than can be claimed for any earlier measurements of conductance.

§ 4. THE DETERMINATION OF THE DAMPING-COEFFICIENT OF A MICROPHONE TUNED TO 512 $\sim$

The observations used in this section are taken from an earlier paper*. The microphone is shown in figure 5 of that paper. The tuning was varied by alteration of the volume of the resonator by means of a sliding portion. The cylindrical neck above the hot-wire grid was 12 mm. long† and 5 mm. in diameter. A section through

* *Proc. Phys. Soc.* **39**, 288 (1927).
† Erroneously stated to be 1 cm. long in the earlier description (*loc. cit.* p. 276).

the neck and the upper part of the resonator is shown in figure 3. As before, the grid was about 1 mm. below the lower end of the neck.

The first two observations previously recorded must be discarded since the volume of the resonator given for the first observation is greater than that for the second whereas it should clearly be less. The error is probably due to a misprint. The remaining observations yielded the figures given in table 2.

It was found from a figure that $(dQ^{-1} d \tan \alpha) = (1 \cdot 40 \, '3 \cdot 7) \times 10^{-2}$ and $Q_m^{-1} = 7 \cdot 665 \times 10^{-2}$ c.c.$^{-1}$ whence $h = 79 \cdot 4$ sec.$^{-1}$ (compared with the value of
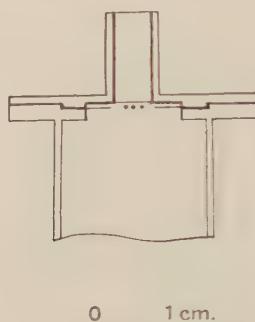


Fig. 3. Section through neck of resonator ($n = 512 \sim$).

81 sec.$^{-1}$ previously given). The temperature was not recorded, but assuming it to be 10° C. we have $a = 33760$ cm./sec. and $c = 0 \cdot 118$ cm., instead of $c = 0 \cdot 114$ cm. as previously given*.

Table 2. Determination of damping-coefficient at 512 $\sim$

| $Q^{-1}$ | sin $ky$ | | $Q^{-1}$ | sin $ky$ |
|---|---|---|---|---|
| c.c.$^{-1}$ | | | c.c.$^{-1}$ | |
| $8 \cdot 64 \times 10^{-2}$ | 0·210 | | $7 \cdot 55 \times 10^{-2}$ | 0·531 |
| 8·38 | 260 | | 7·37 | 459 |
| 8·11 | 344 | | 7·22 | 353 |
| 7·94 | 465 | | 6·90 | 241 |
| 7·72 | 542 | | 6·52 | 182 |
| 7·61 | 549 | | | |

## §5. SOME ADDITIONAL OBSERVATIONS

The following observations of damping-coefficients have been recorded during experiments with hot-wire microphones. The method of experiment was similar in all essential details to that described in § 3. The observations were not made with the object of obtaining specially accurate values for damping and conductance but were recorded during the ordinary course of experiments incidental to the design

* *Loc. cit.* p. 276.

and employment of microphones. All the orifices were cylindrical, and the letters $l$ and $r$ will be used to denote the length and radius respectively.                                 $l, r$

(a)                     $l = 18\cdot4$ mm.                    $h = 20\cdot7$ sec.$^{-1}$.
                        $2r = \phantom{0}5\cdot8$ mm.                    $c = \phantom{0}0\cdot096$ cm.
                        $n = 56\cdot3 \sim.$
                                Temperature, 6° C.

(b)                     $l = 18\cdot4$ mm.                    $h = 21\cdot6$ sec.$^{-1}$.
                        $2r = \phantom{0}5\cdot8$ mm.                    $c = \phantom{0}0\cdot101$ cm.
                        $n = 61\cdot2 \sim.$
                                Temperature, 12° C.

(c)                     $l = 14\cdot95$ mm.                    $h = 26\cdot1$ sec.$^{-1}$.
                        $2r = \phantom{0}5\cdot74$ mm.                    $c = \phantom{0}0\cdot117$ cm.
                        $n = 90 \sim.$
                                Temperature, 7° C.

### § 6. POSSIBLE ERROR DUE TO REACTION BETWEEN MICROPHONE AND SOURCE OF SOUND

There is a possible source of error in the experiments which should be noted. In order to obtain effects of sufficient magnitude to ensure accurate measurement it is necessary to place the microphone near to the source of sound in the first part of the experiment. As the microphone is brought into tune with the source there may be acoustical reaction between resonator and source which will tend to enhance the output of the source when there is unison. In the case of microphones such as those described above for which the radiation damping is small, the effect will probably be quite unimportant. But with microphones which reradiate a larger proportion of sound an appreciable error might be introduced. The error could be avoided by means of an arrangement wherein the amplitude of the source remains constant during a set of observations, for example, by using a hot-wire grid in the throat of a loud-speaker*.

### § 7. THE CONTRIBUTION OF SOUND-RADIATION TO THE OBSERVED DAMPING-COEFFICIENTS

It was pointed out by Tucker and Paris† in 1921 that the contribution of radiation losses to the damping of the small resonators used in the construction of singly-resonant hot-wire microphones was relatively negligible. That this is the case is confirmed by the more accurate observations recorded in the preceding sections.

The damping coefficient, $h$, of a resonator can be regarded as the sum of two parts $h_1$ and $h_2$ representing radiation and viscosity effects respectively. The value     $h_1, h_2$
of $h_1$ may be calculated from‡     $h_1 = \pi n^2 c / 2a$     ......(15).

* Cf. *Proc. Phys. Soc.* **39**, 277 (1927).     † *Phil. Trans.* A, **221**, 399 (1921).
‡ Cf. H. Lamb, *Dynamical Theory of Sound*, p. 265 (1910).

Thus in the case of the resonator used in the experiment described in § 3, $n = 30\cdot66 \sim$, $c = 0\cdot0989$ cm. and $a = 33960$ cm./sec. so that

$$h_1 = 0\cdot0043 \text{ sec.}^{-1},$$

which is to be compared with the observation that

$$h = 15\cdot3 \text{ sec.}^{-1}.$$

The radiation effect is thus quite insignificant, contributing only about 0·03 per cent. to the total damping.

The radiation effect is also negligible in the case of the observations recorded in § 5.

For the resonator used to obtain the observations given in § 4, $n = 512 \sim$, $c = 0\cdot118$ cm., and $a = 33760$ cm./sec., so that

$$h_1 = 1\cdot4 \text{ sec.}^{-1}.,$$

compared with the observation that

$$h = 79\cdot4 \text{ sec.}^{-1}.$$

Although the radiation effects in this case are relatively greater, they account for only 2 per cent. of the total damping. For viscosity alone

$$h_2 = 79\cdot4 - 1\cdot4 = 78 \text{ sec.}^{-1}.$$

## § 8. THEORETICAL EXPRESSIONS FOR THE DAMPING COEFFICIENT AND THE CONDUCTANCE OF AN ORIFICE

The theory of a resonator with a cylindrical neck, with allowance for the effects of viscosity, has been given by G. W. Stewart[*]. The effect is twofold; there is dissipation of acoustical energy and there is an increase in the effective inertia of the air in the neck of the resonator. Stewart deduced the acoustical impedance of a cylindrical neck from the equations of motion used by Helmholtz to compute the effect of viscosity on the velocity of propagation of sound in narrow pipes. Crandall[†] has given a detailed account of the solution of these equations and of the application of the solution to the calculation of the impedance of a cylindrical conduit. He obtained an expression for the resistance-coefficient of a conduit (the ratio of pressure-gradient to particle velocity) of which that part $R$ depending on viscosity is given by

$$R = (2\mu\omega\rho)^{\frac{1}{2}} (1 + \iota)/r \qquad \qquad \ldots\ldots(16),$$

where $r$ is the radius of the conduit and $\mu$ is the coefficient of viscosity of air. By introducing this resistance coefficient into the equation of motion of the air in the neck of a resonator, and omitting the effects of radiation, with which we are not at present concerned, we obtain, instead of (1)

$$\frac{d^2q}{dt^2} + \frac{c}{\rho}\frac{L}{\pi r^2}\frac{1}{r}(2\mu\omega\rho)^{\frac{1}{2}}(1 + \iota)\frac{dq}{dt} + \frac{a^2c}{Q}q = c\frac{d\phi}{dt} \qquad \ldots\ldots(17),$$

[*] *Phys. Rev.* **27**, 488 (1926).
[†] *Vibrating Systems and Sound*, Appendix A, pp. 229–241 (1926).

where $c$ is the conductance of the neck as it would be if viscous forces were non-existent and $L$ is the effective length of the neck. When the length is great compared with the diameter, $L$ will be very nearly the actual length, but in the case of short necks the addition of an end-correction will be necessary to allow for the fact that the viscous effects do not terminate abruptly at the ends of the neck.

Since $\phi$ and $q$ vary as $\epsilon^{\iota\omega t}$, (17) becomes

$$\left[\left(\frac{a^2 c}{Q} - \frac{\omega c}{\rho}\frac{L}{\pi r^3}(2\mu\omega\rho)^{\frac{1}{2}} - \omega^2\right) + \iota\frac{\omega c}{\rho}\frac{L}{\pi r^3}(2\mu\omega\rho)\right] q = \iota\omega c\phi \quad ......(18).$$

If we put
$$h_2 = \frac{cL}{\pi r^3}\left(\frac{\omega\mu}{2\rho}\right)^{\frac{1}{2}} \quad ......(19\cdot1),$$

and
$$c' = c\left(1 - \frac{2\omega Q}{a^2 c}h_2\right) \quad ......(19\cdot2),$$

(18) may be written
$$\left[\left(\frac{a^2 c'}{Q} - \omega^2\right) + 2\iota\omega h_2\right] q = \iota\omega c\phi \quad ......(20).$$

Of the two conductances which appear in this equation $c'$ includes the effect of added inertia due to viscosity and is the conductance that is measured experimentally from observations of the volume and resonance frequency of a resonator. $c$ is the conductance calculated on the assumption that there is no viscosity and can be found from the well-known formula

$$c = \pi r^2/(l + \alpha r) \quad ......(21),$$

where $l$ is the length of the neck and $\alpha r$ is the sum of the end-corrections.

Since $a^2 c/Q = \omega_0^2$ (19·2) may be written
$$c' = c(1 - 2\omega h_2/\omega_0^2) \quad ......(21\cdot1),$$

or
$$c' = c(1 - 2h_2/\omega) \quad ......(21\cdot2),$$

for the limited variations of $Q$ made in the experiments.

(19·1) gives the value of $h_2$ as it would appear from Stewart's expression for the impedance of a resonator.

In the case of necks with lengths greater than their diameters, it seems reasonable to identify $L$ with the reduced length $(l + \alpha r)$ calculated for pure inertia effects, so that

$$h_2 = \frac{1}{r}(\omega\mu/2\rho)^{\frac{1}{2}} \quad ......(22).$$

This is the form in which the expression for the damping coefficient is given by Crandall*.

The resonator necks used in the experiments described in this paper were such that the ratio length/diameter always lay between 2·4 and 3·5, and it will be assumed that $L = l + \alpha r$ with sufficient approximation.

The acoustical impedance of an orifice, with allowance for viscosity, has also been calculated by E. G. Richardson†. His calculation proceeds on an assumption,

---

* *Vibrating Systems and Sound*, p. 56 (1926).    † *Proc. Phys. Soc. Lond.* **40**, 214–215 (1928).

due to Prandtl, that viscosity effects are confined to a thin boundary layer of determinate thickness. Two expressions are given for the acoustical impedance of an orifice, from either of which $h_2$ can be found by use of the fact that the real part of the impedance is equal to $2h_2\rho/c$. Thus from Richardson's equation (10)* we find

$$h_2 = \frac{1}{r}\frac{\mu}{\rho x} \qquad\qquad \text{......(23)},$$

*x*

*v′, μ′*

where $x$ is the thickness of the boundary layer. The second expression† involves an altered coefficient of viscosity, $v'$ or $\mu'/\rho$, and is stated to be obtained from the first expression by means of a substitution equivalent to $x = \sqrt{(2\pi\mu'/\rho\omega)}$. This, however, appears to be an error. In order to obtain Richardson's equation (11) from (10) it is also necessary to substitute $\mu'$ for $\mu$ in (10)‡.

## §9. COMPARISON OF THE OBSERVED DAMPING COEFFICIENTS WITH THEIR VALUES CALCULATED FROM (22)

A comparison of the experimental values of $h_2$ recorded in §§ 3, 4 and 5 with the values of $h_2$ calculated from (22) is contained in table 3.

Table 3. Observed and Calculated Values of $h_2$.

| Frequency (n) | Diameter (2r) | Length/diameter (l/2r) | $h_2$ observed | $h_2$ calculated | Ratio of observed to calculated $h_2$ |
|---|---|---|---|---|---|
| cycle/sec. | cm. | | sec.$^{-1}$ | sec.$^{-1}$ | |
| 30·66 | 0·64 | 3·51 | 15·3 | 12·4 | 1·23 |
| 56·3 | 0·58 | 3·17 | 20·7 | 17·0 | 1·22 |
| 61·2 | 0·58 | 3·17 | 21·6 | 18·1 | 1·19 |
| 90 | 0·574 | 2·50 | 26·1 | 21·8 | 1·20 |
| 512 | 0·5 | 2·4 | 78 | 60·3 | 1·29 |

The mean of the figures in the last column is 1·23, so that the conclusion to be drawn is that calculated values of $h_2$ must be increased by about 23 per cent. in order to procure agreement with observation.

*x*

The frequency of 30·66 ∼ is near to that used in experiments by Richardson§ to measure directly the thickness $x$ of the boundary layer where viscosity effects occur. Measurements were made in an orifice 3 cm. in diameter and 2 mm. long and it was found that $x = 0.075$ cm. at 25 ∼ and $x = 0.05$ cm. at 35 ∼. By using (23) we can calculate $x$ from the observed $h_2$ at 30·66 ∼, and we find in this way

---

\* *Loc. cit.* p. 214.                                † Equation (11), p. 215.

‡ The statement at the foot of p. 215 (Richardson, *loc. cit.*) to the effect that Stewart's form of the expression for impedance can be obtained from Richardson's formulae by the substitution $x = \sqrt{(\mu/\rho n)}$ also appears to be incorrect. To obtain Stewart's impedance from Richardson's (10) we must put $x = \sqrt{(2\mu/\rho\omega)} = \pi^{-\frac{1}{2}}\sqrt{(\mu/\rho n)}$, and to obtain it from (11) we must have $v' = \pi v$, whence

$$x = \sqrt{(v'/n)} = \pi^{\frac{1}{2}}\sqrt{(\mu/\rho n)}.$$

§ *Proc. Phys. Soc.* **40**, 217 (1928).

that $x = 0.029$ cm., that is about half the value that would be expected from Richardson's observations. The discrepancy may be due to the relatively greater length of the orifices used in the present experiments.

### § 10. THE DISCREPANCY BETWEEN THE OBSERVED AND CALCULATED VALUES OF $h_2$

There seems little possibility of there being any experimental error which would account for the large difference between the observed and calculated values of $h_2$. The error mentioned in § 6 would tend to make the observed values of $h_2$ smaller than their true values.

Among the factors which might be suspected of being either wholly or partly the cause of the discrepancy are the following: (i) losses due to viscosity at the sharp edges of the circular hole in the mica disc supporting the hot-wire grid at the lower end of the neck; (ii) losses due to the motion of the air past the heated platinum wire (about 0.0006 cm. in diameter) constituting the grid of the microphone*; (iii) losses due to viscosity during the motion of the air past the porcelain bridge (1 mm. in diameter) which supports the heated wire in the circular hole in the hot-wire grid.

It may be noted, however, in regard to (i) that Stewart† found that viscosity effects were negligible in the case of a Helmholtz resonator with a circular orifice of diameter 4 mm. and length 0.15 mm. Regarded as a separate orifice, the hole in the mica disc has a diameter 6.5 mm. and length 0.13 mm. (the thickness of the mica), and Stewart's results indicate that there is no appreciable damping due to viscosity in an orifice of these dimensions.

Also, so far as I have been able to make out from the well-known work of Sewell‡, it appears that the losses under headings (ii) and (iii) are likely to be relatively insignificant. It must be admitted, however, that the question how much energy is dissipated during the motion of the air past the heated platinum wire requires more attention than I have yet given to it. The high temperature of the wire may be a factor of some importance.

It seems probable, however, that the discrepancy between the observed and calculated damping coefficients cannot be accounted for by any of the factors enumerated above but may be due to the fact that the theory of the vibrational motion of air in a narrow neck is not properly understood. In particular, in view of the experiments of E. G. Richardson§ on the velocity across circular orifices, it seems possible that the velocity distribution implicit in the theory from which formula (22) for the damping coefficient is deduced may not be correct. There is also some evidence that a jet effect exists in small cylindrical necks‖.

---

\* The type of microphone used in the experiment had three loops. It is described in *Phil. Trans.* A, **221**, 391, figure 1 B (1921).

† *Phys. Rev.* **27**, 489 (1926).   ‡ *Phil. Trans.* A, **210**, 239–270 (1910).

§ *Proc. Phys. Soc.* **40**, 215–218 (1928).

‖ W. S. Tucker and E. T. Paris, *Phil. Trans.* A, **221**, 422 (1921).

## § 11. COMPARISON OF OBSERVED AND CALCULATED VALUES OF CONDUCTANCE

Table 4 contains a comparison of the observed conductances recorded in §§ 3, 4 and 5 with values calculated from (21) and (21·2). The value of $\alpha$ in (21) has been taken to be 1·6 on the assumption that a fair value for the end-corrections will be obtained by means of the supposition that both ends of the neck are flanged*. It will be seen from figures 1 and 3 that the lower ends of the necks are much more restricted than by a plane flange while the upper ends are less restricted. The *observed* values of $h_2$ were used to calculate $c'$ from (21·2).

Table 4. Observed and Calculated Values of Conductance.

| Frequency $(n)$ | Diameter $(2r)$ | Length $(l)$ | $c$ calculated from (21) | $c'$ calculated from (21·2) | Observed conductance |
|---|---|---|---|---|---|
| ~ | cm. | cm. | cm. | cm. | cm. |
| 30·66 | 0·64 | 2·25 | 0·119 | 0·098 | 0·0989 |
| 56·3 | 0·58 | 1·84 | 0·115 | 0·102 | 0·096 |
| 61·2 | 0·58 | 1·84 | 0·115 | 0·102 | 0·101 |
| 90 | 0·574 | 1·495 | 0·132 | 0·120 | 0·117 |
| 512 | 0·5 | 1·2 | 0·123 | 0·117 | 0·118 |

The agreement between the figures in the fifth and sixth columns of this table verifies the correctness of the formula (21·2).

It is interesting to note that in the case of the microphone of frequency 30·66 ~ the effect of viscosity was to reduce the conductance by more than 20 per cent.

## § 12. CONCLUSION

The observations on the damping coefficients of resonant hot-wire microphones with small cylindrical necks (table 3) show that the theoretical values are about 23 per cent. below those found by experiment. The observed values for conductance (table 4) agree very closely with those calculated from a formula which takes into account the increase in the effective inertia of the air in the neck due to viscosity.

## § 13. ACKNOWLEDGMENT

My acknowledgments are due to Mr A. Reading for the very considerable assistance he has given in the execution of the experiments described in this paper.

## DISCUSSION

Sir Richard Paget. A possible cause of the differences between observed and calculated conductance may lie in the shape of the resonator. I have found that in resonators such as those shown in figures 1 and 3 the effective resonating cavity is not stopped but is, as it were, smoothed out into a more or less stream-lined form—

* G. W. Stewart, *Phys. Rev.* **27**, 489 (1926), uses a value for end-correction which makes $\alpha$ equal to 1·57.

as if by a smooth surface (of rotation) touching the corners of the steps and merging into the full diameter of the neck and body of the resonator respectively. The effect of this stream-lining is to narrow the neck near its point of abrupt enlargement. The same type of effect occurs at the outer end of the neck where a rectangular cut-off behaves in fact as if the neck were extended outwards, enlarged, and rounded off. This phenomenon corresponds to the well known end-correction.

E. J. IRONS. The present paper increases the debt which we owe to the author for his treatment of resonator problems. I should be pleased to know whether he considers that the method would retain its precision if used for the determination of the conductance of an orifice in a thin wall, i.e. an orifice for which, in terms of (21), $l$ is very small.

DR G. D. WEST asked whether the author had allowed for rise in temperature of the air in the neck of the resonator.

DR A. B. WOOD. It appears that the author is disposed to neglect altogether the damping due to the hot-wire grid. This seems tantamount to assuming that the hot-wire microphone is inefficient as a sound-receiver. Alternatively, assuming the receiver to be efficient, then the grid must absorb an appreciable proportion of the sound-energy falling on it, and this will appear as grid-damping. The latter quantity might conveniently be determined by the introduction of an auxiliary hot-wire grid (or grids) purely as a means of increasing the damping. In this manner also the damping due to the grid at different temperatures could be studied.

DR E. G. RICHARDSON (communicated). I agree with the author that there are at present several uncertain factors that will have to be properly accounted for in any theory which is to give values of the conductances of orifices in agreement with practice. With regard to measurements of the damping-coefficients for comparison with theory, I think that the impedance to the motion of the air in the neck offered by the mica insulator in the author's experiments, and by the fork held over the resonator in my own, is a factor of considerable magnitude. With regard to the difference in the thickness of the boundary layer, as calculated in § 9, the suggestion of the author that this is in part accounted for by the difference in the shape of the orifices used by us (tube and hole respectively) is supported by the corresponding differences of boundary-layer thickness in steady flow past obstacles of various shapes, and at different points along the surface of the same obstacle.

I am grateful to the author for pointing out the slip in the comparison-factor between equation (11) of my paper and the corresponding equation of Stewart, as given by me in the footnote on p. 215.

AUTHOR'S reply. Sir Richard Paget's observations are of great interest and tend to show that the velocity-distribution assumed in the theory may not be that which actually exists in the neck of the resonator. In reply to Dr Irons: I think the experimental method described in the paper could be used to determine the conductance of a hole in a thin wall, but I would recommend the use of a single strand

of fine wire stretched across the hole. In answer to Dr West: I assumed the temperature of the air in the neck of the resonator to be that of the surrounding atmosphere. The true temperature is doubtless higher, but is very unlikely to be high enough to account for the discrepancy between the observed and calculated damping-factors. The matter is certainly one to which attention should be paid in future experiments. With regard to the point raised by Dr Wood, the opinion expressed in the paper is that any damping due to the presence of the grid is small compared with the damping due to viscosity in the neck of the resonator. The experiment which he suggests should however be performed to remove uncertainty. It is not clear to me that the sensitiveness of the hot-wire grid as a detector has any simple relation to its damping effect; a coarser and less sensitive grid would probably produce greater damping than a grid of the more sensitive fine wire.

# THE CURIE POINTS

By L. F. BATES, B.Sc., Ph.D., Senior Lecturer in Physics,
University College, London.

*ABSTRACT.* Attention is directed to the fact that at least three temperatures may require to be specified in a description of the magnetic behaviour of a ferromagnetic substance. These are respectively termed the ferromagnetic critical point, the ferromagnetic Curie point, and the paramagnetic Curie point. The significance of the relative positions of the last two points is discussed, and it is shown that a slight extension of the view that ferromagnetism is due to a magnetic particle consisting of a group of associated atoms may account for the paramagnetic behaviour of iron, nickel and cobalt, and for that of more complicated substances such as the ferrocobalts, magnetite and manganese arsenide.

---

## §1. STATEMENT OF PROBLEM

FOLLOWING a recent discussion on magnetism*, some criticism was directed against the use of the term Curie point. It must be confessed that the term should not be used without discrimination, for in discussing the properties of a ferromagnetic material we may have to bear in mind at least three different temperatures, each of which may loosely be termed a Curie point. Suppose we consider the way in which the intrinsic magnetization of a ferromagnetic substance decreases with rise in temperature. In the first place we have a temperature at which the rate of change of the square of the intrinsic magnetic moment per unit volume with temperature is a maximum. This temperature, often referred to as the Curie point, is important in the discussion of the specific heat of the ferromagnetic substance, for, on the older Weiss theory†, or on the more recent theories of ferromagnetism‡, the specific heat of the substance should be a maximum at this temperature, and experiment has shown that it is so §. It has been suggested by the writer that this temperature should be termed the ferromagnetic critical point, as it is not sufficient to state that a change in specific heat occurs at the Curie point.

*The ferromagnetic Curie point.* A second temperature which is of interest is that at which the intrinsic magnetization may be considered to become zero. This point presents some difficulty, because it is not easy to understand how the intrinsic magnetization can become zero at a sharply defined temperature, as is so commonly supposed. At any rate, we may make our conception of this temperature more precise by supposing that it is obtained by extrapolation from the curve of intrinsic

---

* "Discussion on magnetism," *Proc. Phys. Soc.* **42**, 455 (1930).
† P. Weiss et P. N. Beck, *Journ. de Phys.* **7**, 279 (1908).
‡ R. H. Fowler and P. Kapitza, *Proc. R.S.* A, **29**, 1 (1929).
§ L. F. Bates, *Proc. Phys. Soc.* **42**, 441 (1930).

magnetic moment with temperature, that portion of the curve where the rate of change of the magnetization with temperature is a maximum being used for the purpose. This temperature is the one which is most frequently referred to as the Curie point. In accordance with the suggestion of Forrer*, we shall term it the ferromagnetic Curie point.

*The paramagnetic Curie point.* A third temperature which is of significance comes under consideration when we discuss the variation of the susceptibility with temperature, when the substance has passed into the paramagnetic state. It is frequently assumed that at temperatures considerably above the ferromagnetic Curie point the susceptibility $\chi$ is given by the Weiss law, viz. $\chi = C / (T - \theta)$, where $C$ and $\theta$ are constants and $T$ is the absolute temperature. Forrer terms the constant $\theta$ in the above equation the paramagnetic Curie point. He points out that on the Weiss theory of the internal field we should expect the ferromagnetic and the paramagnetic Curie points to coincide. Actually, however, various experimenters state that they are separated by a temperature range of some 15° to 20° C. Thus, for iron Preuss and Hegg† find a separation of 16° C. For nickel, separations of 15, 14 and 22° C. are given by Bloch, Alder and Peschard‡ respectively. For cobalt Preuss and Bloch‡ respectively give separations of 19 and 25° C. It should be remembered, however, that it is disputed whether the Weiss law holds for these substances at temperatures far above their ferromagnetic Curie points. For example, Terry§ finds that in all three cases a continuous curve is obtained when $1/\chi$ is plotted against the temperature. If tangents are drawn to his curves in the regions of the highest available temperatures, we obtain intersections on the axis of temperature which give separations between the ferromagnetic and paramagnetic Curie points of approximately 80, 30 and 40° C. for iron, nickel and cobalt respectively.

*The reversal Curie point.* Forrer‖ also shows that a fourth temperature may be of interest, for on taking a specially prepared specimen of nickel he obtained with it a series of hysteresis cycles up to, and, more particularly, in the near vicinity of, the ferromagnetic Curie point. The cycles were of distinctive appearance and characterized by very abrupt changes of magnetism when certain critical fields were attained. These critical fields were those at which the reversible portions of the magnetism changed abruptly; the coercive fields were the fields necessary for the irreversible reduction of the magnetism to zero. Incidentally, it was found that the residual magnetism was accurately proportional to the intrinsic magnetization of the specimen. Forrer plotted the above critical fields against the temperatures at which the hysteresis cycles were obtained, and by extrapolation he found the temperature at which the critical field could be taken to be equal to zero. It was also found by extrapolation that the coercive force became zero at the same temperature. This temperature Forrer terms the reversal Curie point. He found it to be some 20° C. above the ferromagnetic Curie point, and, in fact, he considers that it is

*The symbols in the margin:* $\dfrac{\chi}{C, \theta, T}$

---

\* R. Forrer, *Journ. de Phys.* **1**, 49 (1930).

† F. Hegg, *Arch. des Sci.* **31**, 4 (1911) and A. Preuss, *Thèse* (Zurich, 1912).

‡ These values are taken from the paper by R. Forrer mentioned above.

§ E. M. Terry, *Phys. Rev.* **9**, 39 (1917).      ‖ R. Forrer, *loc. cit.*

identical with the paramagnetic Curie point, i.e. that the critical field ceases to exist at the paramagnetic Curie point, so that the simple conception of the Weiss internal molecular field is not adequate to explain the existence of intrinsic magnetization. Hence we need only consider, according to Forrer, the existence of the ferromagnetic and the paramagnetic Curie points, and we may represent the state of affairs diagrammatically as in figure 1. The curve on the left represents the variation of the intrinsic magnetization with temperature, whilst that on the right is supposed to represent the variation of $1/\chi$ with temperature well above the ferromagnetic Curie point. The ferromagnetic and paramagnetic Curie points are denoted by $\theta_f$ and $\theta_p$ respectively. This diagram Forrer considers to represent the behaviour of iron, nickel and cobalt.
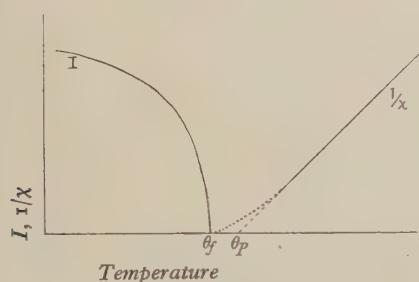
$1/\chi$
$\theta_f, \theta_p$



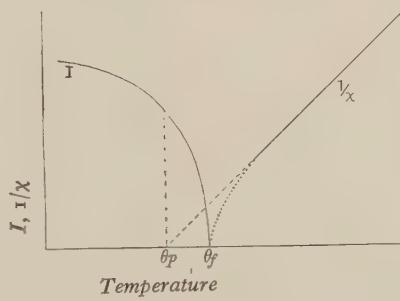Fig. 1. Variation of $I$ and $1/\chi$, with temperature

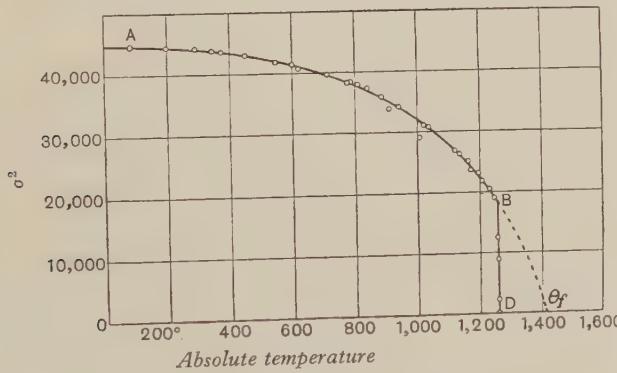Fig. 2. Variation of $I$ and $1/\chi$, with temperature



Fig. 3. Variation of $\sigma^2$ for alloy 40 % Fe, 60 % Co.

*The Curie points of the ferrocobalts.* There are, however, cases where the paramagnetic Curie point is lower than the ferromagnetic Curie point. Such cases occur with the ferrocobalts. Preuss* has found that alloys containing respectively 28·2, 38·1, 48·2, 59·8 and 69·0 parts of cobalt per 100 parts of metal all have very high ferromagnetic Curie points and that the paramagnetic Curie points are respectively 45, 75, 125, 140 and 74° C. lower. In these circumstances we might *a priori* expect that the state of affairs would be represented diagrammatically as in figure 2, but

* A. Preuss, *Thèse* (Zurich, 1912) and R. Forrer, *loc. cit.* Cf. also H. Masumoto, *Sci. Rep. Tokio*, **15**, 449 (1926).

Forrer considers that the free movement which we associate with the magnetic particle in the paramagnetic state is incompatible with the existence of ferromagnetism, and that the latter must disappear abruptly in the neighbourhood of the paramagnetic Curie point, i.e. practically along the ordinate at $\theta_p$. Actually, such cases are found in practice, for Preuss* has shown that all the ferrocobalts containing between 30 to 70 per cent. of iron exhibit this abrupt loss of ferromagnetism. A typical result is shown in figure 3. Let us note in passing that the deduction of the ferromagnetic Curie point now requires a somewhat doubtful extrapolation.

## §2. FORRER'S EXPLANATION

In accepting the existence of the two Curie points, Forrer suggests that two different mechanisms are necessary to explain them. He suggests that the ferromagnetic Curie point corresponds to the disappearance of an intrinsic orientation of the elementary magnetic particle, in which only the direction and not the sense of the magnetic particle is taken into account. This orientation may therefore arise from forces other than those of a purely magnetic origin. On the other hand, he suggests that the paramagnetic Curie point is defined by the fact that below it a finite magnetic field is necessary to reverse the magnetic moment of the substance. Hence, in this case we are concerned only with the sense of the magnetic particle of the elementary particle without reference to its orientation. Forrer finally concludes that for the production of ferromagnetism intrinsic orientation and hysteresis are simultaneously necessary, one of these alone being insufficient.

## §3. RECONSIDERATION OF PREVIOUS RESULTS

Now it appears to the writer that the matter may with profit be considered from another standpoint. Let us suppose that a long cylindrical specimen of ferromagnetic material is suspended vertically in a vacuum between the poles of an electromagnet, as in the Gouy method for the measurement of susceptibility. Let a uniform field $H$ exist at the lower end of the specimen, whilst the upper end is not subjected to any appreciable field. Then the specimen will be acted upon by a force tending to pull it downwards. If the temperature be such that the substance is in a paramagnetic condition, and if it behaves as depicted in figure 1, then the straight portion of the curve may be taken to represent the variation of the reciprocal of the downward pull with temperature for a known value of $H$ at high temperatures. What, then, will be the shape of the curve joining $\theta_f$ to the end of the straight portion? It will be some such curve as that represented by the dotted line, concave upwards, the actual shape of the curve depending on the strength of the field $H$. This is a point which does not appear to be sufficiently emphasized in the published investigations of the paramagnetic susceptibility of ferromagnetic substances. If now we erect an ordinate at $\theta_p$ in figure 1 we have to consider the significance of the portion of the dotted curve to the right of this ordinate. It is at once obvious that the pull recorded experimentally is less than it would be if the substance were actually in the para-

* A. Preuss, *loc. cit.*

magnetic state represented by the continuation of the straight line. The dotted
curve in figure 1 appears to represent the behaviour of iron, nickel and cobalt,
although systematic data, obtained by the method outlined above, appear to be
lacking. There appears to be no doubt, however, that we have to explain why the
pull is less than that theoretically possible over a considerable range of temperature.
Turning now to figure 2, let us suppose that a specified ferromagnetic material gives
the straight line shown when we plot the reciprocal of the pull against the tempera-
ture for a known value of $H$. The dotted curve running from the ferromagnetic
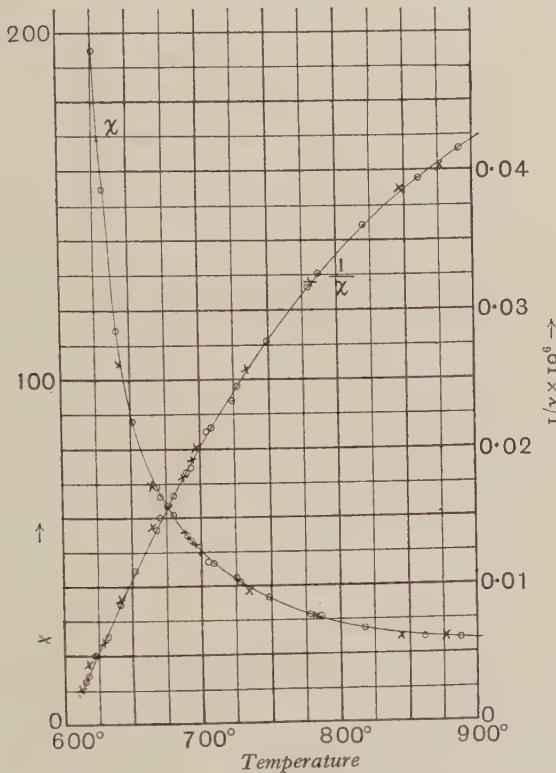


Fig. 4. Variation of $\chi$ and $1/\chi$.

Curie point to the straight portion must now be convex upwards. In this case the
dotted curve always corresponds to a pull which is greater than that which would be
observed if the Weiss law were obeyed throughout the whole range of temperature
above the ferromagnetic Curie point. Magnetite, as far as the writer is aware, appears
to be the only ferromagnetic substance which gives a curve similar to the complete
curve of figure 2. In figure 4 the results obtained by Takagi* are reproduced. His
work was carried out by the Faraday method for the determination of susceptibility
apparently with a single value of $H \cdot dH/dx$ equal to $2\cdot035 \times 10^6$ c.g.s. units. There
does not appear to be a straight portion in the curve thus obtained. We must note,
however, that Takagi does not discuss the relation between $H$ and $\chi$.

\* H. Takagi, *Sci. Rep. Tokio*, **2**, 117 (1913).

In the case of the ferrocobalts which show the abrupt loss of ferromagnetism illustrated in figure 3, Preuss* has shown that the graphs of $1/\chi$ with temperature are straight lines. Just above the temperature at which the ferromagnetism disappears the alloy exists in a $\beta$ state which persists only over a limited temperature range of some 50 to 100° C., depending on the relative proportions of iron and cobalt. It then passes, very suddenly, in some cases, into the $\gamma$ state, which is characterised by a much lower susceptibility. The graph for the $\beta$ state intersects the axis of temperature at the point where the ferromagnetism disappears, within the limits of experimental error. Here, too, the results were obtained by the Faraday method, in which, apparently, only one value of $H.dH/dx$ was used.

## § 4. EXPERIMENTS ON FERROMAGNETIC COMPOUNDS OF MANGANESE

A series of experiments on manganese phosphide† by the Gouy method gave a curve similar to that shown in figure 1, the difference between $\theta_f$ and $\theta_p$ being about 20° C. The values obtained for the susceptibility did not appreciably depend on the applied field, at any rate at temperatures over 10° C. above $\theta_f$. Results obtained with manganese arsenide are, however, of much greater interest in this discussion. This substance has a ferromagnetic critical point at 42·2° C. and a ferromagnetic Curie point at 43·2° C. The curves of the reciprocal pulls against temperature for values of $H$ equal to 3500, 2750 and 1950 gauss are shown in figure 5. The pulls obtained with the lowest field are naturally open to rather larger experimental errors than the others. It was found that the susceptibility varied with the applied field up to 92° C., and it is noteworthy that those portions of the curves which are convex upwards end approximately at 100° C. Above 92° C.



Fig. 5. Results for manganese arsenide

the values of the susceptibility at different temperatures were quite definitely independent of the applied field. The curves eventually become straight lines at higher temperatures, and the value of the paramagnetic Curie point obtained by extrapolation is 1·5° C., i.e. the ferromagnetic Curie point, is considerably higher than the paramagnetic Curie point, as in the case of the $\gamma$ states of iron and of the ferrocobalts.
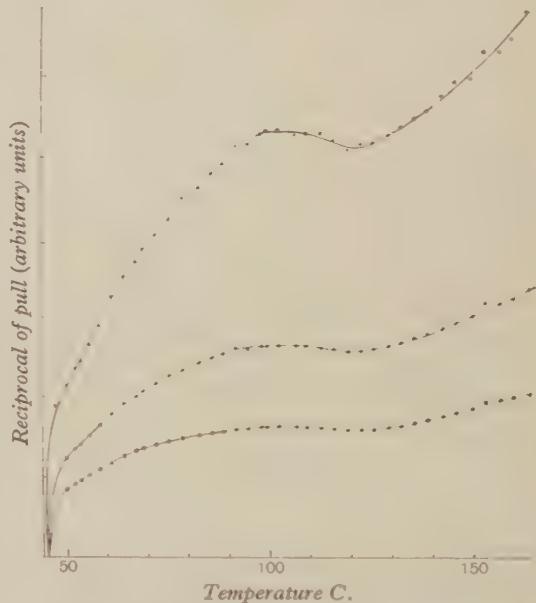
* Preuss, *loc. cit.*                  † L. F. Bates, *Phil. Mag.* **8**, 726 (1929).

## §5. SUGGESTED INTERPRETATION

It appears to the writer that the question whether or not the Weiss law is obeyed at high temperatures is of secondary importance, and that the explanation of the initial curvature of the graph of $1/\chi$ against the temperature is much more important. The explanation appears quite straightforward if we adopt a simple picture of the elementary magnetic particle. Experimental evidence indicates that the latter consists of a group of atoms, the interaction of particular electrons in the group being responsible for its ferromagnetic properties. As the temperature of a ferromagnetic substance rises the number of such groups may change owing to dissociation of the group, thus producing a change in the intrinsic magnetization. There is no reason to suppose that this dissociation is complete at $\theta_f$. We know that the intrinsic magnetization is practically zero at the ferromagnetic Curie point, but that fact need not necessarily imply that the atoms have entirely ceased to be associated in groups. It is easy to see that if the groups still persist above the ferromagnetic Curie point —naturally, in a different state from those below this point—they may possibly produce less magnetic effect than would be produced if all the atoms were free from the forces holding them in the group. In this case the curve of $1/\chi$ with temperature would be concave upwards, and a very slight trace of residual ferromagnetism would be sufficient to cause the shape to change considerably with the applied magnetic field. A tangent drawn at any point on this curve would strike the temperature axis at a point above the ferromagnetic Curie point. As we have seen, iron, nickel and cobalt give curves of this type. If Terry's results* are accepted, then we must admit that the association of the atoms persists over large ranges of temperature above the ferromagnetic critical point. In any case, the work of all experimenters appears to show that the amount of residual ferromagnetism in all three cases must be very small, although a detailed study exists only in the case of nickel†. If, however, the ferromagnetism does not entirely disappear at the ferromagnetic Curie point, but persists in amounts sufficient to mask the paramagnetic effect of the individual atoms, then we should expect the curve of $1/\chi$ against the temperature to be convex upwards, owing to the continual decrease in ferromagnetism with rise in temperature. The curve would, however, depend markedly upon the strength of the applied field, and it is therefore unfortunate that in the case of magnetite, we possess no detailed investigation of the variation of the susceptibility with the applied field. Broadly speaking, then, if association of the atoms persists without ferromagnetism we get a curve concave upwards, whilst if ferromagnetism persists slightly we get a curve convex upwards. It is clear that if ferromagnetism persists slightly over a limited range of temperature above the ferromagnetic Curie point whilst association of the atoms in groups persists over a greater range, we may obtain curves which are at first convex upwards and then concave upwards, and possibly giving a straight portion when the association has entirely disappeared. In these cases we should expect the shape of the convex portion to vary with the strength of the applied field. This is precisely the type of curve which is found with manganese

* E. M. Terry, *loc. cit.*        † P. Weiss and R. Forrer, *Ann. de Phys.* 5, 153 (1926).

arsenide, and it is noteworthy that above 100° C., where the susceptibility is independent of the applied field, the curve approximates closely to those obtained for iron, nickel and cobalt. If further evidence in favour of the views advanced here to explain the behaviour of manganese arsenide is necessary, it is provided by the behaviour of the temperature-hysteresis of the substance as described in an earlier paper*. One further point is of interest. The value of the Weiss constant of the internal molecular field is calculated from the straight portions of such curves. This constant is used in calculations dealing with the properties of the substance below the ferromagnetic Curie point. It is clear from the above views, which we have adopted to explain the complete course of the curves, that its use should more correctly be restricted to regions above the ferromagnetic Curie point. The fact that the agreement between the experimental and calculated values, e.g. of the specific heat, below the ferromagnetic Curie point is so good, is only further evidence that the forces which cause the groups of atoms to associate and form magnetic particles are small compared with the forces which bind the atom in the crystal.

Let us now turn to the results obtained by Preuss with the ferrocobalts, such as those depicted in figure 3. It seems most reasonable to suppose that in these cases the groups of atoms suddenly and completely break up. Hence there is a complete loss of ferromagnetism and the individual atoms are also completely free of the forces which caused them to associate in groups. We should therefore expect the substance to be perfectly paramagnetic, and to give a graph of $1/\chi$ with temperature intersecting the temperature axis at the point at which the ferromagnetism completely disappears. There is some additional evidence for this view, for if the groups are so completely broken we should expect a temperature-hysteresis to occur. Such hysteresis in the ferrocobalts has been shown to exist by Masumoto†.

### § 6. CONCLUSION

It is therefore considered that a reasonable extension of the view that ferromagnetism is due to the association of atoms in groups may account for the paramagnetic behaviour of the simpler elements iron, nickel and cobalt and for that of more complicated substances such as the ferrocobalts, magnetite and manganese arsenide. The position of the paramagnetic Curie point is relatively unimportant. Our survey of existing knowledge indicates that more detailed investigation of the variation of the susceptibility of ferromagnetic bodies just above their ferromagnetic Curie points, particularly with respect to the applied magnetic field, is desirable. The existing experimental evidence in the case of iron, nickel and cobalt indicates that the existence of a true paramagnetic Curie point is doubtful and may only be assumed for the purpose of an approximate calculation of the Weiss constant of the internal molecular field, but it certainly appears desirable to employ the terms ferromagnetic Curie point and paramagnetic Curie point in our discussion of magnetic behaviour.

\* L. F. Bates, *Phil. Mag.* **8**, 714 (1929).
† H. Masumoto, *Sci. Rep. Tokio*, **15**, 449 (1926).

## § 7. ACKNOWLEDGMENT

## DISCUSSION

The PRESIDENT referred to the diagram for the ferrocobalts, which showed a very abrupt loss of ferromagnetism, and asked whether the graph obtained by plotting the reciprocal of the susceptibility against the temperature in the region above the ferromagnetic Curie point was a straight line or a curved line.

Dr BATES, in reply, showed lantern slides of the graphs of the reciprocal of the susceptibility against temperature for various ferrocobalts, reproduced from Preuss's dissertation. The graphs for regions just above the ferromagnetic Curie points were straight lines. At higher temperatures more or less abrupt changes, corresponding to the $\beta$–$\gamma$ change in the case of iron, were observed.

# VARIATION OF SPARK-POTENTIAL WITH TEMPERATURE IN GASES*

## By H. C. BOWKER, B.Sc. (Eng.), Ph.D., A.K.C.

*Communicated by Mr E. B. Wedmore, April 5, 1930, and in revised form, August 6, 1930. Read and discussed November 21, 1930.*

*ABSTRACT.* The effect of temperature on spark-potential in hydrogen and nitrogen at ordinary pressures has been studied up to 860° C., over 6000 voltmeter-readings having been taken. The spark-potential is found to depend on the density of the gas and to be independent of temperature and pressure for a given density. Additional ionization of limited amount does not lower the spark-potential at ordinary densities.

---

### §1. OBJECT AND SCOPE

THE object of the research described in this paper was to determine the effect on the spark-potential of the temperature of the gas in which sparking takes place. This research, which has been carried to much higher temperatures than any reached by previous experimenters in the same field, leads to the conclusion that, over the range of the experiments, the spark-potential is only affected by variation of temperature in so far as it alters the density of the gas. This is in agreement with Paschen's law which, in its general form, states that in a uniform field and in any particular gas the spark-potential is a function of the mass of gas between the electrodes.

Tests have been made at temperatures up to 860° C. at pressures ranging from about 0·25 to 2 atmospheres absolute in hydrogen and nitrogen, the electrodes used being spheres both of copper and of nickel, having a radius of 1 cm. Earlier investigators who have worked within the above range of pressure, have only carried out tests up to about 300° C.† in air, so that a considerable advance has been made. (For details see next section.) Higher temperatures could not be reached with the present apparatus, as the quartz vessel, being necessarily hotter than the spark-gap which it enclosed, showed signs of devitrification. In order to reach higher temperatures, apparatus of a different type must be designed.

---

* Abridged from a thesis approved for the degree of Doctor of Philosophy in the University of London.

† Since the experiments described here were completed, an account of similar work in Germany has been published by S. Franck, *Archiv f. Elekt.* **21**, 318 (1928). Although Franck's curves do not agree with standard calibrations, they lead to the same conclusions as are given here, except that he finds a drop in the spark-potential at temperatures above 700° C. for gaps greater than 4 mm. As he apparently used steel spheres in air, the surface may have been covered with oxide at that temperature, and some such effect as the roughness of the surface might account for this deviation from the usual law.

## §2. INTRODUCTION

*Theoretical considerations.* It is well known that the spectrum of a spark corresponds to that of the gas through which the spark passes, whereas the spectrum of an arc contains that of the electrodes. Hence spark-over depends on the ionization of the gas. Usually a few ions diffuse into the gap from the surrounding space, and then, when the spark-potential is reached, the number of ions is multiplied enormously, and a spark takes place. Townsend's theory, which is to a large extent accepted, accounts for this intense ionization by collision of negative and positive ions. Ionization by collision is affected by the density of the gas, as well as the kind of gas, since the kinetic energy of the ions and their mean free path are concerned. The effect of the density of the gas is therefore of great importance, and many investigators have examined the relation between pressure and spark-length in uniform fields.

The problem on which this research is an attempt to shed light is whether the number of ions is increased as the temperature rises, to such an extent that the spark-potential is appreciably lowered.

*Previous work on the effect on spark-potential of variation of pressure.* A large number of experimenters have investigated the effect of variation of the pressure and gap-length at atmospheric temperature, chiefly between electrodes giving a uniform or nearly uniform field. Paschen[1] made a series of tests on a number of different gases between spheres of 1 cm. radius, using gap-lengths of 1 to 10 mm. at pressures from atmospheric down to a few cm. of mercury. As a result of these tests he formulated the law known as Paschen's law in the form: "Spark-potential is a function of (pressure × spark-length)." Similar tests had been made by Baille[2], Wolf[3], and de la Rue and Muller[4], and have since been confirmed by many other workers. Further references are not given here, as a long bibliography of earlier work is given at the end of a paper by Edler[5] in 1925, and the whole of this subject is treated by Whitehead[6], who gives a large number of useful references. An important work which should be mentioned here is Schumann's *Elektrische Durchbruchfeldstarke von Gasen* (Berlin, 1923). He also gives a large bibliography (pp. 94–96).

In 1903 Carr[7] made several series of tests with a gap of 3 mm. between parallel plates at low pressures down to 0·5 mm. His curves show a rise in spark-potential at the lowest pressures, but he still finds that Paschen's law holds. The work of Cardani[8], published about the same time as that of Paschen, is cited by Guye and C. Stancescu[9] in support of the use of density, instead of pressure, in Paschen's law. They made tests with a short gap, at pressures ranging from atmospheric up to about 10 atmospheres, using commercial carbon dioxide, and found that Paschen's law holds for the whole range if used in the more general form: "Spark-potential is a function of (mass of gas between electrodes) × (spark-length)."

Tests made by Hayashi[10] at higher pressures still (up to 70 atmospheres) indicate that the spark-potential falls off above 10 atmospheres, and tends towards a limiting value for a given gap-length.

7

Before leaving the work of the earlier investigators, it is well to draw attention to the fact that many of them made tests in a number of different gases. Very little appears to have been done recently in this direction. Generally speaking, their results show that high spark-potentials are associated with high molecular weights, but the spark-potential is by no means proportional to the molecular weight. This is brought out clearly by Carr's results [7].

*Previous work on the effect on spark-potential of variation of temperature.* The variation of spark-potential caused by changes in temperature has not attracted so much attention. In 1834, W. Snow Harris [11] performed some experiments on the potential required to cause spark-over between two spheres in a glass receiver. The volume was fixed, and the temperature was varied between 10° and 150° C., "but without in the least affecting the result." "The insulating power of the air was found to be quite independent of its temperature, and to depend only on the density."

An improvement on this method was made by Cardani [8], in 1888. The volume was again fixed, but the pressure of the air was measured with a manometer, the temperature being calculated from the change in pressure. Temperatures up to 300° C. were obtained, but above this the glass vessel became conducting. The temperature-distribution was far from uniform, so that great accuracy could not be expected, but the results were sufficiently consistent to enable Cardani to conclude that the spark-potential is a function of the mass of gas traversed by the spark, and that a temperature-effect is not to be expected until the temperature becomes high enough to reduce the stability of the molecule.

The only further tests* on the effect on the spark-potential of variation of temperature appear to have been made at very low pressures by Bouty [12] (in 1903), and Earhart [13] (in 1910), in air, hydrogen, and carbon dioxide. Bouty's tests were made at temperatures up to 190° C. with pressures ranging from 4 to 10 cm. at atmospheric temperature. Earhart's work does not apply to the region with which the present paper is concerned, as the air he used was only at a few mm. pressure. Under these conditions, up to 600° C.†, he found that the spark-potential in air and carbon dioxide, in this region, depends on the mass of gas between the electrodes and is otherwise independent of temperature. A more recent investigation on the effect of temperature was made by Peek [14] with concentric cylinders, but the electric discharge in this case was visible corona, and not the spark. The range of temperature was − 20° C. to 140° C., and the results show excellent agreement with curves obtained by variation of the pressure only.

From the preceding sections it is seen that Paschen's law holds in its most general form for a wide range of densities, from a pressure of a few cm. up to about 10 atmospheres. The effect of temperature (over the small range studied) appears to be confined to the alteration of the density of the gas, and is, therefore, auto-

* See footnote on p. 96.

† Earhart continued his tests up to 1000° C. in air, but, owing to the experimental difficulties, the results for this higher range do not exhibit the same close agreement, so that it is uncertain whether the above conclusion holds for the higher range.

matically included in the general form of Paschen's law. It remains to be shown whether this holds for temperatures above 300° C. at ordinary pressures. The agreement among Cardani's results is not close enough to remove all question of any deviation, even up to 300° C., and certainly warrants no extrapolation.

*Experimental details.* In order that the results might be comparable with those of other investigators and with standard calibrations, it was decided, at the beginning of this research, to use a spark-gap comprising spheres 1 cm. in radius. The spheres were made of copper and nickel, the latter being chosen on account of its high melting point, about 1450° C., and its slowness to oxidize. Hydrogen was the gas chiefly used, as it gives a definite spark-over voltage with spheres and keeps the electrodes clean and free from oxide. One series of tests was made in nitrogen as a check, this gas being selected on account of its inert nature. After a considerable time spent in overcoming experimental difficulties a suitable apparatus was evolved having the spheres enclosed in a quartz tube. A heater of the resistance-wire-wound type surrounded this tube, and was found adequate for the immediate requirements, although, in the light of the experience gained during the tests, many improvements might be made with advantage.

The particular object was to compare values of spark-potential obtained at low temperatures with those obtained at higher temperatures, with a view to detecting any decrease in spark-potential at constant density as the temperature rose.

On account of the difficulty of obtaining accuracy in measurements of high temperatures and spark-over voltages, a large number of tests was made, involving over 6000 voltmeter-readings, besides many other measurements. The frequency of supply in all these tests was approximately 51·5 ∼. No special attempt was made to maintain a constant frequency or to check it often, as the spark-potential of the sphere-gap is independent of it at all ordinary frequencies. According to Peek[15] and Reukema[16], the same results are obtained for frequencies ranging from 10 ∼ to 20,000 ∼, after which the spark-potential falls until 60,000 ∼ is reached, when the decrease ceases and a steady value is obtained.

### §3. DESCRIPTION OF APPARATUS

*General remarks.* The apparatus consisted of a spark-gap chamber of quartz in the form of a tube arranged vertically, in which were enclosed the spheres forming the spark-gap, and the thermo-couple for measuring the temperature. Apparatus for supplying the gas and high voltage were connected to the spark-gap chamber, which was surrounded by a heater at the middle.

*Spark-gap chamber.* To enclose the spheres in an atmosphere of gas at the required conditions a spark-gap chamber was used, the main part of which was a vitreosil tube $A$, figure 1, $2\frac{1}{4}$ in. in bore and 16 in. long, fixed in a flanged brass casting $B$ at the bottom with a sealing-wax joint. A tube $\frac{5}{8}$ in. in bore and 6 in. long was sealed on the top of the main tube, and terminated in a copper tube fixed in with a lead seal. The upper electrode rod, the top part of which was of nickel $\frac{3}{16}$ in. in diameter, passed through the copper tube, and was held by several brass nuts and

adaptors, a washer of special rubber and paint being used to make the joint gas-tight. It was possible to see that the spheres were aligned and that the thermo-couple was placed in its correct position as only the lower part of the large tube was opaque, the rest being transparent. The flanged brass end-piece $B$ was bolted down to the base $C$, which also was made from a brass casting. A large washer of the same special rubber was used here, and both sides of the washer and both brass surfaces were carefully greased with tap grease before bolting-up to render the vessel gas-tight. The inlet for gases was through a copper tube, which was screwed and soldered into the base.

*Arrangements for measuring spark-gap.* One of the most important measurements was the length of the spark-gap. In order to obtain an accuracy of about 1 per cent. on a gap of 5 mm., measurements had to be made to hundredths of a millimetre. To provide for measurement and variation of the gap, the lower electrode rod projected downwards through a stuffing box in the centre of the base $C$. It was of nickel, $\frac{5}{16}$ in. in diameter and 22 in. long. At the top it was turned down on a taper and screwed to take the spheres, which were 20 mm. in diameter. A length of about 3 in. at the bottom also was turned down and screwed ($\frac{1}{4}$ in. Whitworth). The next 4 in. was carefully turned, so as to be smooth and straight for passing through the stuffing box.

To prevent the electrode rod turning round, and also to carry a small steel ball used in measuring the gap, a small brass plate $D$ was screwed on the rod, and fixed with a lock-nut. Two rods, screwed into the base $C$, projected vertically downwards, and passed through two holes in this plate. Two strips, shown in section at $E$, were fixed on these rods at the bottom, and formed stops for the nut by which the electrode rod was raised or lowered. Another steel ball was fixed in the bottom of the base vertically above the one on the plate $D$, and an internal micrometer was used to measure the distance between them. This distance was first measured with the spheres just touching, and, when the electrode rod was lowered, the increase in the micrometer reading indicated the length of the spark-gap.

*Arrangements for measurement of temperature.* This is a measurement of the greatest importance. Owing to the uneven temperature-distribution, it was found necessary to measure the temperature actually in the spark-gap. For this purpose a thermo-couple of platinum and platino-rhodium was used and was mounted in two concentric vitreosil tubes, 22 in. long, which supported and insulated the thermo-couple wires, the lower 12 in. being surrounded by a brass tube $\frac{3}{8}$ in. in diameter, shown at $F$. All three tubes were closed up at the bottom with sealing-wax. The brass tube was smooth and strong for passing through the stuffing box, which was provided in the base $C$ for this purpose. The thermo-couple wires terminated in an oil bath in which a thermometer was placed, and copper leads, heavily rubber-covered, connected the thermo-couple from this cold bath to the instrument on which the temperature readings were obtained.

The calibration used was obtained by the National Physical Laboratory for similar thermo-couples taken from the same ingots. The thermo-couple was also compared with another pyrometer, and was found to agree as closely as could be

expected. A curve was obtained giving the E.M.F. in micro-volts corresponding to the cold bath temperature, and this was added on when the temperature was estimated.

*Heater.* In order to heat the spheres and the gas in the spark-gap, a heater surrounded the main tube of the spark-gap chamber and was capable of raising it to
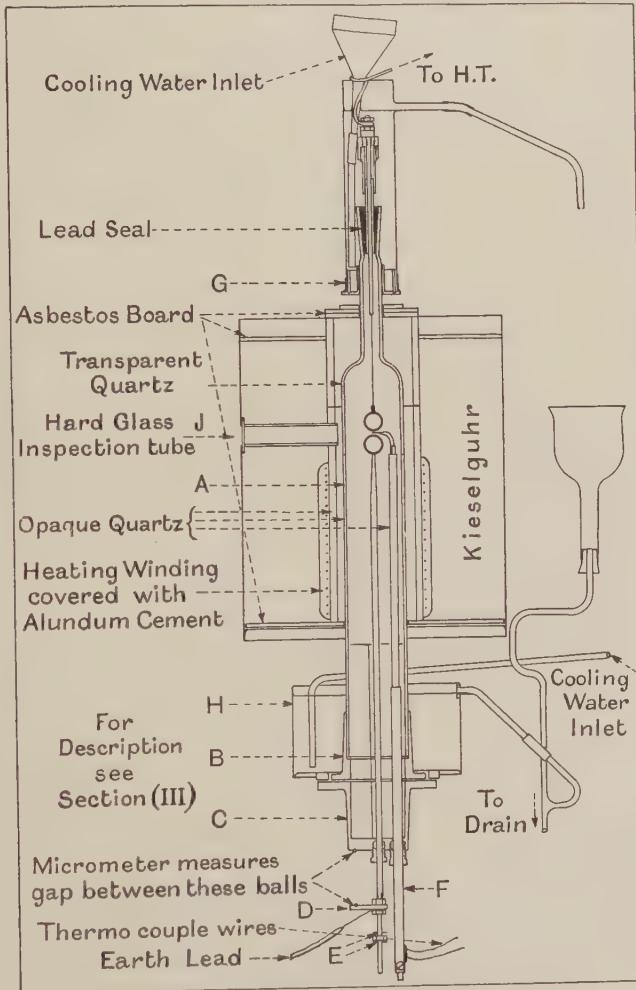
Cooling Water Inlet

To H.T.

Lead Seal

G

Asbestos Board

Transparent Quartz

Hard Glass J Inspection tube

A

Opaque Quartz

Heating Winding covered with Alundum Cement

Kieselguhr

For Description see Section (III)

H

B

C

Cooling Water Inlet

To Drain

Micrometer measures gap between these balls

F

D

Thermo couple wires

Earth Lead

E

Fig. 1. Diagram of apparatus without supporting framework.

temperatures of about 1000° C. The heating-winding was wound non-inductively on an opaque vitreosil tube $3\frac{3}{4}$ in. in outside diameter, and was about $6\frac{1}{2}$ in. long, "brightray" wire, which is made from an alloy of 80 per cent. of nickel with 20 per cent. of chromium, being used. The winding was covered with alundum cement. To reduce the loss of heat by radiation the furnace tube was surrounded with kieselguhr, which formed an effective lagging material. A sheet iron drum 11 in.

in diameter and $13\frac{1}{2}$ in. high had a hole cut in the bottom, and a sheet of asbestos board, having a hole $3\frac{1}{4}$ in. diameter in the centre, placed in it. The tube carrying the heating-winding was placed vertically over this hole, and two hard glass tubes for inspection fitted in position as shown at *J*, figure 1. A short length of similar quartz tube was placed above the other, and the space between the tubes and the outer drum was filled in with kieselguhr. Another sheet of asbestos board covered it, and the whole formed a compact unit quite separate from the rest of the apparatus. The base *C* was bolted down in a framework of angle-steel, and cross pieces were arranged for the heater to stand on. Uprights were fixed in this framework to act as guides, so that, when the spark-gap chamber was in position, the heater could be let down over it, into its place, without any danger of knocking against it. Pieces of asbestos board were placed on top of the heater tube to prevent a constant stream of air passing through the inside of the heater. The heater was supplied during the tests and for some time previously from a 100-volt storage-cell battery, but while the temperature was being raised the 100-volt mains were used. For this purpose a double-pole double-throw switch was connected to the heater, and the circuit included a number of rheostats, an ammeter and a fuse.

Interference with the field between the spheres due to the presence of the heating-winding, or due to the magnetic effect of the heating current, has been so reduced as to become negligible, except for the larger gaps of 8 and 10 mm. This has been brought about by placing the heating-winding entirely below the gap, and by employment of a non-inductive winding.

*Cooling jackets.* Cooling jackets were provided at the top and bottom of the spark-gap chamber. The top jacket protected the lead seal and the joint by which the upper electrode rod was fixed in. It consisted of a glass tube 2 in. in bore with an overflow tube, and it was supported on a special brass cup *G* pushed on to a layer of asbestos string and red lead wrapped round the quartz tube. A piece of thin rubber tube made a water-tight joint between the glass tube and the brass cup. The water was able to reach the bottom of the brass cup, and no trouble was experienced through the asbestos packing getting hot or loose. Both inlet and outlet from this jacket were by drip feed, and sufficient cooling and insulation were obtained in this way up to about 15 kV, when the flow sometimes had to be stopped, as it tended to form a continuous stream. A cylinder with a flange at the bottom on the inside formed the lower water-jacket *H*. It was bolted down to the base, keeping the sealing-wax joint cool and free from strain, as well as cooling the stuffing boxes in the base.

*Gas supply.* Gas was let into or exhausted from the spark-gap chamber through a copper tube, which was screwed and soldered into the base supporting it and was connected to a glass tube by a sealing-wax joint. This glass tube was several feet long and was connected through a stop-cock to one side of a phosphorus-pentoxide drying-tube, a branch between the stop-cock and the drying-tube being joined to a closed mercury manometer about 12 in. long and an open U-tube, also containing mercury, about 4 ft. long. The U-tube was used for measuring the pressure of the gas, in conjunction with a standard barometer, and the closed manometer indicated

the degree of exhaustion obtained before fresh gas was admitted, or when tests for leaks were being made. In order to connect the apparatus with the vacuum-pump, with a cylinder of gas or with the atmosphere, there were several branch tubes on the other side of the drying-tube, each provided with stop-cocks. The pump was a pulsometer 4-inch Geryk rotary vacuum pump, stated by the makers to be capable of reaching pressures as low as 0·02 mm. It dealt rapidly with the volumes of gas used.

The gases* used were hydrogen and nitrogen, and were obtained from cylinders without any subsequent purification, other than passage through the drying-tube.

*High tension supply*. The high voltage supply was obtained from an alternator and a small high-tension transformer having a ratio of 75 : 20,000. The field of the
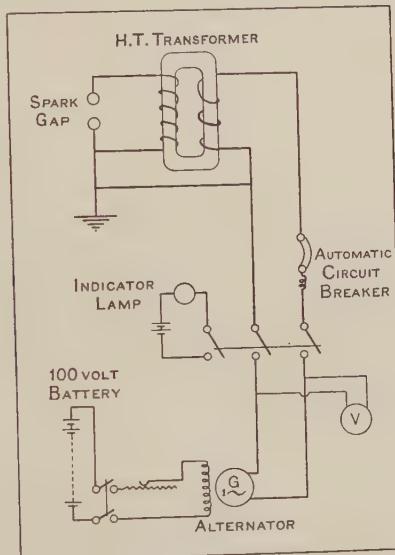


Fig. 2. Wiring diagram.

alternator was separately excited from a 100-volt storage-cell battery, the field-current being controlled by several sliding rheostats conveniently placed so that they could be adjusted while the voltmeter was being read. The voltmeter-readings recorded are those of primary voltage. The primary voltmeter was calibrated against a sphere-gap on the secondary, but an accurate knowledge of the actual secondary voltage is not important, since the primary object is to detect a decrease, if any, in the spark-potential at constant density, and not to compare different spark-potentials. The voltmeter on the primary side provided an accurate and convenient method of measuring the voltage, much quicker than other methods.

The frequency was approximately 51·5 ∼ in all the tests. The wiring diagram is shown in figure 2. The primary circuit included a small automatic circuit-breaker

* The British Oxygen Co., Ltd., gave the following approximate analyses: *Hydrogen* 99·5 per cent. pure, the balance being oxygen with a trace of nitrogen; *nitrogen* 99·2–99·8 per cent. pure, the balance being oxygen with traces of helium and neon.

and a three-pole switch. Two poles of this switch connected the alternator to the transformer, and the third connected a small red indicator-lamp, for a danger-signal, to an accumulator. The automatic circuit-breaker was set so that it would come out as readily as possible. All sparks, except those formed at the lowest voltages, caused the breaker to operate very quickly. This was a distinct advantage, as it greatly reduced the heating of the spheres caused by continued sparking.

### §4. PROCEDURE DURING TESTS

Four series of tests were made as follows: (i) nickel spheres in hydrogen (preliminary); (ii) copper spheres in hydrogen; (iii) nickel spheres in hydrogen; (iv) nickel spheres in nitrogen. The main series was the third. The chief object of the first series was to obtain data about the heater and the temperature distribution: see figure 8. The temperature was raised by steps of nearly 50° C. when nickel spheres in hydrogen were used, and by 100° C. in the second and fourth series. These two series were made to discover what effects, if any, are due to the use of a different metal in series (ii) and of a different gas in series (iv). The spheres were carefully polished with metal-polish before being put in the apparatus, and remained quite clean in hydrogen. They were not touched during each series of tests.

At each temperature the spark-gap chamber was filled with gas to about 2 atmospheres' pressure, which was a convenient upper limit to the range of pressure used. The spheres were then brought together, so that they were just touching. The micrometer zero-reading was then obtained, and the gap was set to 4 mm. The thermo-couple was replaced in the centre of the gap and the temperature was taken, after which the thermo-couple was pulled down several inches so as not to disturb the spark-gap during tests. The gas-pressure was then read and testing began. About five voltmeter-readings were recorded for each gap, the first one or two sparks being usually not counted. Readings were taken at gaps of 4, 5, 6, 8 and 10 mm. at each pressure, and the pressure was reduced by several steps —usually four or five pressures were used at each temperature —until the primary volts were as low as 8 or 10.

To confirm the temperature-reading and to find out if it had altered by the end of the test, the gap was set to 4 mm., the thermo-couple was again carefully adjusted to the centre of the gap and the temperature-reading was taken. After this the spheres were made to touch again, and the zero checked. As the measurement of the gap depended on the constancy of the zero-reading this was important. Usually it agreed to within 0·02 mm. On a few occasions, when the difference was fairly large, the whole test was repeated. A gradual change of temperature could be allowed for in the calculations by interpolation, but changes in the gap-length had to be corrected for by the drawing of preliminary curves, as mentioned in the next section. Changes not greater than 0·10 mm. were allowed for in this way.

## § 5. RESULTS

*Graphical representation.* About five voltmeter-readings were recorded for each set of conditions, and the average of these was taken. These average voltmeter-readings were first plotted against the spacing between the spheres for each density, for one temperature only, and in this way variation in the length of the gap could be cor-
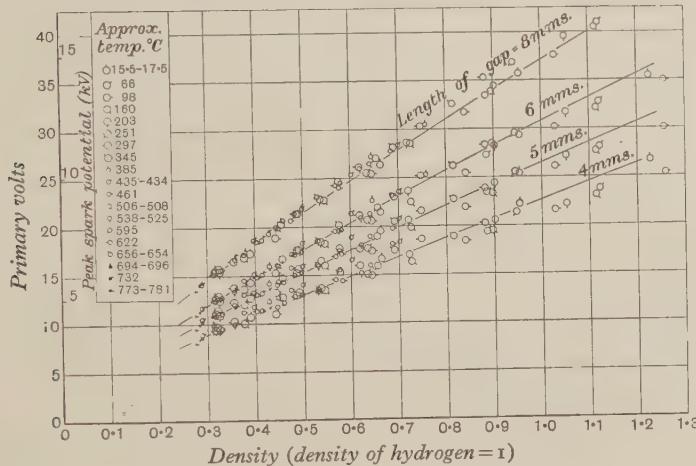


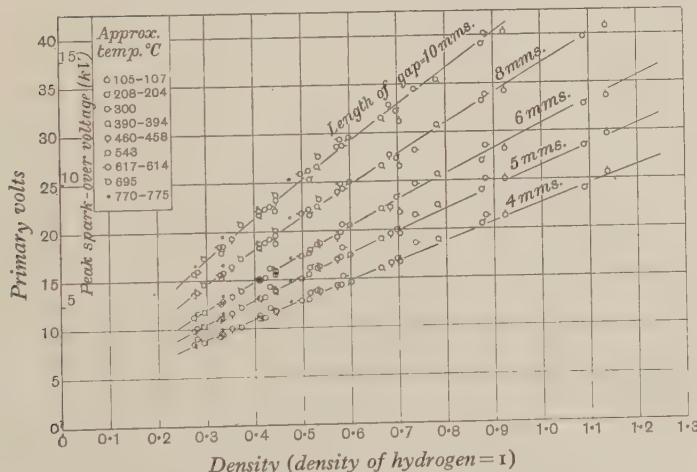Fig. 3 (1st series).  Nickel spheres in hydrogen.



Fig. 4 (2nd series).  Copper spheres in hydrogen.

rected for and any discrepancies due to other factors were exposed. After this, the readings were all plotted against density, in figures 3–6, and fell on different curves according to the length of gap. The figures for density give the density of the gas compared with that of the same gas at 0° C. and 760 mm. pressure, the latter density being taken as unity.

It appeared, when the preliminary curves for series (i) and (iv) were plotted, that the readings taken with a gap of 10 mm. were too inconsistent for any conclusions to be based on them. They have, therefore, not been shown among the results plotted in figures 3 and 6, which are confined to shorter gaps.
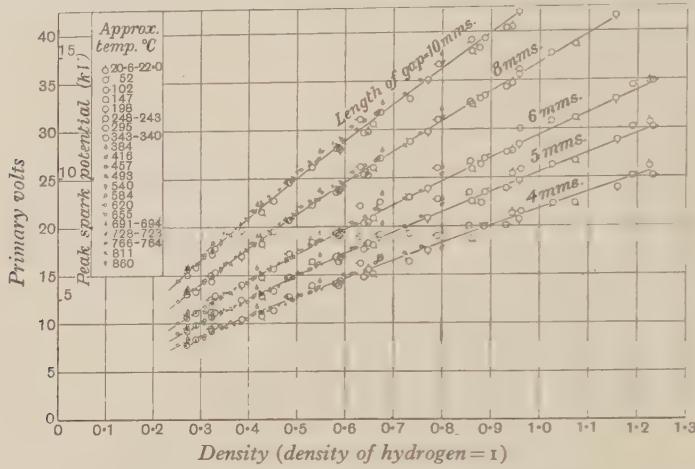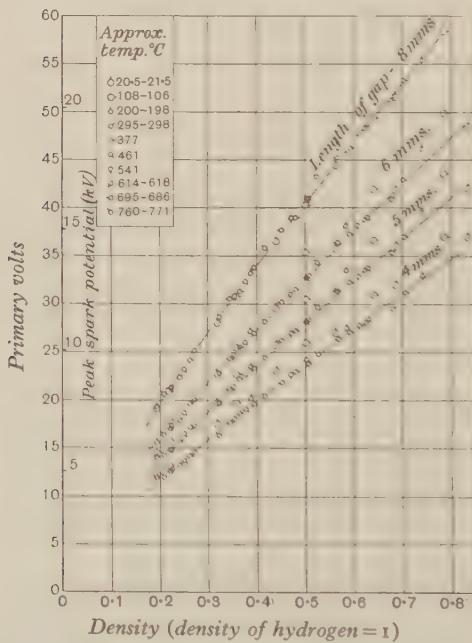


Fig. 5 (3rd series). Nickel spheres in hydrogen.



Fig. 6 (4th series). Nickel spheres in nitrogen.

The temperature-readings are shown to the nearest degree, in order to indicate the extent of the temperature-change during each test. In estimating the actual temperature, it is advisable to allow for a possible error of ± 2 per cent.

Separate curves were also drawn for the 5 mm. gap only, at each temperature, from the data of series (iii). Primary volts, being a measure of spark-potential, were plotted against density as before. The volts at densities 0·4 and 0·5 were read off from these curves, and then plotted against the temperature in figure 7. The points lie approximately along a horizontal line, thus demonstrating that spark-potential is independent of temperature over the range of the experiments.

*Effect of temperature on the relation between spark-potential and density.* When the results are plotted against density as in figures 3–6, there are, for each gap-length, a number of arrays or sets of points, each set being composed of points obtained at the same temperature. A different sign for each temperature is used to mark the points, so that the sets can be distinguished. Each set, since it represents tests at a given temperature, shows the effect of varying the pressure only at its particular
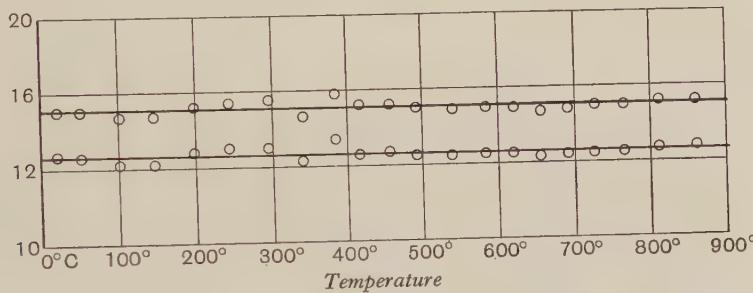


Fig. 7. Relation between temperature and spark-over at constant density
(0·4 for lower, 0·5 for upper curve).

temperature. In the method employed the density of the gas was calculated from both temperature and pressure and the points were plotted against density. It was then found that the curves through each set of points, for a given gap, are practically coincident. All the points together produce a smooth curve giving the relation between spark-over and density for all the temperatures, with these particular electrodes.

This agreement leads to two observations about the curve connecting spark-potential with density: (1) that the shape of the curve, and (2) that the position of the curve is unaltered by changes in the temperature, over the range of the experiments. Of course, the points themselves are found on different parts of the curve, in dependence on the density, which does alter with temperature.

These observations lead to the conclusion that, over the range studied, the spark-potential depends on the density of the gas, and is independent of whether the changes in density are caused by changes of pressure or temperature or both. In other words, if the density is kept constant the spark-potential is independent of the temperature. The latter form of the statement follows immediately from an inspection of figure 7, where values of spark-potential for twenty-one different temperatures are plotted for the same density. All the points lie close to a horizontal straight line.

*Different gases.* The tests of series (iv), in nitrogen, were made in order to find out if there was any effect due specially to the use of hydrogen. The results are similar, the slightly greater irregularity being due probably to the fact that nitrogen is not so good a conductor of heat as hydrogen. It was often some time before the fluctuation of pressure and temperature, caused by changing the pressure, had ceased, and this made the determination of the density difficult. Hydrogen settled down more quickly than the mercury in the manometer.

It might be thought that Paschen's law, which is applicable only to a given gas, might be applied to spark-over in different gases if the term expressing the density were taken to be proportional to either the number of molecules or the mass of gas between the electrodes. Either form applies in any one gas only. By referring to
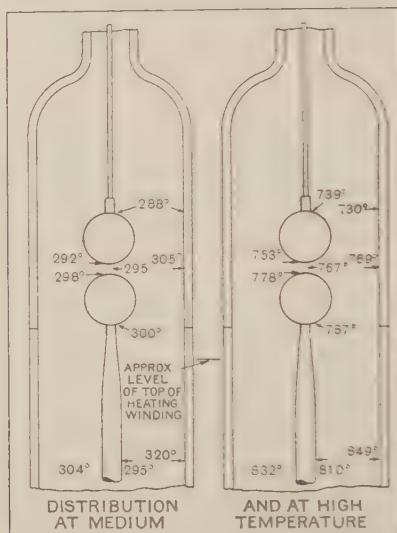


Fig. 8. Approximate temperature distribution in neighbourhood of spark gap.

figures 5 and 6, it is seen, for example, that, with a 4 mm. gap, at density 0·4, the spark-potential in hydrogen is 4·6 kV approximately, and in nitrogen 8·5 kV. These figures, showing the spark-potential in nitrogen to be nearly double that in hydrogen, do not confirm either suggestion. The ratio of the mass of gas in each case is 7 : 1, and if the number of molecules were the basis, the spark-potentials should be identical. It may be mentioned that Paschen and other investigators, who have studied spark-over in nitrogen, hydrogen and other gases, have also obtained results which show that spark-potentials in different gases cannot be related in such a simple manner as that mentioned earlier, i.e. by the taking of the term expressing the density as proportional to either the number of molecules or the mass of gas between the electrodes.

*Different metals.* Two different metals, nickel and copper, were used as electrodes in these temperature tests. No difference in their behaviour was noticed while the tests were being made. The gas used was hydrogen. When the results for copper in

figure 4 are compared with those in figures 3 or 5, which are both for nickel spheres in hydrogen, practically no difference is observable.  Hence it may be concluded that for copper and nickel electrodes, over this range of density, the metal of which the electrodes are formed makes no apparent difference.  It is probable that the same results would be obtained with most metals.

At low pressures of the order of 10 mm. or less a number of investigators have obtained different results when using different metals.  Dubois[17] found that the presence of impurities on the electrodes caused large differences in the breakdown-voltage, but came to the conclusion that, with perfectly clean electrodes, the sparking-potential is independent of the nature of the metal of which the electrodes are made. Variations, however, are still found with different metals, carefully puri-fied, particularly with sodium[18], and some photo-electric effects have been observed. It seems that these effects are only noticeable when the spark-potential is of the order of a few hundred volts, and no appreciable variation occurs at ordinary densi-ties, when the spark-potential is several kilovolts at least.  No alteration in the spark-potential appears to be caused by photo-electric effects at higher pressures and ordinary frequencies, for, according to Reukema[16], at atmospheric pressure and 60 ~ flooding of the spheres with ultra-violet light only serves to increase the accuracy of the sphere gap as a voltmeter, and neither raises nor lowers the spark-over voltage.

*Effect of temperature on the initiation of the spark.*  On comparing voltmeter-readings obtained at high temperatures with those obtained at low or atmospheric temperatures, we at once notice that there is a remarkable regularity among the high temperature-readings, while the low temperature-readings vary slightly. This appears to suggest that at the higher temperatures (say 600° C. upwards) there is a continual supply of ions, which is sufficient to start the discharge directly the applied voltage reaches the spark-potential, but which is not present at low or moderate temperatures. There is, as the curves show, not sufficient ionization to alter the type of discharge, or to reduce the potential required.

When the tests were being made it was found that at high temperatures several readings, practically identical, could be obtained with no difficulty when the voltage was raised gradually.  If the voltage was raised to a value slightly below the spark-over voltage and left there no discharge took place, but directly it was raised above this value a spark was produced. At low temperatures, and in the open, it was nearly always found that the voltage could be raised above the value which afterwards appeared to be the spark-potential, and when at last the spark took place a comparatively heavy current passed. The next attempt almost invariably resulted in spark-over at a lower voltage, after which normal values were obtained. If the voltage was raised very slowly it was usually found possible to get well above the normal spark-potential before breakdown occurred. This irregularity at the lower temperatures may be explained by a lack of casual ions or by the presence of some surface effect. The heating of the spheres caused by the spark also accounts for some irregularity, particularly for the low readings.

Reukema[16] mentions a similar irregularity, but overcame it by providing

additional ionization by flooding the spheres with ultra-violet light. He states that, at ordinary frequencies with ultra-violet light, spark-over was obtained directly the voltage reached the required potential, no point differing more than $\frac{1}{4}$ per cent. from the mean curve, whereas, without ultra-violet light, a difference of about 2 per cent. might occur with any point. The same average value was obtained in both cases.

These results show that at ordinary densities and frequencies some additional ionization does not lower the spark-potential.

### §6. CONCLUSIONS

Allowance being made for irregularities due to uneven temperature distribution, difficulties in measuring high temperatures, and difficulties in obtaining the correct spark-potential, the results plotted for widely differing temperatures show remarkable agreement. *This indicates that the spark-potential for any particular gap is dependent only on the density, and is independent of any effect due solely to the temperature, over this range,* i.e. *up to* 860° C. The results confirm the part of Paschen's law which relates to density, so far as the range extends; this, in its general form as applied to an individual gas, is: "The spark-potential is a function of the mass of gas between electrodes."

Paschen's law, as applied to different pressures and gap-lengths, of course only holds within a finite but wide range of limits, with uniform fields, and in any one gas. Probably the general conclusion, that changes of temperature and pressure make no difference so long as the density remains constant, holds over a wide range of densities and for non-uniform fields. This conclusion, which applies to both hydrogen and nitrogen, will probably hold for most gases, but the curves relating spark-potential with density, for any two gases, will not be identical in form.

The exceedingly close agreement between series (ii) and series (i) (see §4 and figures 3 and 4) warrants the conclusion that, so far as copper and nickel* are concerned, *the metal of which the electrodes are made does not directly affect the results,* and it is probable that, if the surfaces are clean and smooth, the results would be practically the same with most metals.

As a result of the deductions in §5 on the effect of temperature on the initiation of the spark, it appears that additional ionization of a limited extent does not lower the spark-potential at ordinary densities.

### §7. ACKNOWLEDGMENTS

---

* It may be mentioned that the melting points of copper and nickel are 1083° C. and 1452° C. respectively. See *Smithsonian Tables*, p. 198 (1927).

## REFERENCES

(1) F. PASCHEN. *Ann. der Phys. und Chem.* **37**, 85 (1889).
(2) J. B. BAILLE. *Ann. de Chim. et de Phys.* **5**, 25, 486 (1882).
(3) M. WOLF. *Ann. der Phys. und Chem.* **37**, 306 (1889).
(4) W. DE LA RUE and H. W. MULLER. *Phil. Trans.* **171**, 109 (1880).
(5) R. EDLER. *Elekt. und Masch.* **12**, 875 (1925).
(6) S. WHITEHEAD. *Dielectric phenomena—Electrical Discharges in Gases*, pp. 40–51 (1927).
(7) W. R. CARR. *Phil. Trans.* A, **201**, 403 (1903).
(8) P. CARDANI. *R. Accademia dei Lincei, Rendiconti*, **4**, 44–51 (1888).
(9) C. E. GUYE and C. STANCESCU. *Arch. des Sciences*, **43**, 131–160 (1917).
(10) HAYASHI. *Ann. der Phys.* **45**, 431–453 (1914).
(11) W. SNOW HARRIS. *Phil. Trans.* **124**, 230 (1834).
(12) M. E. BOUTY. *Comptes Rend.* **136**, 1646, and **137**, 741 (1903).
(13) EARHART. *Phys. Rev.* **29**, 293 (1909), and **31**, 652 (1910).
(14) F. W. PEEK. *A.I.E.E.J.* **31**, 1059–1064 (1912).
(15) F. W. PEEK. *Dielectric Phenomena in High Voltage Engineering*, pp. 106–107 (1920).
(16) REUKEMA. *Trans. A.I.E.E.* **47**, 38 (1928).
(17) DUBOIS. *Annales de Phys.* **20**, 160–211 (1923).
(18) J. TAYLOR. *Phil. Mag.* **3**, i, 368, and **3**, ii, 753 (1927).

## DISCUSSION

Mr S. WHITEHEAD. I should like to ask the author whether he has considered his results in connexion with recent theories put forward to replace or extend the classical Townsend theory. In the theory of Slepian the main causes of the spark-discharge appear to be thermal ionization together with space-charge effects. Although very little thermal ionization takes place at a temperature of 800° or 900° C., yet if the spark normally has a high effective local temperature an increase of 500° or 600° C. ambient temperature, if reflected in the local temperature, would cause a considerable increase in the amount of thermal ionization, if the ionization-potentials were not too high. One would rather expect to find some effect at the temperatures employed by the author if the ionization potentials were of the order of 4 to 10 or 15 volts, which would be more or less true for the gases he employed.

Prof. W. WILSON said that the thermionic effect would not necessarily be large at the temperatures in question: its magnitude would depend on the metal used.

Dr L. F. BATES pointed out that the best-known experiment devised by the founder of the Physical Society was one in which a red-hot ball may lose positive instead of negative charge.

AUTHOR'S reply. In reply to Mr Whitehead: I agree that an effect of the type he described might occur at still higher temperatures, but it is not apparent at 500° or 600° C. If thermal ionization is a cause of the spark-discharge, breakdown will take place when the appropriate temperature is attained, by which time the layers of gas surrounding the inner core, which ultimately becomes the discharge

path, will also be heated, chiefly by conduction from the inner core. The time required to reach this state will be shortened as the ambient temperature is increased, but the final temperature of the inner core will depend on the potential-drop and the properties of the gas.

Thermionic emission, undoubtedly present though small, appears merely to facilitate spark-over.

## DEMONSTRATION

Demonstration of an Instrument for Combining Two Curves into One (devised by J. L. HAUGHTON, D.Sc.), *given on November 21, 1930*, by Mr R. PAYNE.

In certain apparatus for recording on a thread recorder the changes of a physical property of a metal with change of temperature, two curves are obtained, one representing change of temperature plotted against time, while the other represents change of the property being measured, also plotted against time. While such pairs of curves can be used to determine the value of the physical property at any temperature, it is often advisable to replot the data obtained, so as to give one curve representing the temperature property function of the material. The instrument exhibited does this replotting semi-automatically. The thread-recorder drum, containing the two records, is driven slowly below two cross wires which can be moved, by means of lead-screws, in a direction parallel to the axis of the drum. By rotation of the lead-screws while the drum is rotating it is possible to cause the cross-wires to follow the curves. Small lenses are carried above the cross-wires to facilitate reading. One of the lead-screws drives a table whose motion is, therefore, proportional to the ordinates of one curve, say to the temperature. The other lead-screw drives a pencil through the intermediary of a pair of $45°$ bevel wheels, so that the pencil moves at right angles to, and in proportion to, the ordinates of the other curve. The motion of the pencil relative to the plate will therefore trace out a curve connecting temperature and the physical property being studied.

# REVIEWS OF BOOKS

*A Text Book of Sound*, by A. B. WOOD, D.Sc. Pp. xiv + 519. (London: G. Bell and Sons, Ltd.) 25s.

This work, as one would expect from the author's reputation, possesses a decidedly practical bias, and, although the mathematical treatment is adequate, mathematics is, throughout the book, a tool used to subserve the needs of the experimenter.

The subject-matter reported is conveniently arranged in five sections, the first of which gives an excellent account of the theory of vibrations and the second of vibrating systems and sources of sound—in particular the maintained tuning-fork and the quartz oscillator. Besides much that is common to most text-books on the subject there are paragraphs on relaxation oscillations, motional impedance, and alternating-current sources, while the analogy between electrical and mechanical oscillating systems is emphasized both here and throughout the book.

The velocity of sound-waves of small and finite amplitude and of normal and ultrasonic frequencies, the effect of change of medium, and the attenuation of waves are among the subjects treated in the next section; here it is satisfactory to find included a comparatively full treatment of diffraction, which is so often considered as peculiar to the domain of physical optics. We note that the author seems to imply that Dixon's method for determining the effect of temperature on the velocity of sound in a gas is a resonance-tube experiment, while recent work by Partington and Shilling using this method is unmentioned.

The section on the reception, transformation and measurement of sound-energy is an important one dealing *inter alia* with the ear, the conversion of sound-energy into electrical energy, directional reception and the analysis of complex sounds, and concluding with the theory of wave-filters in which the line-impedances are "lumped."

In the final section the measurement of distance by sound, the acoustics of buildings, and the reproduction of sound are described, but the author, in view of the magnitude of the subject, has refrained from considering musical instruments. Tables of velocities are given in appendices.

The claim on the jacket of this 25s. book that it *amply covers* the requirements of students preparing for university degrees is very modest, inasmuch as the essential requirements in sound for most degrees could be written in an elegant hand on the back of a halfpenny postage stamp and sold for a handsome profit at a penny. The additional claim that it serves as a valuable text-book of reference is justified by the amount of matter reported and a supply of references to original papers. A few tests of the index showed that it was dependable, but disclosed that, although the references to two papers are each given no fewer than three times in the text, the entries for Webster's classical paper introducing the concept of acoustical impedance are omitted.

To sum up: the author has, subject to a few of the clerical errors unavoidable in a first edition, dealt, and dealt well, with "the ever-increasing bulk of new data and methods of investigation which is now available," and has placed upon the market a full, well illustrated and reliable work.

E. J. I.

*Lecture Experiments in Optics*, by B. K. JOHNSON. Pp. 112. (London: E. Arnold and Co.) 8s. 6d.

Those of us who, nurtured on the pages of Lewis Wright, have felt the need for some more modern exposition of lecture methods in optics, heard with pleasure that Mr B. K. Johnson was drawing on his wide experience in these matters in order to prepare such a volume.

8

In all experimental lecture work, there is a host of detail concerning those practical matters of lighting, dimensions, interchangeable fitments and the like which each lecturer must painfully acquire for himself, or obtain more agreeably from the painful experience of others. Mr Johnson's book is designed to expedite this process, and he has provided his readers with a mass of valuable practical details concerning lecture experiments on reflection and refraction, lenses and mirrors, photometry, the eye, optical instruments, the spectrum, polarization, interference and diffraction.

Some of the experiments seem more suited to the laboratory than the lecture table, and it is with a certain measure of regret that the reviewer finds that Mr Johnson makes practically no use of that very effective method of exhibiting the properties of lenses, mirrors and prisms, which consists in studying the passage through the appropriate system of a series of narrow parallel beams grazing a white vertical board mounted on the lecture table.

Mr Johnson's book can be commended, and we trust that in the near future he will be able to offer to the public a considerably enlarged edition.

A. F.

*Applications of Interferometry*, by W. EWART WILLIAMS. Pp. viii + 104. (London: Methuen and Co.) 2s. 6d.

Mr Williams has produced a scholarly but far from elementary book. He groups apparatus for obtaining interference-systems into two broad classes, those based on a division of wave-front, of which the biprism may be taken as typical, and those based on a division of amplitude, as shown in the Michelson interferometer. He discusses carefully and thoroughly the fundamental principles of the methods, devoting special attention to just those difficult points which the average text-book is wont to scamp, and concerning which an inquiring student is apt to put awkward posers.

In so small a volume it is impossible to do more than make a selection of one or two important applications, and Mr Williams has chosen some very apt and interesting instances. In particular, his description of Michelson's method of measuring stellar diameters may be quoted as the clearest account in brief compass with which the present reviewer is acquainted.

Unassuming as it is, the book is a very useful and welcome addition to the literature of physical optics.

A. F.

*The Physics of Solids and Fluids*, by P. P. EWALD, TH. PÖSCHL and L. PRANDTL. Pp. xii + 372. (London: Blackie and Son, Ltd.) 17s. 6d.

Among the volumes which have recently appeared dealing, from the point of view of the advanced student, with general properties of matter, this work, which is a translation of certain articles selected from the latest edition of Muller-Pouillet, holds a high place. The book opens with two chapters, from the pen of Professor Pöschl, which deal with elasticity, strength of materials and solid friction. The mathematical treatment, though adequate, is simple, and practical considerations are kept well to the foreground.

Professor Ewald writes on the mechanical structure of solids from the atomic standpoint, and gives, in the compass of some seventy pages, a remarkably interesting account of the lattice theory of polar crystals and the mechanical properties of metallic crystals, concluding with a critical comparison of mechanical properties in metals and non-metals.

The larger portion of the book is devoted to a series of chapters dealing with certain hydrostatic and hydrodynamic problems and is written by Professor Prandtl. Is it necessary to say more than that the reader who opens the book anticipating a thorough

and stimulating treatment of the fundamentals of hydromechanics will not be disappointed? Here again, practical considerations are continually emphasized, and not the least valuable portion of this section is that devoted to problems of aviation.

Those of us who have been nurtured on the arid treatment beloved of the Cambridge school can only sigh and congratulate the more fortunate students of a newer generation.

The translation reads pleasantly, the book is well produced, and the price is modest. It can be recommended unreservedly.

A. F.

*Étoiles et Atomes*, by A. S. EDDINGTON, F.R.S., M.A., D.Sc., LL.D. Pp. ix + 188 with 13 illustrations. (Paris: Herman et Cie.) Paper cover. 35 fr.

Last summer we learnt from the daily press of a long-haired, frowsy fraternity, anxious to expose their bodies to the sun's radiation in Hyde Park, at the Welsh Harp at Hendon, and elsewhere—sun-bathers, forsooth. Why even Shadrach, Meshech and Abednego, the three youths who, according to holy writ, walked in a fiery furnace, had the "bulge on them" so far as their studies of the effects of radiation on human tissue were concerned. The true cult of sun-bathing is of very recent growth, and its prophets are a select and choice group of our most brilliant physicists, Eddington, Fowler, Jeans, Milne and one or two others. And Sir Arthur Eddington is the champion sun-bather of them all. Listen, "Personnellement je suis mieux chez moi sous la surface du soleil, et j'ai hâte d'y pénétrer" (p. 4). And to think that the temperature beneath the surface may be as high as 40,000,000° (p. 8). Our author is a veritable salamander!

This volume, largely an account in popular terms of Sir Arthur's brilliant contributions to our knowledge of stellar cosmology, is based upon the author's evening discourse before the British Association at Oxford in 1926, and three lectures given at King's College, London, in the same year. The English edition, comprising three chapters, appeared first in 1927. A French translation appeared in the *Bulletin de la Société astronomique de France* in 1928–1929. Since then, our author, following the technique characterizing a Turkish bath, has taken a "cooler" in intersidereal space, where the temperature is of the order of 3° absolute. His experiences there were broadcast as a B.B.C. National Lecture in April 1929. Here they are recounted for the first time in a French edition. It were surely a work of supererogation for me to refer to the contents of the volume. Sir Arthur's contributions to astronomical physics are, or should be, known to all physicists; his style makes one regret the approaching end of the volume as the reading proceeds. Personally, I have been fascinated by his account of the interior of a star (chapter I), recent researches relating to Algol, Sirius, Betelgeuse (chapter II), the age of the stars (chapter III) and the matter of intersidereal space (chapter IV). The translation has been well done—M. Rossignol is a sweet-voiced, capable and well-known translator, and no *rossignol d'Arcadie*—who long since took his *premier essor*. The book is well printed on good paper, is well illustrated and the price is extremely reasonable. I recommend it to physicists generally and, more especially, to examinee students of physics of whom a knowledge of French is required in their examinations. "French, physics and astrophysics without tears" sums up my recommendation of the work.

J. S. G. T.

*Band Spectra and Molecular Structure*, by R. DE L. KRONIG, Ph.D. Pp. x + 163. (London: Cambridge University Press.) 10s. 6d.

This book is an elaboration of lectures given at Cambridge in 1929. It is divided into five chapters which deal respectively with the classification of the energy levels of diatomic molecules, the wave-mechanical properties and fine structure of those levels, selection rules and intensity relations, the macroscopic properties (dielectric constants, magnetic susceptibilities, specific heats, etc.) of molecular gases, and the theory of molecular forma-

tion and chemical binding. Generally, the subject matter may be classified into (i) a concise but fairly complete statement of the theoretical results, (ii) an adequate outline of the derivation of these results, and (iii) a very brief indication of the comparison of the theoretical with the experimental results. It is so arranged that certain sections (indicated by asterisks at the beginning and end) in which a knowledge of the wave-mechanics is indispensable, may, with the minimum of interruption of the train of thought, be omitted by the reader who has not the necessary mathematical equipment. After the omission of such sections, very little is left of some of the articles into which the chapters are divided. Of two articles (on the theoretical classification of rotational energy levels), indeed, only the opening paragraph and the closing paragraph remain in each case: so remarkable is Dr Kronig's power of concise expression, and so much of the present theory has the non-mathematical reader to take for granted.

The symbols used conform to the notation recently recommended by Mulliken, for the quantum numbers but not for the energies, frequencies, etc. The following examples of the differences may assist the reader of both authors:

| Kronig | Mulliken | Kronig | Mulliken |
|---|---|---|---|
| $W, W_j, W_{j'}$ | $E, E', E''$ | $\nu_o, B_o, \rho_o$ | $\omega_e, B_e, r_e$ |
| $W^o{}_{q\Lambda\Omega}, W^o{}_{q\Lambda}$ | $E_e$ | $v, \mathcal{J}; v', \mathcal{J}'$ | $v', \mathcal{J}'; v'', \mathcal{J}''$ |
| $W^o{}_{q\Lambda\Omega v}, W^o{}_{q\Lambda v}$ | $E_e + E_v$ | even terms ($\times$) | positive terms ($+$) |
| $W^o{}_{q\Lambda\Omega vJ}$ (in case $a$) $\}$ | $E_e + E_c + E_c$ | odd terms ($o$) | negative terms ($-$) |
| $W^o{}_{q\Lambda\Omega rK}$ (in case $b$) $\}$ | | | |

Particularly, the reader must note that Prof. Kronig still uses the words "even" and "odd" in the sense in which he himself first used them, where Hund and Mulliken now use the words "positive" and "negative" and in quite a different sense from the latter writers' use of *gerade* and *ungerade*.

The published records accessible to the reviewer do not justify the statement on p. 97 that "the fact that the molecules $O^{16}O^{17}$, $O^{16}O^{18}$, and $C^{12}C^{13}$ do not have half of the lines missing like the molecules $O^{16}O^{16}$ and $C^{12}C^{12}$ led Birge and King to the discovery of the isotopes $O^{17}$, $O^{18}$ and $C^{13}$." Actually, the discovery of $O^{17}$ and $O^{18}$ was announced by Giauque and Johnston, the fact that $O^{16}O^{18}$ has two lines to every one of $O^{16}O^{16}$ was first pointed out by Babcock, and $C^{13}$ was discovered by King and Birge, who, however, made no mention of there being two lines of $C^{12}C^{13}$ to one of $C^{12}C^{12}$ (though they would be expected, of course). $^2\Pi_1$ on the second line of p. 52 is obviously a misprint for $^3\Pi_1$.

The work closes with a subject-index and a well classified list of 352 references, of which only about half a dozen are to publications earlier than 1923.

With Prof. Kronig's authoritative account of the purely theoretical aspect, Prof. Mulliken's comprehensive "Interpretation of Band Spectra" now appearing in *Reviews of Modern Physics*, the same writer's forthcoming book, and a book which is being written (in English) by a well-known Scandinavian investigator, the English student would appear to be well provided with descriptive works on this subject for several years hence. In addition, there are two recent German monographs (one of which is shortly to re-appear in English), and a forthcoming book by a prominent German band-spectroscopist. At present, however, there is a definite lack of a volume of well-chosen and well-arranged numerical data for the many known band-systems and reliable values of the molecular constants derived from their analyses, with a profusion of energy-level and other diagrams and a bare minimum of descriptive matter. Such a volume, no doubt, would be a useful supplement to the works just mentioned, and would also facilitate the identification of band-spectra in the laboratory. The reviewer is here venturing to express a long-held and considered opinion, for which he has recently found support in conversations with several spectroscopists including Prof. Mulliken himself. But perhaps all this is irrelevant in a review of Prof. Kronig's very welcome book.

W. J.

*The Principles of Quantum Mechanics*, by P. A. M. Dirac. Pp. x + 258. (London: Clarendon Press.) 17s. 6d.

In the preface to the *Mécanique Analytique* Lagrange remarks, "On ne trouvera point de figures dans cet ouvrage." Dr Dirac's book is conceived in much the same spirit and on p. 18 we find the significant observation, "One does not anywhere specify the exact nature of the symbols employed, nor is such specification at all necessary." The prejudice of the present reviewer in favour of the wave-mechanical language and symbolism, though not entirely removed, has been greatly shaken by studying this work, and he feels compelled to describe it as a notable achievement and one which is not unworthy of comparison with the great French classic.

The difficulties which have beset the path of the growing quantum theory are very largely due to our inveterate insistence on building up theories in terms of concepts and images borrowed from our immediate experience and observation. It is becoming more and more evident that a logical account of sub-microscopic phenomena cannot be given in terms of familiar concepts in the old-fashioned causal space-time manner. This accounts for the unspecified nature of the symbols in Dr Dirac's symbolic method. They are as it were the expression of new concepts, and the author has pursued the ideal of presenting the new mechanics in terms of them in a rigorously logical form, shorn of all irrelevancies. He claims, perhaps rightly, that his method goes more deeply into the nature of things than does that of wave mechanics; but it would seem to have profited greatly by suggestions from the latter mode of exposition, as the constant use of such terms as "superposition," "interference," "phase" and the like indicates.

While the practical physicist will probably prefer the wave-mechanical form of theory to Dirac's symbolic form (and will probably profit more from it), he cannot afford to ignore the other. Notwithstanding the abstract character of parts of the book it is, as the author maintains, in close contact with physics and contains many important applications. It begins with a chapter on the principle of superposition followed by chapters on the symbolic algebra of states and observables, *eigen* values and *eigen* functions (it is to be regretted that Dr Dirac has not seen fit to render *eigen* by an English equivalent), transformation theory, etc.; while the latter part of the book is devoted very largely to applications.

The book can be recommended to physicists (perhaps also to pure mathematicians, though there is a slight doubt whether they will understand it) not only because the author is one of the chief contributors to the new theory, but because there is much in it of interest and value even for purely experimental physicists. Moreover, once the reader has mastered the first four or five chapters he will find the book extraordinarily fascinating.

W. W.

*Geophysical Memoir No. 50. Practical Examples of Polar-Front Analysis over the British Isles in* 1925–6, by Dr J. Bjerknis, Director of the Geophysical Institute, Bergen. 4to, pp. 21, and 27 plates. (London: H.M. Stationery Office, 1930.) 3s. net.

The advances which have been made in dynamical meteorology in recent years by Norwegian meteorologists make it very desirable that their methods should be tested by application to the conditions which are found to exist in other countries, and in the present memoir Dr Bjerknis applies them to the Meteorological Office records of the weather for a period of high pressure, March 31–April 1, 1925; one of moderate pressure, February 10–11, 1925; and one of somewhat lower pressure, January 22–23, 1926. He shows that the theory of the polar front allows the physical processes involved in the weather-changes

experienced to be followed readily, and adds to it in this memoir an explanation of the changes of the fronts from sharp to diffuse or *vice versa* which agrees with that suggested by the late Mr A. Giblett in 1923.

C. H. L.

*Geophysical Memoir No. 51. A Study of Visibility and Fog at Malta.* By J. WADS-WORTH, M.A. 4to, pp. 23. (London: H.M. Stationery Office, 1930.) 1s. 6d. net.

The observations of Mr Wadsworth were made at Valetta at 8 a.m., 2 and 7 p.m. from 1919 to 1925. He finds that mist or fog on the coast is more frequent in winter than in summer and that it tends to disappear by midday. In the absence of fog, visibility extends to 30 miles at least; it is best in winter with N.W. winds and least in summer with E. winds.

C. H. L.

*Meteorological Office Reseau Mondial* 1923. 4to, pp. xv + 115. (London: H.M. Stationery Office, 1930.) 25s. net.

This annual account of the variation of pressure, temperature and precipitation over the surface of the earth from 80° N. to 70° S. has now appeared for 13 years; and for nearly all the observing stations, of which there are two to each 10° square, normal mean values of the three quantities are available. Many years must elapse before sufficient observations have accumulated to justify statements as whether and how they are changing with time.

C. H. L.

*Magnetic, Meteorological and Seismographic Observations made at the Government Observatories, Bombay and Alibag in* 1926. Reduced and tabulated by Dr S. K. BANERJI. Fsc. pp. iii + 135, and 5 plates. (Calcutta, 1930.) 17s. 6d.

This volume is on the same lines as the one for 1925 and extends the record of continuous meteorological and magnetic observations to 81 years and of seismological observations to 28 years. Pressure, rainfall, wind-velocity and direction, temperature, and humidity are tabulated for each hour, cloud at seven periods each day, magnetic declination, horizontal and vertical forces for each hour, and the time, amplitude and period of each seismic disturbance.

C. H. L.

# PUBLICATIONS OF THE PHYSICAL SOCIETY

## PROCEEDINGS

Vol.
1 ( 3 pts) 12s. each.
2 ( 5 „ ) 12s. each.
3 ( 4 „ ) 12s. each.
4 ( 5 „ ) Pts 1, 2, 3 and 5, 7s. each.
           Pt 4, 12s.
5 ( 5 „ ) 7s. each.
6 ( 4 „ ) Pt 1, 12s. Pts 2, 3 and 4, 7s.
           each.
7 ( 4 „ ) 7s. each.
8 ( 4 „ ) 7s. each.
9 ( 4 „ ) 7s. each.
10 ( 4 „ ) 7s. each.
11 ( 4 „ ) Pt 1, 7s. Pts 2, 3 and 4, 12s.
           each.
12 ( 4 „ ) Pt 1, 12s. Pts 2, 3 and 4, 7s.
           each.
13 (13 „ ) 7s. each, except pt 12, 12s.
14 (12 „ ) 7s. each, except pt 12, 12s.
15 (12 „ ) 7s. each.
16 ( 8 „ ) 7s. each.
17 ( 7 „ ) 7s. each.
18 ( 7 „ ) 7s. each.
19 ( 8 „ ) 7s. each.
20 ( 6 „ ) 7s. each.
21 ( 7 „ ) 7s. each.

Vol.
22 ( 4 pts) 7s. each, except pt 2, 12s.
23 ( 5 „ ) Pts 1, 3, 4 and 5, 7s. each.
           Pt 2, 12s.
24 ( 6 „ ) 7s. each, except pt 1, 12s.
25 ( 5 „ ) 7s. each.
26 ( 5 „ ) 7s. each.
27 ( 5 „ ) 7s. each.
28 ( 5 „ ) 7s. each.
29 ( 5 „ ) 7s. each.
30 ( 5 „ ) 7s. each, except pt 5, 12s.
31 ( 5 „ ) Pts 1, 2, 3 and 4, 7s. each.
           Pt 5, 12s.
32 ( 5 „ ) 12s. each.
33 ( 5 „ ) 7s. each.
34 ( 5 „ ) Pts 1, 3, 4 and 5, 7s. each.
           Pt 2, 12s.
35 ( 5 „ ) 7s. each.
36 ( 5 „ ) 7s. each.
37 ( 5 „ ) 7s. each.
38 ( 5 „ ) Pts 2, 3, 4 and 5, 7s. each.
           Pt 1, 12s.
39 ( 5 „ ) 7s. each.
40 ( 5 „ ) 7s. each.
41 ( 5 „ ) 7s. each.
42 ( 5 „ ) 7s. each.

Postage is charged extra. The sale of Parts the price of which is 12s. is restricted, and permission to purchase them must be obtained from the Council of the Society.

The Proceedings can be supplied in bound volumes at an additional charge of 5s. per volume.

## SOME SPECIAL PUBLICATIONS

THE TEACHING OF GEOMETRICAL OPTICS. Price 4s. 6d.

REPORT ON SERIES IN LINE SPECTRA. By *A. Fowler*, F.R.S. Second Edition, with index. Price 12s. 6d.; in cloth, 15s. 6d.

REPORT ON RADIATION AND THE QUANTUM THEORY. By *J. H. Jeans*, Sec. R.S. Second Edition. Price 7s. 6d.; in cloth, 10s. 6d.

REPORT ON THE RELATIVITY THEORY OF GRAVITATION. By *A. S. Eddington*, F.R.S. Third Edition. Price 6s.; in cloth, 8s. 6d.

THE EFFECT OF ELECTRIC AND MAGNETIC FIELDS ON SPECTRAL LINES (Seventh Guthrie Lecture). By *Niels Bohr*. Price 2s. 6d.

THE SCIENTIFIC PAPERS OF JAMES PRESCOTT JOULE. In cloth. Vol. I, 18s.; Vol. II (Joint Papers), 12s.

THE SCIENTIFIC PAPERS OF SIR CHARLES WHEATSTONE. In cloth. Price 12s.

DISCUSSIONS. Photo-Electric Cells and their Applications, 12s. 6d.; The Making of Reflecting Surfaces, 5s.; Lubrication, 1s. 6d.; Ionisation in the Atmosphere, 3s.; Hygrometry, 5s.; Metrology in the Industries, 1s. 6d.; Absolute Measurement of Electrical Resistance, 2s. 6d.; X-Ray Measurements, 2s. 6d.; Physics and Chemistry of Colloids, 2s. 6d.

Postage is charged extra.

*Fellows of the Society may obtain any of the above publications for their* PERSONAL *use at* HALF-PRICE. *An additional charge is made for binding.*

Orders for any of the above publications should be sent to the

ASSISTANT SECRETARY, THE PHYSICAL SOCIETY, 1 LOWTHER GARDENS,

EXHIBITION ROAD, LONDON, S.W. 7

from whom a full list of the Society's publications may be obtained.